Cardiovascular Disease, Endothelial Cell Gene Expression, and Renal Dysfunction in Insulin Resistant, Hyperlipidemic Swine

Elizabeth Parker Merricks

A dissertation submitted to the faculty of the University of North Carolina at Chapel Hill in partial fulfillment of the requirements for the degree of Doctor of Philosophy in the Department of Pathology and Laboratory Medicine.

Chapel Hill
2010

Approved by:

Timothy C. Nichols, M. D., Advisor

Marjorie S. Read, Ph.D.

Dwight A. Bellinger, Ph.D., DVM

Thomas H. Fischer, Ph.D.

Caterina Gallippi, Ph.D.

©2010
Elizabeth Parker Merricks
ALL RIGHTS RESERVED

ABSTRACT

Elizabeth Parker Merricks: Cardiovascular Disease, Endothelial Cell Gene Expression, and Renal Dysfunction in Insulin Resistant, Hyperlipidemic Swine
(Under the direction of Timothy C. Nichols, M.D.)

Globally, the prevalence of insulin resistant (IR), type-2 diabetes mellitus (DM) is increasing. Both IR and DM are associated with an increase in cardiovascular events and renal pathology. The underlying cause for this increase is, as yet, not completely understood. A thoroughly characterized model is needed to identify mechanisms connecting insulin resistance with cardiovascular and renal disease. Through selective breeding we have produced hyperinsulinemic pigs that develop hypercholesterolemia when fed a high fat diet. A subgroup of these pigs develops severe and diffuse proximal and distal abdominal aorta and coronary artery atherosclerosis compared to the other group which has moderate disease. Through aortic endothelial cell gene expression studies we have identified three genes (*MERP-1, RABGAP1L, COL12A1*) that are uniquely expressed in the atherosclerotic endothelium of the severe disease group. Additionally, a subgroup of the pigs develops renal histopathology that mirrors the phenotype of an insulin resistant/diabetic nephropathy when albuminuria is present. All pigs have been monitored over the course of one year on a high fat, high sodium diet for weight, backfat, blood pressure, insulin sensitivity, total and LDL cholesterol, triglycerides, oxidized LDL, fructosamine, inflammatory makers, and aldosterone. The goals of

this proposal were to characterize this pig model with regards to 1- presence and severity of coronary and aortic atherosclerosis and its association with markers of oxidative stress, 2-changes in endothelial cell gene expression as it relates to the severity of aortic atherosclerosis, and 3-extent of renal pathology and its resemblance to human diabetic renal disease. This will support the long range goal of this laboratory, which is to provide the scientific community with a well-characterized, useful animal model of insulin resistance and/or type-2 diabetes, which develops human-like coronary and aortic atherosclerosis and IR/diabetic like nephropathy.

To my sons, Jeffrey and Justin

Material possessions will come and go but an education can stay with you forever.
It is never too late!
I love you more than you'll ever know!

ACKNOWLEDGEMENTS

First - this has taken too darn long! While this dissertation took 8 calendar years to finish only a small portion of that time was actually spent on this project. I have undergone this endeavor with the foolish notion that I could still work full time, raise two kids, and do everything else entailed in my busy life! Praise and thanks first and foremost to God for all the answered prayers! Additionally, there are many people that I need to thank for their help and encouragement.

It is always hard to know where to begin. I guess I should start with my origins in the Department of Pathology by thanking Dr. Katherine Pryzwansky, PhD, who took a chance on a naïve, freshman work-study student many, many years ago. She has been a wonderful teacher, mentor, and friend. I can truly say that without her, I would not be where I am today.

Second, and no less important, I would like to thank Dr. Marjorie Read, PhD, for taking me into her lab when my time with Kathy was over. She also has been a wonderful teacher, mentor, and friend. She was a big factor in my decision to undertake this challenge. Without our lunch outings and her constant support, guidance, encouragement, and friendship, this would not have happened. Additionally, I would like to thank her for taking time out from her retirement to be a part of my committee. I couldn't and wouldn't have done this without her!

I would also like to thank the other members of my committee. Timothy Nichols, MD, has been my mentor and supervisor throughout this endeavor. He has always been supportive and has given me the resources, time, and space that were needed to do this research. He knows how important family is, especially how important my family is to me, and has always understood the fact that my family comes first. For that I am eternally gratefully. When I got frustrated with lab matters and needed advice, Thomas Fischer, PhD, was always there to cheer me up and tell me I needed to drink more! Dwight Bellinger DVM, PhD, has been a wonderful resource as veterinarian. He always tells me exactly what he thinks! Caterina Gallippi PhD is a great inspiration as a young mother, researcher, and friend. I wish I had started this when I was her age!

Additionally, I need to thank Dr. Charles Jennette, chair of the Department of Pathology and Laboratory Medicine, not only for allowing me to work and pursue my degree, but also for his help and expertise with the renal portion of this dissertation. Thanks also to Dr. Gary Koch and his staff and students at the Biometrics Consulting Lab for help with all statistics.

I would like to thank all of the staff at FOBRL (aka –The Blood Lab); it has been a great place to work. There are a few people I need to mention specifically: 1-Robin Raymer – well, most people may not know it, but Robin is the cornerstone of the Blood Lab. If you need to know anything about the lineage, treatment, etc. of any of the animals, or anything in general about FOBRL, Robin is THE person. Not only has she been a great resource, she has been a great friend. We have had numerous adventures traveling the world together and I value her friendship and

advice. 2- Kent Passingham - without Kent, a lot of the actual “pig work” would not be done. Thus far he is the only person I have seen move an 800 lb pig around and make it look like there’s nothing to it! His pig knowledge and handling skills are invaluable. Thanks Kent for all your hard work! 3- Mark Kloos was my right hand in the laboratory. The gene expressions studies would not be complete without his hard work and advice. Not to mention, he always had some interesting story to tell – never a dull moment. To Robin, Kent, and Mark – Thanks for making Bergmans more fun or at least more bearable than they were meant to be!

Last and most importantly, I would like to thank my family. I know this has been a long road, but they have stood back and let me pursue my degree without any undue pressures. Thank you to my Mom and Dad, Carolyn and Johnnie Parker! I could not have asked for better parents. They have always given encouragement and support and have never given up on me. Also, thanks to my uncle and aunt, Alvin and Judy Parker. They are like second parents to me and I would not be at this point in my education without their support. Thank you to my sisters, Lori Hollowell and Joy Byrum. I appreciate all the pep talks over the phone when I was frustrated, depressed, or just at my wit’s end!

Most of all, I need to thank “my boys” – my husband, Jeff Merricks and my sons, Jeffrey and Justin. **They are my world!** Thanks for hanging through this with me! I love you guys more than anything.

TABLE OF CONTENTS

LIST OF TABLES

LIST OF FIGURES

LIST OF ABBREVIATIONS

AMDCC	Animal Models of Diabetic Complications Consortium
APO E	apolipoprotein E
aPTT	activated partial thromboplastin time
ARFI	acoustic radiation force impulse
CETP	cholesterol ester transfer protein
CIRC	circumflex coronary artery
CRP	C reactive protein
CVD	cardiovascular disease
DEPC	diethyl pyrocarbonate
DH	dietary hypercholesterolemic
DM	diabetes mellitus
EC	endothelial cell
EIA	enzyme immunoassay
ELISA	enzyme linked immunosorbent assay
eNOS	endothelial nitric oxide synthase
FC	fibrous cap
FDR	false discovery rate
FH	familial hypercholesterolemic
FSGS	focal segmental glomerulosclerosis
FSIVGTT	frequently sampled intravenous glucose tolerance test
GBM	glomerulobasement membrane
GITC	guanidine thiocyanate
HDL	high density lipoprotein
HFH	heterozygous familial hypercholesterolemic
IL-6	interleukin 6
IM	intramuscular
IR	insulin resistance/resistant
IS	insulin sensitive

IT	intimal thickening
IV	intravenous
LAD	left anterior descending coronary artery
LDL	low density lipoprotein
MA	moderate disease, atherosclerotic endothelium
MAP	mean arterial pressure
MAPK	mitogen activated protein kinase
MM	mesangial matrix
MMA	mesangial matrix area
MMP	matrix metalloproteinase
MN	moderate disease, normal endothelium
MT	medial thinning
NA	not available
NaCl	sodium chloride
ND	not detected
NGS	normal goat serum
NO	nitric oxide
ORG	obesity related glomerulopathy
Ox LDL	oxidized low density lipoprotein
PAI-1	plasminogen activator inhibitor 1
PAS	periodic acid Schiff's
PBS	phosphate buffered saline
PCA	principal component analysis
PT	prothrombin time
RAAS	renin-angiotensin-aldosterone system
RCA	right coronary artery
RIA	radioimmunoassay
RMA	robust multi-array average
SA	severe disease, atherosclerotic endothelium

SD	standard deviation
Si	insulin sensitivity index
SMC	smooth muscle cell
SN	severe disease, normal endothelium
TNF-α	tumor necrosis factor alpha
$U_{A/C}$	urine albumin/creatinine ratio
VWF	Von Willebrand factor
WT-1	Wilm's tumor antigen 1

Chapter 1

Introduction

Insulin resistance (IR) is defined as a condition where there is a decreased biological response to normal concentrations of serum insulin. The body is able to produce insulin, but there is improper use of insulin by muscle, fat, and liver cells in the conversion of glucose to energy. This often results in a compensatory insulin secretion by the pancreas which leads to increased insulin in the blood. IR generally has no symptoms, may be present for years without detection, and is commonly a precursor of diabetes mellitus (DM). When the pancreas can no longer compensate for the needed increase in insulin, glucose increases as well. Patients with high normal glucose and increased insulin are in a “pre-diabetic” state. According to the United States Department of Health and Human Services, pre-diabetes is on the rise in the US. Many of these patients go on to develop DM. The incidence of insulin resistant, type 2 DM is increasing at epidemic rates globally. In the United States alone, in 2007, there were 1.6 million new cases of diabetes diagnosed in people aged 20 years or older and a total of 7.8 percent of the population with diabetes.[1] According to the International Diabetes Federation, the number of people living with diabetes in 2010 is expected to reach 285 million worldwide.[2]

For insulin resistance alone, the prevalence among those 20 years or older may be as much as 34%.[3] Obesity is not only a major risk factor for insulin

resistance but may also add to its severity. During obesity there may be dysregulated release of non-esterified fatty acids, glycerol, hormones, and proinflammatory cytokines from adipose tissue which may contribute to the development of IR.[4, 5] Additionally, insulin resistance may contribute to the development of obesity[6] as adipocytes are highly responsive to insulin. In the last 25 years there has been a drastic rise in obesity among adults in the United States with >30% of the adult population now considered obese.[7]

Insulin Resistance, Endothelial Dysfunction and Cardiovascular Disease

Normal, healthy endothelium has numerous beneficial effects, including: promotion of vasodilation; antioxidant, anti-inflammatory, anticoagulant, and profibrinolytic effects; and inhibition of leukocyte adhesion and migration, smooth muscle cell proliferation and migration, and platelet aggregation and adhesion.[8] Endothelial dysfunction, while an early and potentially reversible step, can lead to the initiation and progression of atherosclerosis.

Atherosclerosis is the basis of cardiovascular disease (CVD) - the leading cause of death in the world today.[9] Atherosclerosis is a process that occurs in large to medium sized arteries. Mass transport, low density lipoprotein (LDL) receptors, and damage to the endothelium allow the accumulation of LDL in the vessel wall where it is then oxidized. Damaged endothelium also allows adhesion of platelets and monocytes. Monocytes migrate into the subendothelial space, transform to macrophages, and phagocytize oxLDL to become foam cells. Both platelets and macrophages secrete factors that activate smooth muscle cells to

migrate from the media to the intima, where they can proliferate and form a fibrous cap over the plaque. The arterial walls thicken and lose their elasticity.

Atherosclerosis is a complicated process. The initial step is thought to be chronic endothelial injury, leading to endothelial dysfunction. This dysfunction can be brought about by diabetes and a number of risk factors including hypertension, smoking, viruses, and immune reactions, but the two key factors are thought to be hyperlipidemia and hemodynamic disturbances. While atherosclerosis most often occurs in the arteries supplying the heart, it also occurs in arteries supplying the brain, kidneys, and lower extremities.

The progression of endothelium from normal to dysfunctional to atherosclerotic may parallel the progression of insulin resistance to overt diabetes.[10] Studies have shown that insulin resistance co-associates with other factors that lead to endothelial dysfunction, especially changes in lipoproteins.[11] Insulin works through both the phosphatidylinositol 3-kinase pathway to regulate endothelial nitric oxide (NO) production and as a growth factor through the mitogen activated protein kinase (MAPK) pathway to affect cell growth and movement, increase endothelial cell adhesion markers and mediate expression of certain prothrombotic factors.[11]

Numerous large population studies have shown that both IR and DM are associated with an increase in cardiovascular events.[12-18] However, the underlying cause for this increase is, as yet, not completely understood.

Insulin Resistance and Nephropathology

Hypercholesterolemia and hypertension (key risk factors for atherosclerosis) as well as obesity, insulin resistance and diabetes affect renal function. Endothelial dysfunction may also play a significant role in insulin resistance and diabetic renal complications. Insulin resistance and hyperinsulinemia have been independently associated with chronic kidney disease in numerous analyses[19]. Insulin is thought to alter urinary sodium excretion by effects on the tubules, to promote mesangial cell proliferation, and increase the action of angiotensin II.[19] One study found patients receiving peritoneal dialysis have an increase in insulin levels and insulin resistance when compared to healthy controls.[20] A ten year follow-up community based study found obesity, amongst other factors, to be a predictor of chronic kidney disease.[21] This finding is thought to be mediated through insulin resistance and endothelial dysfunction.[22] Insulin resistance itself may be an independent predictor of the development of nephropathy in diabetics.

Pigs as Model of Human Disease

A thoroughly characterized model is needed to investigate the connection between insulin resistance and cardiovascular disease and nephropathy. Pigs have long provided experimental models of human disease. Swine have many phenotypic similarities to humans including cardiovascular anatomy and function, renal architecture and function, metabolism, lipoprotein profile, size, tendency to obesity, and omnivorous habits. Swine are also similar to humans in that they carry a large part of cholesterol in LDL and develop atherosclerosis with aging. The

phenotypic susceptibility to coronary atherosclerosis makes pigs an attractive species for related mechanistic studies.

Dissertation Overview

Through selective breeding, our group has developed a hyperinsulinemic pig model that develops worsening insulin resistance when fed a high fat diet for twelve months. A subgroup of these pigs develops severe and diffuse proximal and distal abdominal aorta and coronary artery atherosclerosis compared to the other group which has moderate disease. Additionally, a subgroup of these pigs develops albuminuria which appears to predict the presence of renal histopathological changes that are consistent with those seen in IR/diabetic humans. In the current studies, all pigs have been monitored over the course of one year on a high fat diet for weight, backfat, blood pressure, insulin sensitivity, total and LDL cholesterol, triglycerides, oxidized LDL, fructosamine, inflammatory makers, and aldosterone. Changes in specific markers of oxidative stress have been identified in these animals.

Several swine models of both type I and II diabetes are being explored. A recent comprehensive review by our group explains the available swine models of type 2 DM and/or IR.[23] This review also lists steps for validating a model of type 2 IR-DM. The model presented in this dissertation addresses these steps including documentation of fasting hyperinsulinemia, insulin sensitivity, serum glucose levels, body fat measurements, lipoprotein concentrations, serum markers, blood pressure and end-organ damage.

The overall goal of this dissertation is to characterize these pigs with regards to cardiovascular disease, changes in endothelial cell gene expression, and renal pathology as related to insulin resistance and obesity and the similarity of each to what is seen in human disease. This will support the long range goal of this laboratory, which is to provide the scientific community with a well-characterized, useful animal model of insulin resistance and/or type-2 diabetes, which develops human-like coronary and aortic atherosclerosis as well as nephropathology.

Chapter 2

Atherosclerosis in Insulin Resistant Pigs Fed a High Fat/High NaCl Diet

Abstract

Objective: To investigate if the severity of atherosclerosis that develops in pigs fed a high fat/high NaCl diet is associated with elevated oxLDL, fructosamine, and aldosterone. *Methods and Results*: The primary endpoint was atherosclerosis severity in adult pigs (n= 18) fed a high fat diet that also contained high NaCl (56% above recommended levels) for 1 year. Nine pigs developed severe and diffuse distal coronary atherosclerosis (i.e., intimal area as percent medial area ≥ 75% in at least 2 sections = severe and ≥ 75% over 3 sections separated by 2 cm in the distal half of the coronary artery = diffuse distal) and proximal abdominal aortic atherosclerosis that was severe (i.e., ≥ 6 mm^2 intimal area) and diffuse (i.e., ≥ 40 % surface with raised lesions). The other nine pigs had moderate atherosclerosis. Both groups of pigs developed comparable elevations in total and LDL and HDL cholesterol, weight gain, increase in backfat, blood pressure, and inflammatory markers, and increase in insulin resistance (Bergman S_i, $p \leq 0.008$) without overt diabetes. Insulin resistance did not correlate with atherosclerosis severity. Most importantly, when compared to the 9 pigs with moderate atherosclerosis, the 9 pigs

with severe and diffuse atherosclerosis had significantly higher oxLDL and greater increases in fructosamine and aldosterone values consistent with increased oxidative stress.

Introduction

The increasing prevalence of insulin resistance and type 2 diabetes is likely to be attended by a significant increase in cardiovascular disease (CVD).[24-26] Insulin resistance (IR) is defined as a decreased biological response to normal concentrations of serum insulin that over time leads to compensatory hyperinsulinemia.[25] Insulin resistant and diabetic humans often develop diffuse coronary atherosclerosis involving long arterial segments and including multiple distal lesions.[27-31] These patients require intensive medical therapy and their lesions are less amenable to angioplasty, stent placement, surgical reconstruction or bypass.[32, 33] Often disease progression outside of the stented segment of the coronary artery or bypass insertion site limits the duration of benefit in patients with IR and diabetes and even the most aggressive medical treatment regimens do not lower the risk for CVD to the non-diabetic level.[33-36] These findings strongly suggest that available treatments are not addressing key pathophysiological mechanisms that, when activated in these patients, augment the development of atherosclerosis. Thus, there is a need for relevant animal models of both insulin resistance and type 2 diabetes that also exhibit severe and diffuse coronary and aortic atherosclerosis.

Animal model systems with coexistent diabetes and hyperlipidemia have been developed in mice, rabbits, non-human primates and pigs in an attempt to determine the effect of hyperglycemia and/or insulin resistance on the development of atherosclerosis.[35, 36] In general, injection of streptozotocin has been used to create a model of type 1 diabetes.[37] Often this drug has been given to APO E or

LDL receptor deficient mice to produce a combined model that is predisposed to aortic atherogenesis.[38, 39] These mice develop subintimal deposition of lipid and oxidized LDL and inflammatory cell infiltrates,[40] but their degree of smooth muscle cell hyperplasia and other characteristics of advanced atherosclerotic lesion development are not similar to human lesions.[41] Furthermore correlations between metabolic changes and hyperlipidemia with severity of atherosclerosis progression have not been established therefore attributing changes in lesion severity to changes in either hyperglycemia or insulin resistance independent of changes in cholesterol has been difficult.[42]

Models of type 2 diabetes have been more difficult to generate. OB/OB (leptin deficient) mice and db/db (leptin receptor mutation) mice have been crossed with APO E deficient or LDL receptor knockout mice, which if fed a western diet develop more severe insulin resistance and type 2 diabetes.[43] However proving that the presence of more severe insulin resistance or diabetes in these animals is the sole cause of increased atherosclerosis has been difficult since an increase in hyperlipidemia is occurring simultaneously.[44] Diabetic rabbits and pigs have also been studied but to a much lesser extent.[45-49] In both cases these models have used either Alloxan or streptozotocin for inducing diabetes and then fed high fat diets. These models also have had difficulty determining the extent to which atherosclerosis is increased due to the induction of diabetes as opposed to lipoprotein abnormalities.[41] One study showed substantial differences in coronary and aortic atherosclerosis but the interpretation was confounded by concomitant

changes in the severity of the lipoprotein phenotype and whether the animals had extensive distal coronary atherosclerosis was not reported in detail.[49]

Our objective was to investigate how severity of atherosclerosis is associated not only with lipoproteins, weight, blood pressure, inflammatory markers and severity of IR in an animal model but also changes in parameters that correlate with change in oxidative stress. Our experimental approach was to study normocholesterolemic pigs fed a high fat diet that also contained increased NaCl. The results show that the experimental pigs developed varying degrees of atherosclerosis which were grouped as moderate or severe. Atherosclerosis severity was not associated with increases in body weight, backfat, insulin or glucose levels, insulin resistance, total or LDL or HDL cholesterol levels, blood pressure, or inflammatory markers. Three other variables, however, that have been associated with increased oxidative stress, (i.e. oxLDL, fructosamine, and aldosterone) were found to be significantly higher in animals with the severe atherosclerosis phenotype as compared to animals with less severe disease. Thus, our paradigm suggests that feeding a high fat/high NaCl diet may enhance the severity of atherosclerosis development through changes in oxidative stress in insulin resistant, hypercholesterolemic pigs.

METHODS

Experimental Pigs, High Fat/High NaCl Diet, and Sampling Protocol during Year Long Study

All pigs were treated according to the standards set in the Guide for Care and Use of Laboratory Animals (National Institutes of Health publication No. 85-23). All procedures and protocols were in accordance with institutional guidelines and approved by the Institutional Animal Care and Use Committee. All pigs were produced and maintained in the same environmental conditions at the Francis Owen Blood Research Laboratory at the University of North Carolina at Chapel Hill and are from Spotted Poland/China and Yorkshire crosses. Pigs from the following two genotypes were used: normocholesterolemic (n=10), heterozygous familial hypercholesterolemic (FH) that are also normocholesterolemic at baseline (n=8).[50-52] Neither normocholesterolemic nor heterozygous FH pigs exhibit hypercholesterolemia unless they are fed a high fat diet. Eighteen pigs were entered into the year-long study as they became available (11 males, 7 females) and the entire group was studied over 24 months. The mean age at study entry was 3.9 ± 2 yr. All study pigs were fed a high fat diet that consisted of pig chow (5NP8 Wayne™ 15% Pig & Sow Pellets, Granville Milling, Granville NC) supplemented with 1% cholesterol, 20% beef tallow, and 0.75% cholate by weight.[53, 54] The NaCl content of the diets was measured (Eurofins Scientific Inc, Des Moines, IA) and 5NP8 provided 0.35% or 8 grams/day as recommended[55] and the high fat diet provided 0.55% or 12.5 grams/day, a 56% increase. The total calories in the high

fat/high NaCl diet were distributed as: 43% fat, 12.5% protein, and 44.5% carbohydrate. Weight, backfat, blood pressure, total and LDL and HDL cholesterol, oxLDL, fructosamine, aldosterone, triglycerides, Bergman Frequently Sampled Intravenous Glucose Tolerance Test (FSIVGTT), and serum and plasma inflammatory markers (TNF-alpha, IL-6, PAI-1, CRP) were obtained at baseline (BL), 3, 6, and 12 months of the year-long study. Serum glucose was measured monthly while the pig was fully conscious in addition to when it was sedated for the Bergman FSIVGTT. At study termination all pigs were euthanized with an overdose of pentobarbital (6 grains/10 lbs. IV) and tissue samples for morphometry were collected from all three coronary arteries and the abdominal aorta.

Bergman Frequently Sampled Intravenous Glucose Tolerance Test (FSIVGTT).

Each pig was sedated with ketamine 4-6 mg/kg intramuscular (IM) and acepromazine 0.1-0.3 mg/kg IM. Two intravenous catheters were placed, one for sampling and one for infusing glucose and insulin. A bolus of glucose (0.3 gm/kg IV) was administered as a 50% solution over ~5 to 10 min. Serum was prepared from blood samples obtained at -15, -10, -5, -1, 2, 3, 4, 5, 6, 8, 10, 14, and 19 minutes to measure insulin and glucose concentrations. At 20 minutes, an insulin bolus (0.03U/kg IV, Novolin R Human Insulin Regular, Novo Nordisk) was injected and blood samples for insulin and glucose concentrations were collected at 22, 25, 30, 40, 50, 70, 100, 140, and 180 minutes. The data were analyzed by the Bergman method to calculate an insulin sensitivity index (S_i) using MINMOD Millennium version 6.02.[56] This method has been widely used to estimate insulin

sensitivity.[57-61]

Measurement of Body Weight, Backfat, and Arterial Blood Pressure

Pigs were weighed on a FlexWeigh scale (model LPF-4824) with a digital readout (Velcon/FlexWeigh Model 5). Backfat has been used as an index of total body fat in pigs[62-67] and was measured by ultrasound over the last rib with the pig standing (Fukuda Denshi, model UF750XT). The intra-animal variability is < 7%. Arterial blood pressure was measured in the tail of conscious pigs (Veterinary Blood Pressure Monitor, model 9301V, CAS Medical Systems, Inc).[68-70] The results are the mean of 5 measurements taken over 5 min.

Total and LDL and HDL cholesterol, triglycerides, insulin, and glucose

Serum cholesterol and triglycerides were measured by an automated method (ANTECH® Inc. Cary, NC)[53]. LDL and HDL cholesterol were measured by colorimetric endpoint reactions using the Liquid Direct LDL and HDL Cholesterol Kits, respectively (Amresco, Solon, OH). Reactions were performed according to the manufacturer's instructions modified for a 96 well plate and optical density was read using a Vmax kinetic microtiter plate reader (Molecular Devices). Serum insulin was measured by a solid phase RIA (ICN, lower unit of detection is 2 μU/ml). The intraassay variability was 4% and the interassay variability was 6%. Serum glucose was measured with a 2300 STAT PLUS (YSI, Yellow Springs, Ohio).

Inflammatory Markers, oxLDL, Fructosamine, and Aldosterone

Pig specific ELISAs were used according to the manufacturer's instructions to measure TNF-alpha (Biosource),[71] IL-6 (R&D Systems), PAI-1 (Molecular Innovations, Southfield, MI),[72] CRP (Pig CRP, Tri-Delta Diagnostics), and oxLDL (Mercodia, Uppsala, Sweden).[73-75] Fructosamine was measured in serum by a colorimetric endpoint reaction according to the manufacturer's instructions (Raichem, San Diego, CA). Aldosterone was measured by enzyme immunoassay with a commercially available kit (Aldosterone EIA, Alpco Diagnostics, Salem, NH) using serum samples that were ether extracted, dried and reconstituted in sample buffer.

Morphometry of Coronary and Abdominal Aortic Atherosclerosis

Coronary artery and aortic atherosclerosis were measured as described previously.[54, 76]

Definition of Severe and Diffuse Distal Coronary Artery and Abdominal Aortic Atherosclerosis

Severe coronary atherosclerosis was defined as mean intimal area as a percent of medial area of ≥ 75 % in at least two coronary artery cross sections. Severe and diffuse distal coronary atherosclerosis was defined as a mean intimal area as a percent of medial area of ≥ 75% over three coronary artery cross sections separated by 2 cm in the distal half of the coronary artery.

Abdominal aortic atherosclerosis in swine and humans begins at the aortoiliac junction and progresses in a retrograde fashion.[77-81] Severe abdominal aortic

atherosclerosis was defined as the proximal half having a mean intimal area of ≥ 3.5 mm^2 and diffuse abdominal aortic atherosclerosis was defined as the proximal half having ≥ 40% of the surface area covered with raised lesions.

Total IEL Area as an Assessment of Coronary Artery Remodeling

The total area contained within the IEL has been used to assess coronary arteries for remodeling during atherogenesis in humans and pigs.[28, 82, 83] Thus, the total IEL area for all three coronary arteries from the two groups of pigs was measured as described[54, 76] and the results were expressed in mm^2 for each of the three arteries from all pigs.

Percent of Coronary Artery Cross Sections with Fibrous Caps and Measurement of Fibrous Cap Thickness

The presence or absence of a fibrous cap was determined from visual inspection of all sections of each coronary artery from all pigs. The results are expressed as the percent of cross sections with fibrous caps. Maximal fibrous cap thickness was measured on the cross section with the greatest percent stenosis for a given coronary artery and is expressed in mm.

Statistical Analysis

For all groups, descriptive statistics are reported as means ± SD for weight, backfat, blood pressure, triglycerides, total and LDL and HDL cholesterol, oxLDL, fructosamine, aldosterone, inflammatory markers, insulin, glucose, Bergman S_i

values, coronary and aortic atherosclerosis measurements. The Wilcoxon rank sum statistic was used as the primary method for comparisons between two groups for coronary and aortic atherosclerosis measurements. Parametric repeated measures ANOVA/ANCOVA models with group, time, and baseline as explanatory factors were used as the primary method for oxLDL (as logarithms), fructosamine, and aldosterone (as logarithms). For all other variables, Wilcoxon rank sum statistics for comparisons between groups and Wilcoxon signed ranks statistics for comparisons within groups were used with parametric repeated measures ANOVA/ANCOVA models in mutually supportive ways and with comparable results for blood pressure, total and LDL and HDL cholesterol, and triglycerides. The ANOVA/ANCOVA models additionally included gender. A p-value being less than 0.05 was the criterion for identifying a change within groups, a difference between groups, or an association of interest for future investigation.

Results

The detailed results of the atherosclerosis data are presented first followed by the metabolic parameters that were monitored during the year-long study to determine which were associated with the development of either the severe and diffuse versus moderate atherosclerosis phenotype. Additional analyses that assessed the effect of gender and genotype (i.e., normocholesterolemic and FH heterozygous) had similar results.

Severity of Coronary Artery Atherosclerosis

At the end of the study, the pigs were found to have developed two different degrees of atherosclerosis severity: Severe = severe and diffuse atherosclerosis, n = 9 (4 males and 5 females), age 4.7 ± 1.9 years old; and Moderate = moderate atherosclerosis, n = 9 (7 males and 2 females), age 5.0 ± 2.3 years).

The nine pigs meeting the criteria for severe atherosclerosis were found to have a mean intimal area as a percent medial area ≥ 75% in all but one RCA and all but one LAD cross section (Figure 2.1). The mean intimal area as a percent medial area in the distal half of the coronary arteries for all 9 pigs in this group was ≥ 75% in at least 3 consecutive cross sections over 2 cm in all three coronary arteries (Figure 2.1). When the extent of coronary atherosclerosis was compared between the severe and moderate atherosclerosis groups for the proximal and distal halves of the coronary arteries, the severe group had significantly larger intimal area, percent stenosis, and intimal area as a percent medial area (Figures 2.1 and 2.2 and Table 2.1, $p \leq 0.001$).

Coronary Artery Remodeling Assessed by Total IEL Area

The severe atherosclerosis group had significantly larger total IEL areas when compared to the moderate group for all three coronary arteries (Table 2.2, $p<0.01$). These data are consistent with a greater degree of positive remodeling.[28, 82, 83] There was no evidence of pair wise vessel to vessel differences in the total IEL area within either group ($p>0.10$).

Percent of Coronary Artery Cross Sections with Fibrous Caps

The percent of coronary artery cross sections containing fibrous caps was significantly greater in the severe atherosclerosis group for all three coronaries (Table 2.2, $p<0.01$). There was no evidence among animals with detectible fibrous caps of differences between the mean fibrous cap thickness for the groups ($p>0.05$).

Severity of Abdominal Aortic Atherosclerosis

The animals that had severe coronary disease also had an average intimal area of 6.6 ± 5.4 mm^2 in the proximal half of the abdominal aorta, and therefore had severe aortic atherosclerosis (Table 2.3). They also had an average of 59.4 ± 21.3 % surface area in the proximal half covered by raised lesions, and therefore had diffuse disease (Table 2.4). The pigs with moderate disease had a significantly lower ($p = 0.003$) percent surface area covered by raised lesions in the proximal half (23.0 ± 8.5%, Table 2.4). Likewise, the intimal area was significantly less ($p = 0.034$) than the severe atherosclerosis group (2.5 ± 4.1 compared to 6.6 ± 5.4 mm^2). The

pigs with severe atherosclerosis also had significantly greater intimal area as a percent of medial area for the proximal half of the abdominal aorta compared to the moderate group (Table 2.3, 16.8 ± 9.2 compared to 7.0 ± 11.8, $p = 0.027$). Differences between the groups for the distal half of the abdominal aorta tended to be absent or less evident than those for the proximal half.

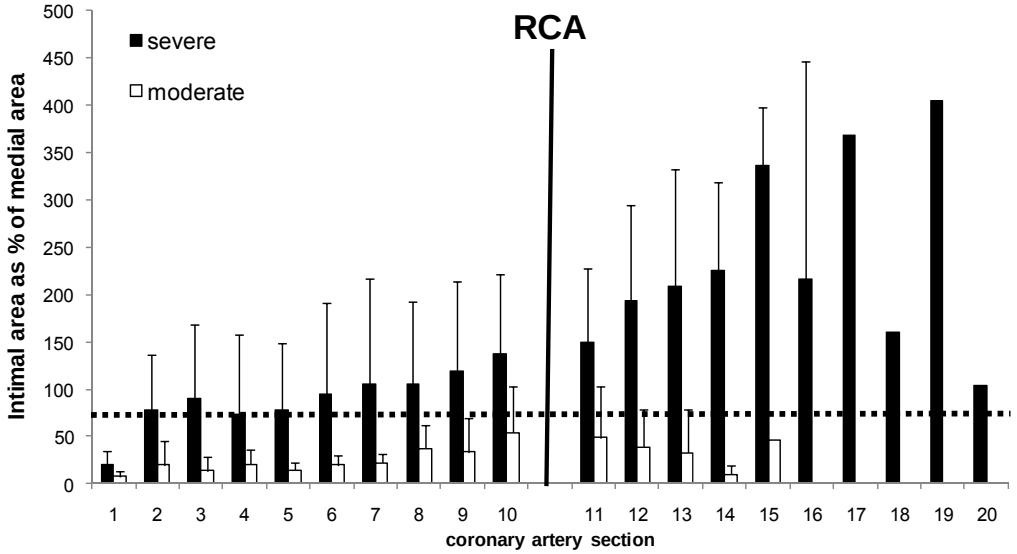
RCA
severe
moderate
Intimal area as % of medial area
500
450
400
350
300
250
200
150
100
50
0
1 2 3 4 5 6 7 8 9 10 11 12 13 14 15 16 17 18 19 20
coronary artery section

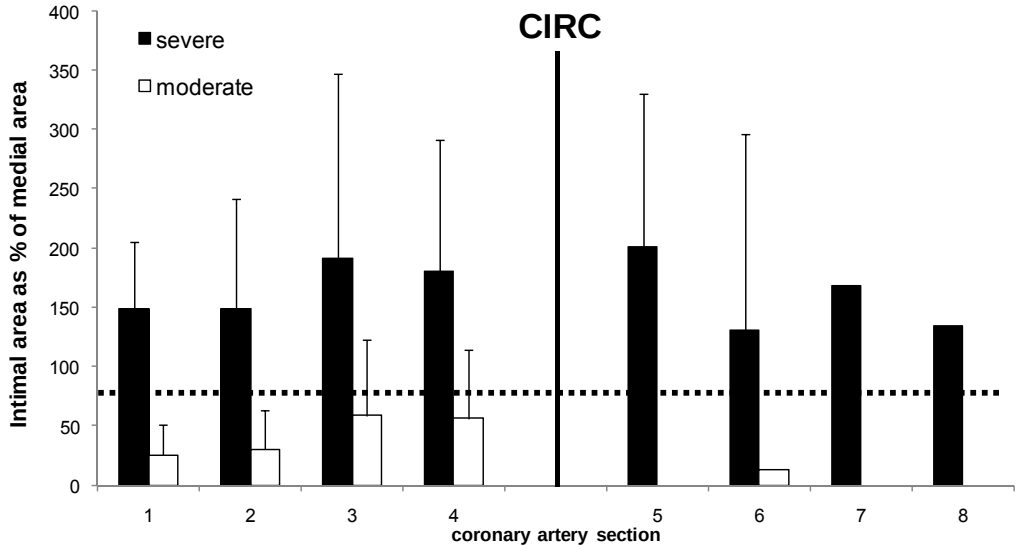
CIRC
severe
moderate
Intimal area as % of medial area
400
350
300
250
200
150
100
50
0
1 2 3 4 5 6 7 8
coronary artery section

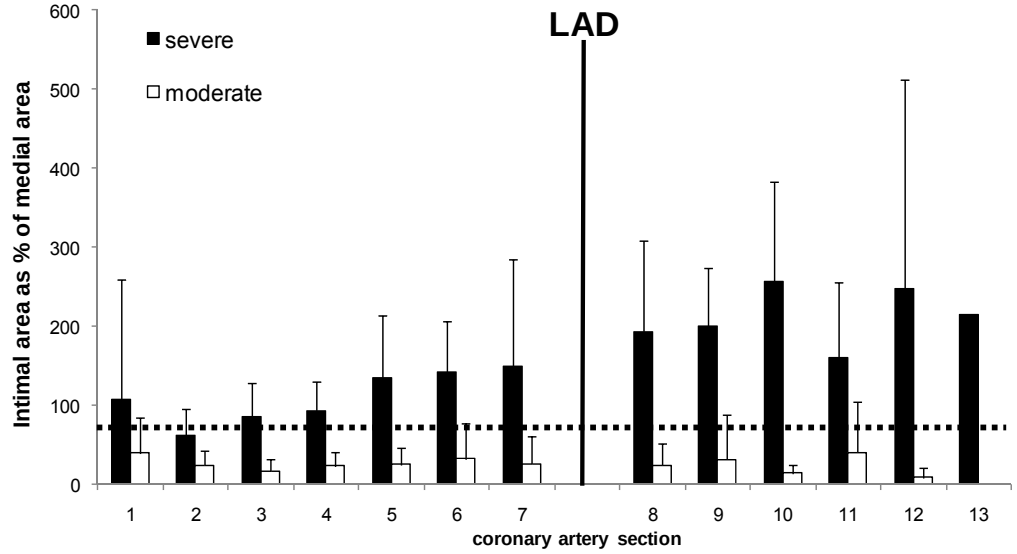
LAD
severe
moderate
Intimal area as % of medial area
600
500
400
300
200
100
0
1 2 3 4 5 6 7 8 9 10 11 12 13
coronary artery section

Figure 2.1. Intimal Area as % Medial Area from Serial Coronary Artery Sections. The mean ± SD for intimal area as % medial area of all sections from all three coronary arteries are shown by severe (black) or moderate (white) atherosclerosis phenotypes. Sections were taken at 1 cm intervals. The solid black vertical line indicates the division between the proximal and distal halves of each coronary artery. The horizontal dashed line = 75%, the criteria for severe coronary atherosclerosis. The presence of lesions with a value of ≥ 75% over 3 sections (i.e., 2 cm) in the distal half was defined as severe and diffuse distal disease. Using this definition, pigs in the severe atherosclerosis group exhibited severe and diffuse distal coronary atherosclerosis in all three coronary arteries.

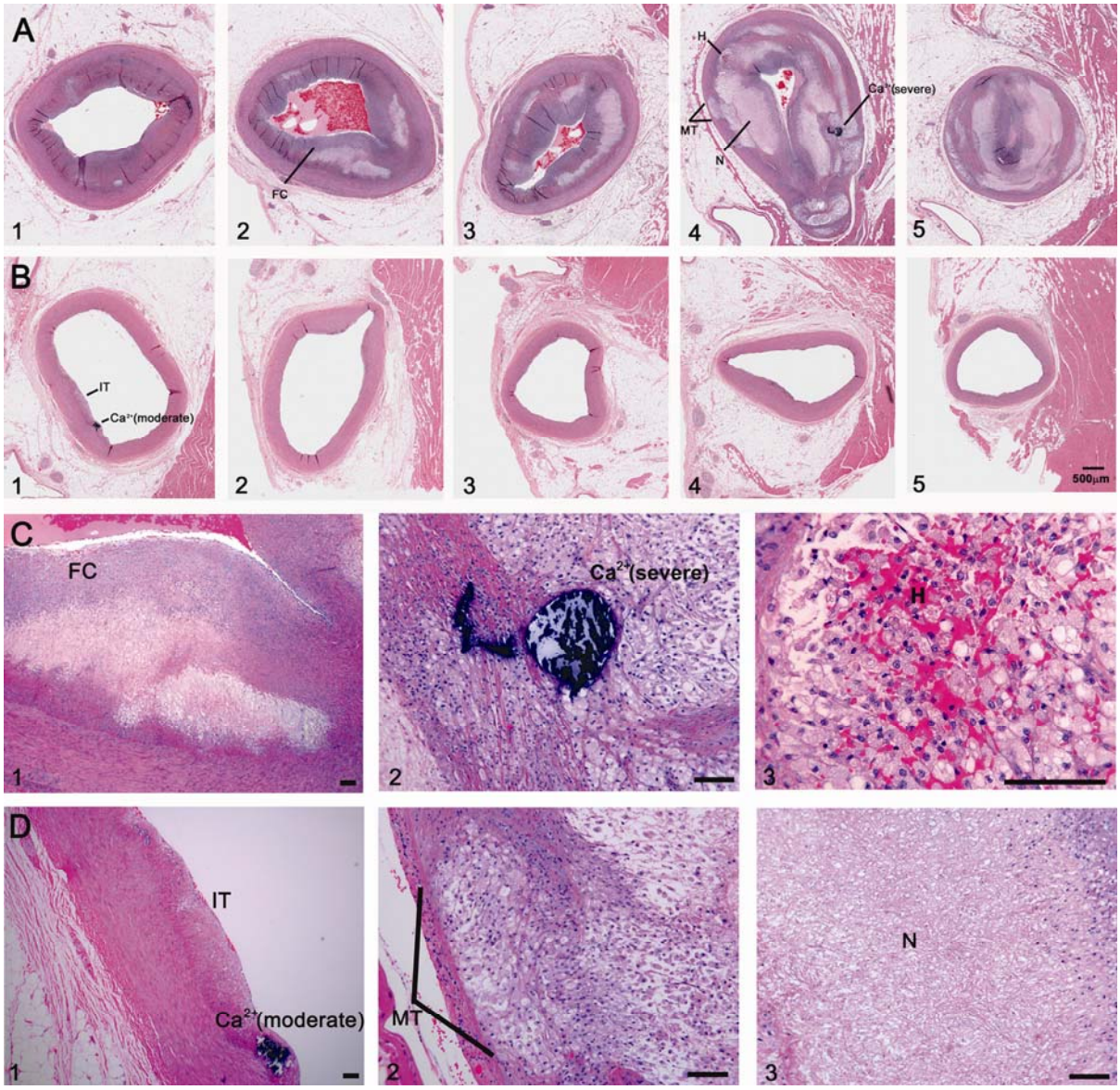
A
1
2
FC
3
4
H
MT
N
Ca2+(severe)
5
B
IT
Ca2+(moderate)
1
2
3
4
5
500μm
C
FC
1
Ca2+(severe)
2
H
3
D
IT
Ca2+(moderate)
1
MT
2
N
3

Figure 2.2. Coronary Artery Atherosclerosis in Insulin Resistant Pigs. Panels A1 to A5: Representative serial sections from the proximal to distal left anterior descending coronary artery are shown from an IR pig with severe and diffuse distal coronary atherosclerosis. The mean intimal area as a percent of medial area for all three coronary arteries for this pig (35G) was 203.9% proximally and 338.5% distally. Panels B1 to B5: In contrast, a pig (05I) with moderate coronary atherosclerosis had a mean intimal area as a percent of medial area for all three coronary arteries of 11.3% proximally and 5.8% distally. Features of coronary atherosclerosis in rows A and B are shown at higher magnification in rows C and D, respectively: intimal thickening (IT) and calcification in a pig with moderate atherosclerosis (Ca^{2+} (moderate), Panels B1 and D1), calcification in a pig with severe atherosclerosis (Ca^{2+} (severe), Panels A4 and C2), fibrous cap (FC, Panel A2 and C1), hemorrhage into the plaque (H, Panels A4 and C3), medial thinning (MT, Panels A4 and D2), necrosis (N, Panels A4 and D3). (Hematoxylin and Eosin, mag bar = 500 μm is shown in B5 for rows A and B; mag bar = 10 μm in all panels in rows C and D).

Table 2.1. Proximal and Distal Coronary Artery Atherosclerosis Morphometry in IR Pigs

	Severe Atherosclerosis (n = 9)	**Moderate** Atherosclerosis (n = 9)	p*
Proximal Coronary Arteries			
Medial area (mm^2)	7.8 ± 1.2	7.1 ± 2.4	0.480
Intimal area (mm^2)	5.9 ± 2.2	1.6 ± 1.4	0.001
% stenosis	60.7 ± 11.3	23.2 ± 13.8	< 0.001
Intimal area as % medial area	98.0 ± 47.2	21.9 ± 14.5	< 0.001
Distal Coronary Arteries			
Medial area (mm^2)	3.8 ± 1.1	3.3 ± 1.5	0.380
Intimal area (mm^2)	6.3 ± 2.4	1.3 ± 1.0	< 0.001
% stenosis	83.3 ± 6.4	32.4 ± 19.1	< 0.001
Intimal area as % medial area	185.5 ± 73.6	36.2 ± 22.5	< 0.001

* Wilcoxon rank sum statistic for differences between groups

Table 2.2. Mean Coronary Artery Total IEL Area (mm^2), Percent of Coronary Artery Cross Sections Containing Fibrous Caps, and Fibrous Cap Thickness (mm) in IR Pigs

	Severe Atherosclerosis (n = 9)	**Moderate** Atherosclerosis (n = 9)	p†
Right			
Total IEL area	8.62 ± 2.12	5.30 ± 1.60	0.008
% with Fibrous Cap	74.1 ± 17.1	21.3 ± 17.1	0.001
Fibrous Cap Thickness	0.591 ± 0.168	0.412 ± 0.165 (n = 8)*	0.06
Circumflex			
Total IEL area	7.39 ± 2.55	3.86 ± 1.89	0.008
% with Fibrous Cap	90.0 ± 15.6	32.4 ± 39.8	0.006
Fibrous Cap Thickness	0.658 ± 0.241	0.442 ± 0.271 (n = 5)*	0.35
Left Anterior Descending			
Total IEL area	8.64 ± 2.25	4.84 ± 2.71	0.006
% with Fibrous Cap	83.6 ± 17.8	22.2 ± 32.3	0.002
Fibrous Cap Thickness	0.461 ± 0.096	0.322 ± 0.140 (n = 5)*	0.11

* The difference in "n" values for Fibrous Cap Thickness reflects the absence of detectible fibrous caps in the respective artery from a given pig.
†Wilcoxon rank sum statistic for differences between groups

Table 2.3. Proximal and Distal Abdominal Aortic Atherosclerosis Morphometry in IR Pigs

Histomorphometry	**Severe** Atherosclerosis (n = 9)	**Moderate** Atherosclerosis (n = 9)	p*
Proximal Half Abdominal Aorta			
Medial area (mm^2)	35.0 ± 13.2	36.9 ± 9.7	0.427
Intimal area (mm^2)	6.6 ± 5.4	2.5 ± 4.1	0.034
Intimal area as % medial area	16.8 ± 9.2	7.0 ± 11.8	0.027
Distal Half Abdominal Aorta			
Medial area (mm^2)	40.1 ± 14.8	33.4 ± 9.5	0.427
Intimal area (mm^2)	8.0 ± 4.4	4.4 ± 4.9	0.052
Intimal area as % medial area	19.2 ± 8.2	12.7 ± 14.1	0.064

* Wilcoxon rank sum statistic for differences between groups

Table 2.4. Proximal and Distal Abdominal Aortic Atherosclerosis Morphometry in IR Pigs

En Face Measurements	**Severe** Atherosclerosis (n = 9)	**Moderate** Atherosclerosis (n = 9)	p*
Proximal Half Abdominal Aorta			
Total aortic surface area (cm^2)	15.9 ± 2.9	15.0 ± 3.6	0.536
Area with raised lesion (cm^2)	9.7 ± 4.6	3.5 ± 1.6	0.005
% aortic surface with raised lesions	59.4 ± 21.3	23.0 ± 8.5	0.003
Distal Half Abdominal Aorta			
Total aortic surface area (cm^2)	15.3 ± 3.9	15.0 ± 4.1	0.791
Area with raised lesion (cm^2)	11.0 ± 4.7	7.9 ± 4.2	0.216
% aortic surface with raised lesions	68.9 ± 16.0	51.0 ± 18.8	0.077

* Wilcoxon rank sum statistic for differences between groups

Change in Fasting Glucose, Insulin, and Insulin Sensitivity by Bergman FSIVGTT, and Serum Fructosamine Levels during the Year Long Study

Throughout the study, fasting glucose values in conscious pigs did not change significantly (Table 2.5). In contrast, when the pigs were sedated for the Bergman FSIVGTT, the glucose values were higher, possibly due to the stress of the procedure or the sedatives used (Table 2.6).[84, 85] Fasting insulin values measured during the Bergman FSIVGTT were higher at 3 ($p = 0.05$) and 12 ($p = 0.01$) months when compared to baseline values for the severe atherosclerosis group, whereas the moderate group showed little or no evidence of change (Table 2.6). Fasting glucose during the Bergman FSIVGTT was significantly elevated at 12 months compared to baseline in the severe group ($p = 0.01$) but had no evidence of change in the moderate group. The mean S_i values decreased significantly in all pigs at 6 and 12 months consistent with increased insulin resistance ($p = 0.023$ and 0.004 for the severe atherosclerosis group, and $p = 0.047$ and 0.008 for the moderate atherosclerosis group compared to baseline, respectively). There was little or no evidence of differences in mean fasting glucose, insulin or S_i values during the Bergman FSIVGTT between the severe and moderate atherosclerosis groups at any time point (Table 2.6, $p > 0.05$). With adjustments for baseline, such absence of differences for all time points had further confirmation from the repeated measures ANCOVA ($p= 0.764$ for fasting insulin, $p= 0.616$ for fasting glucose, and $p= 0.351$ for Bergman FSIVGTT, with each as logarithms).

The serum fructosamine levels were similar at baseline for the moderate and severe groups ($p=0.566$). They increased significantly at 3, 6, and 12 months

compared to baseline in the group that developed severe atherosclerosis (Table 2.7, $p < 0.05$). There was no evidence of change in the group with moderate atherosclerosis. Accordingly, the serum fructosamine level was significantly higher at 6 months in the severe group when compared to the moderate atherosclerosis group ($p< 0.001$); moreover, with adjustment for baseline, the repeated measures ANCOVA indicated that serum fructosamine levels for the severe group comparably exceeded those for the moderate group by an average of 0.227 mmol/L or ~15% at all post-baseline determinations ($p<0.001$, 95% CI (0.113, 0.340)).

Table 2.5. Fasting Glucose in Conscious IR Pigs on the Year Long Study

	Severe Atherosclerosis (n = 9)	**Moderate** Atherosclerosis (n = 9*)
Fasting Glucose (mg/dl)		
Month: 1	75 ± 6	73 ± 8
2	76 ± 6	73 ± 6
4	77 ± 4	74 ± 9
5	72 ±7	76 ± 13
7	77 ± 7	72 ± 5
8	76 ± 9	73 ± 11
9	72 ± 5	79 ± 15
10	74 ± 6	75 ± 11
11	73 ± 4	76 ± 8

*One pig was euthanized due to inappetance at 6 months, thus n = 8 for months 7 to 12.

Table 2.6. Fasting Insulin and Fasting Glucose Values in IR Pigs While Sedated For Bergman S_i Measurements during 12 Month Study

	Severe Atherosclerosis (n = 9)		**Moderate** Atherosclerosis (n = 9†)	
Fasting Insulin (µU/ml)		p*		p*
Baseline	10.0 ± 3.6		16.6 ± 12.3	
3 month	14.3 ± 6.6	0.05	16.0 ± 4.5	0.84
6 month	15.6 ± 15.3	0.25	17.4 ± 9.0	0.82
12 month	16.8 ± 7.1	0.01	17.9 ± 7.4	0.08
Fasting Glucose (mg/dl)				
Baseline	102.6 ± 19.3		120.2 ± 24.0	
3 month	109.7 ± 38.2	0.82	112.7 ± 12.9	0.65
6 month	115.0 ± 42.4	0.57	115.0 ± 38.4	0.91
12 month	126.0 ± 29.5	0.01	119.0 ± 20.0	0.55
Bergman S_i				
Baseline	4.0 ± 0.5		3.8 ± 0.3	
3 month	3.8 ± 0.5	0.109	3.6 ± 0.4	0.063
6 month	3.7 ± 0.6	0.023	3.5 ± 0.5	0.047
12 month	3.4 ± 0.5	0.004	3.4 ± 0.3	0.008

* Wilcoxon signed rank statistic for change from baseline within group.
p>0.05, Wilcoxon rank sum statistic for differences between groups at all time points
†One pig was euthanized due to inappetance at 6 months, thus n = 8 for month 12.

Table 2.7. Fasting Fructosamine Values in IR Pigs

Fasting Fructosamine (mmol/L)	**Severe** Atherosclerosis (n = 9)	p*	**Moderate** Atherosclerosis (n = 9[§])	p*
Baseline	1.47 ± 0.17		1.45 ± 0.24	
3 month	1.77 ± 0.17[‡]	0.004	1.61 ± 0.21[‡]	0.07
6 month	1.82 ± 0.14†[‡]	0.004	1.45 ± 0.15†[‡]	0.59
12 month	1.60 ± 0.19[‡]	0.027	1.43 ± 0.17[‡]	0.74

*Wilcoxon signed rank statistic for change from baseline within group
† p<0.001, Wilcoxon rank sum statistic for differences between groups.
‡ p<0.001, ANCOVA
§ One pig was euthanized due to inappetance at 6 months, thus n = 8 at 12 months.

Change in Weight, Backfat, and Blood Pressure during Year Long Study

The baseline, 3, 6, and 12 month weight and backfat values and blood pressure values are shown in Tables 2.8 and 2.9, respectively. Weight increased significantly over time compared to baseline in the moderate atherosclerosis group ($p < 0.05$) and there were trends for increases in the severe group ($p \leq 0.10$). Backfat increased significantly in both groups by 12 months ($p < 0.05$). There was no evidence of differences between the two groups for weight or backfat at study entry, nor at any of the time points ($p \geq 0.05$). With adjustments for baseline, such absence of differences for all time points had further confirmation from the repeated measures ANCOVA ($p= 0.316$ for weight, $p= 0.609$ for backfat).

Blood pressure was in a range that would be considered mildly hypertensive in humans with no evidence of differences between the two groups (Table 2.9). Blood pressure had little or no evidence for increase over time in either group except diastole at 12 months in the moderate group ($p = 0.03$). With adjustments for baseline, such absence of differences for all time points had further confirmation from the repeated measures ANCOVA ($p=0.671$ for systolic, $p=0.659$ for diastolic, $p=0.728$ for MAP, and $p=0.506$ for pulse).

Table 2.8. Weight and Backfat in IR Pigs on Year Long Study

	Severe Atherosclerosis‡	**Moderate** Atherosclerosis‡
Weight (lb)	(n = 9)	(n = 9)
Baseline	489 ± 66	491 ± 53
3 month	527 ± 80*	536 ± 74†
6 month	545 ± 79*	582 ± 71†
12 month	594 ± 115*	643 ± 76†
Backfat (cm)	(n = 7)	(n = 8)
Baseline	8.1 ± 1.1	6.2 ± 2.1
3 month	8.4 ±1.0	7.3 ± 1.4†
6 month	9.0 ± 1.3	7.9 ± 0.9†
12 month	9.6 ± 1.1†	8.9 ± 1.0†

* $p \geq 0.05$, Wilcoxon signed rank statistic for change from baseline within group
† $p \leq 0.05$, Wilcoxon signed rank statistic for change from baseline within group
‡ $p > 0.05$, Wilcoxon rank sum statistic for differences between groups
Data are listed for pigs for which there was a complete 12 month data set except for one pig with moderate atherosclerosis that was euthanized at 6 months due to inappetance.

Table 2.9. Arterial Blood Pressure (mm Hg) in IR Pigs on the Year Long Study

	Severe Atherosclerosis (n = 7)	**Moderate** Atherosclerosis (n = 8)
Systolic		
Baseline	142 ± 27	135 ± 19
3 month	147 ± 14	139 ± 20
6 month	153 ± 28	148 ± 24
12 month	146 ± 17	145 ± 23
Diastolic		
Baseline	96 ± 21	83 ± 13
3 month	96 ± 14	91 ± 20
6 month	110 ± 32	98 ± 18
12 month	103 ± 16	97 ± 22
MAP*		
Baseline	113 ± 25	103 ± 15
3 month	119 ± 15	114 ± 20
6 month	127 ± 32	119 ± 22
12 month	118 ± 18	115 ± 23
Pulse		
Baseline	96 ± 16	94 ± 23
3 month	105 ± 17	96 ± 17
6 month	109 ± 9	94 ± 29
12 month	93 ± 12	100 ± 17

*MAP = mean arterial pressure

p>0.05, Wilcoxon signed rank statistic for change from baseline at all time points for all values except diastole at 12 months for which p = 0.03 in the moderate atherosclerosis group.

p≥0.09, Wilcoxon rank sum statistic for differences between groups at all time points

Data are listed for pigs for which there was a complete 12 month data set except for one pig with moderate atherosclerosis that was euthanized at 6 months due to inappetance.

Total, LDL, and HDL Cholesterol and Triglyceride Levels

Fasting total and LDL and HDL cholesterol and triglyceride values were similar for the moderate and severe groups at study entry (Table 2.10). Fasting total and LDL and HDL cholesterol increased significantly at 3, 6, and 12 months relative to baseline values within groups ($p < 0.05$) but triglycerides had no evidence of change ($p > 0.05$). There was no evidence of differences between the moderate and severe groups at 3, 6, or 12 months ($p \geq 0.100$). With adjustments for baseline, such absence of differences at all time points had further confirmation from the repeated measures ANCOVA ($p = 0.153$ for total cholesterol, $p = 0.186$ for LDL cholesterol, and $p = 0.175$ for HDL cholesterol, $p = 0.194$ for triglycerides, with each as logarithms).

Table 2.10. Fasting Total, LDL, and HDL Cholesterol and Triglycerides in IR Pigs on Year Long Study

	Severe Atherosclerosis† (n = 9)	**Moderate** Atherosclerosis† (n = 9 ‡)
Total cholesterol (mg/dl)		
Baseline	82 ± 23	73 ± 12
3 month	476 ± 177*	386 ± 113*
6 month	422 ± 148*	305 ± 108*
12 month	372 ± 66*	336 ± 76*
LDL cholesterol (mg/dl)		
Baseline	45.0 ± 15.8	40.0 ± 11.3
3 month	213.1± 68.9*	176.1 ± 49.6*
6 month	184.8 ± 45.3*	144.4 ± 50.1*
12 month	160.5 ± 27.1*	141.3 ± 24.2*
HDL cholesterol (mg/dl)		
Baseline	32.5 ± 9.8	29.2 ± 6.0
3 month	101.7 ± 31.1*	79.6 ± 27.6*
6 month	82.7 ± 22.7*	79.7 ± 30.8*
12 month	72.0 ± 23.4*	84.7 ± 15.8*
Triglycerides (mg/dl)		
Baseline	24 ± 9	23 ± 7
3 month	31 ± 13	24 ± 13
6 month	31 ± 20	20 ± 15
12 month	29 ± 12	22 ± 13

*p<0.05, Wilcoxon signed rank statistic for change from baseline within group
† p ≥0.10, Wilcoxon rank sum statistic for differences between groups
‡ One pig in this group was euthanized due to inappetance at 6 months, thus n = 8 for month 12.

Changes in Oxidized LDL

The mean oxLDL levels were similar for the moderate and severe groups at baseline ($p = 0.724$, Table 2.11). The values increased significantly relative to the baseline at 3, 6, and 12 months in both groups ($p < 0.01$). OxLDL was significantly greater in the severe atherosclerosis group at 6 months ($p = 0.008$) and trends for increases at 12 months ($p=0.061$). Moreover, with adjustment for baseline, the repeated measures ANCOVA (for logarithms) indicated that oxLDL levels for the severe group comparably exceeded those for the moderate group by an average of 14.6% at all post-baseline determinations ($p=0.025$, 95% CI (1.9, 28.8)). Thus, oxLDL was found to be more sensitive to differences in atherosclerosis between groups than LDL cholesterol, but an independent effect beyond that of total LDL could not be identified.

Table 2.11. oxLDL Levels (units/L) in IR Pigs on Year Long Study

	Severe Atherosclerosis (n = 9)	**Moderate** Atherosclerosis (n = 9[§])	p[†]
oxLDL (units/L)			
Baseline	21.74 ± 2.42	21.19 ± 2.43	0.724
3 month	32.59 ± 5.44*[‡]	31.46 ± 7.02*[‡]	0.596
6 month	35.75 ± 6.33*[‡]	27.91 ± 5.20*[‡]	0.008
12 month	35.61 ± 4.37*[‡]	30.34 ± 6.39*[‡]	0.061

*p≤0.01, Wilcoxon signed rank statistic for change from baseline within group
[†] Wilcoxon rank sum statistic for differences between groups
[‡]p = 0.025, ANCOVA
[§]One pig was euthanized due to inappetance at 6 months thus n = 8 at 12 months.

Changes in Aldosterone

The mean aldosterone levels were similar for the moderate and severe groups at baseline (p=0.48, Table 2.12). The values did not increase in the group with moderate atherosclerosis whereas with severe disease there was a highly significant increase above baseline values. With adjustment for baseline, the repeated measures ANCOVA (for logarithms) indicated that aldosterone levels for pigs that developed severe atherosclerosis comparably exceeded those for pigs with moderate atherosclerosis by an average of 47.4% at all post-baseline determinations (p=0.023, 95% CI (6.0, 105.1)). Serum potassium and sodium levels were assayed monthly and remained within the normal range (not shown).

Table 2.12. Fasting Aldosterone Values in IR Pigs

	Severe Atherosclerosis (n = 9)	**Moderate** Atherosclerosis (n = 9 ‡)
Aldosterone (pg/ml)		
Baseline	149.9 ± 109.1	176.2 ± 117.4
3 month	170.2 ± 96.7*†	148.8 ± 90.0†
6 month	177.7 ± 77.1*†	131.2 ± 64.3†
12 month	212.2 ± 66.6*†	155.0 ± 87.0†

*p<0.05 for increase from baseline (ANCOVA)
† p = 0.023, ANCOVA
‡One pig in this group was euthanized due to inappetance at 6 months, thus n = 8 for month 12.

Change in Inflammatory Markers during Year Long Study

The inflammatory markers had no evidence of differences between the moderate and severe groups when the mean values are compared at all time points during the 12 month study (Table 2.13, $p \geq 0.05$). The inflammatory marker TNF-alpha was significantly increased from baseline in the severe atherosclerosis group at 3 and 12 months ($p < 0.05$). IL-6 had no evidence of change within either group. PAI-1 increased significantly in both groups at 3 months and in the moderate atherosclerosis group at 6 months ($p < 0.05$). CRP increased significantly in the group that developed moderate atherosclerosis at 3 months ($p < 0.05$) and exhibited a trend at 12 months ($p = 0.06$). With adjustments for baseline, the absence of differences between the moderate and severe groups for the inflammatory markers at all time points had further confirmation from the repeated measures ANCOVA ($p=0.138$ for TNF-alpha, $p=0.411$ for IL-6, $p= 0.288$ for PAI-1, and $p= 0.846$ for CRP, with each as logarithms).

Table 2.13. Inflammatory Markers in IR Pigs on Year Long Study

	Severe Atherosclerosis (n = 9)	**Moderate** Atherosclerosis (n = 9 †)
TNF-alpha (pg/ml)		
Baseline	24.2 ± 35.2	32.8 ± 29.9
3 month	84.9 ± 88.6*	66.0 ± 84.8
6 month	35.0 ± 38.1	50.3 ± 43.0
12 month	96.5 ± 119.7*	50.1 ± 52.8
IL-6 (pg/ml)		
Baseline	31.0 ± 92.9	10.0 ± 15.4
3 month	20.9 ± 56.5	37.4 ± 42.3
6 month	37.2 ± 73.9	ND
12 month	35.3 ± 62.3	16.0 ± 29.7
PAI-1 (ng/ml)		
Baseline	3.7 ± 4.1	2.2 ± 3.9
3 month	9.2 ± 8.1*	7.0 ± 4.3*
6 month	3.7 ± 3.0	4.0 ± 4.7*
12 month	1.5 ± 1.3	2.9 ± 5.3
CRP (µg/ml)		
Baseline	10.7 ± 11.5	4.3 ± 2.3
3 month	10.0 ± 9.4	14.4 ± 19.8*
6 month	10.9 ± 7.2	8.2 ± 9.7
12 month	13.5 ± 14.3	7.7 ± 3.6

ND = not detected
$p>0.05$, Wilcoxon rank sum statistic for differences between groups at all time points for all markers.
*$p \leq 0.05$, Wilcoxon signed rank statistic when compared to baseline within group.
†One pig was euthanized due to inappetance at 6 months, thus n=8 for month 12.

Discussion

The study shows that 18 adult pigs fed a high fat diet with increased NaCl exhibited a significant increase in IR that was accompanied by comparable weight gain, increased backfat, elevation in total and LDL and HDL cholesterol levels, blood pressure, and inflammatory markers. Those pigs that exhibited more severe as well as diffuse distal coronary artery and proximal abdominal aortic atherosclerosis had significant increases in fructosamine and aldosterone levels during the study. Both groups had significant increases in oxLDL but the degree of increase was significantly greater in the group of animals with severe and diffuse disease. Although all animals developed increased IR during the study, the severity of IR did not correlate with the severity of atherosclerosis. Since none of the IR pigs had diabetes, it appears that severe and diffuse atherosclerosis can develop in response to a high fat/high NaCl diet in the absence of overt hyperglycemia but in association with increased oxLDL, fructosamine, and aldosterone levels consistent with increased oxidative stress. These findings suggest that this degree of IR is not sufficient by itself to increase atherosclerosis severity in this model. Definitive proof of a single mechanism that predisposes to severe atherosclerosis among these parameters, the determination of whether or not these parameters are additive or synergistic, or the establishment of a hierarchy among them is beyond the scope of this work.

Insulin Resistance

Although fully manifested diabetes mellitus confers a greater risk for

cardiovascular disease and other complications as compared to isolated IR without hyperglycemia, the presence of IR is a major independent risk factor with relative risk ratios between 2.2 and 2.7 when multifactorial linear regression analysis is utilized to assess risk.[25, 86, 87] Thus, both IR and hyperglycemia appear to independently confer additional vascular disease risk. The manner in which the hyperinsulinemic state or the loss of insulin sensitivity leads to increased atherosclerosis remains poorly defined. In addition to increased oxidative stress, changes in markers of vascular inflammation that are related to changes in fat mass, changes in lipoprotein metabolism, and altered sensitivity of vascular cell types to other hormones such as angiotensin II have been proposed as mechanisms. Additionally the presence of IR is associated with hypertension, lipoprotein abnormalities, and chronic kidney disease that further accentuate atherosclerosis risk.[88-93]

Our IR pigs had elevated glucose levels during the Bergman FSIVGTT when sedated but not when fully conscious (Tables 2.5 and 2.6). It is possible that the sedatives used in these pigs contributed to the glucose elevations. Isoflurane has been shown to alter insulin sensitivity in pigs, possibly from direct drug effects as well as procedure-related stress.[84, 85] Importantly, since all S_i measurements were done with sedation and indicate a significant reduction in S_i, the reduction over 12 months is interpretable and was clearly progressive. In addition, studies have shown that stress induced hyperglycemia correlates with subsequent development of diabetes and that the subjects who were predisposed to develop glucose intolerance during the FSIVGTT had higher fructosamine levels at baseline (see

discussion on fructosamine below).[94] It is noteworthy that a group of insulin sensitive pigs (n = 6) fed regular pig chow in other studies exhibited a range of mean S_i values from 4.5 ± 0.6 to 4.8±0.6 and range of mean glucose values of 75.4± 4.5 to 88 ± 13 mg/dl measured on samples drawn using the same sedation protocol (data not shown). Therefore, it is probable that feeding the high fat/high NaCl diet induced some degree of glucose intolerance that was detectible during stress.

Fructosamine

Fructosamine is used as an index of mean blood glucose in pigs since pig red blood cells are relatively impermeable to glucose and thus hemoglobin A1c is not a reliable index of mean glucose concentrations.[95] In our study, the fructosamine levels measured during the fasting state rose relative to baseline values in the group of animals that developed severe and diffuse disease but the levels were not elevated to a point that they would reflect significant and/or sustained hyperglycemia.

Fructosamine has also been shown to correlate with 2 hr postprandial glucose[96] and relatively short periods of hyperglycemia have been shown to increase protein glycation even if fasting glucose is not increased.[97] In general most reports have compared the degree of fructosamine change that occurs with impaired glucose tolerance to subjects with normal glucose tolerance and correlated this with a change in atherosclerotic risk. Studies in experimental animal models have reported increases in fructosamine over the range noted in our animals as being associated with biochemical changes that are believed to predispose to

increase risk of atherosclerosis and some studies have demonstrated an increase in lesion formation.[98] However, studies in which fructosamine changes alone predispose to increased risk have not been reported. Presumably the increase in fructosamine in the group of pigs with severe atherosclerosis reflects modest increase in mean daily glucose levels, although periods of post prandial hyperglycemia of short duration cannot be excluded. Regardless of the cause, the degree of increase was significantly greater than the change that occurred in the group with moderate atherosclerosis. Therefore, it is possible that even this modest change (0.227 mmol/L or ~15%) in fructosamine reflects a contribution of increased mean glucose values to increased oxidative stress and on lesion development.

oxLDL

Increases in oxidized LDL in humans, pigs, and rodents correlate with increased atherosclerosis and reduction in oxLDL correlates with reduced atherosclerosis.[96, 99-104] In our study, the increase in oxLDL was probably due in part to increases in total cholesterol in both groups although increases in glycated proteins as reflected by fructosamine in the group with severe atherosclerosis may have contributed to the greater degree of increase in oxLDL in that group. The animals with increased fructosamine had greater increases in oxidized LDL compared to total LDL suggesting that the change in fructosamine may have been a significant component of the change in oxLDL, thus leading to a more severe atherosclerosis phenotype.

In humans increased glycemic index correlates with increased oxLDL when

total LDL remains unchanged.[99, 105-107] Also, reductions in fat mass, dietary fat, and blood glucose have been shown to be associated with decreases in oxLDL.[108-111] More modest increases in postprandial glucoses in subjects with impaired glucose tolerance can also lead to increases in oxLDL[112-115] and treatment in those subjects also lowers oxLDL.[116-119] A few studies have reported increases in oxLDL in nondiabetic subjects with impaired glucose tolerance[120-122] and one reported a correlation between oxLDL in normal subjects with higher fructosamine.[120] Moreover, even small increases in postprandial glucose that are within the normal range can lead to increases in oxidized LDL[99, 123] and small reductions in postprandial glucose in patients with type 2 diabetes also lead to decreased oxidized LDL.[99, 123] Since oxidized LDL was increased in our animals with severe atherosclerosis, it is possible that increases in their postprandial glucoses were sufficient to contribute to the increased LDL oxidation to levels that were greater than the group of animals that tended to have slight or no changes in fructosamine.

Aldosterone

The significant increase in aldosterone in pigs with severe atherosclerosis is consistent with the suspected role of the renin-angiotensin-aldosterone system (RAAS) in insulin resistance, oxidative stress, and severity of atherogenesis.[124] Activation of the RAAS system has been associated with increased reactive oxygen species formation. In statistical models that controlled for oxLDL or fructosamine and baseline levels (i.e., change over time), gender, and atherosclerosis severity,

pigs with severe atherosclerosis had significantly higher aldosterone levels ($p<0.05$, ANCOVA). This result suggests that the increased aldosterone levels may have contributed to the increased oxLDL in the pigs with severe atherosclerosis. Also, pigs with increased aldosterone levels did not have higher blood pressure than those with lower aldosterone levels. While this finding seems counterintuitive, the experimental cholesterol ester transfer protein (CETP) inhibitor torcetrapib increased aldosterone levels by a mechanism that did not explain the pressor effect of the drug.[125, 126] Thus, significant elevations in aldosterone do not predictably increase blood pressure but can still contribute to increases in oxidative stress.

Inflammatory Markers

TNF-alpha, IL-6, PAI-1, and CRP were not significantly different between groups. In some cases, these values were significantly increased over baseline values but this was an inconsistent finding. Thus, these values do not appear to be robust markers of IR or atherosclerosis in this model.

Atherosclerosis Morphology in Insulin Resistance

Coronary artery atherosclerosis in the IR pigs showed fibrous cap formation, foam cells, medial thinning, plaque hemorrhage, necrosis, and calcification (Figure 2.2). All of these characteristics have been described in atherosclerotic plaques from IR and diabetic humans.[28, 30] Similar histological findings have been described in pigs given streptozotocin and fed a high fat diet.[49] An important characteristic is the presence of distal coronary atherosclerosis which has been a

consistent finding in asymptomatic IR and diabetic patients screened by electron beam computed tomography and magnetic resonance imaging,[27, 31] clinically symptomatic IR patients by quantitative angiography[29] and in type 2 diabetic patients who died suddenly.[28] Thick fibrous caps (>64 μm) are more common in coronary atherosclerotic plaques of humans with type 2 diabetes that died suddenly.[28] In our study, the fibrous caps were more abundant in pigs with severe atherosclerosis than those with moderate atherosclerosis. Clinical studies have reported an increase in remodeling in diabetic victims of sudden death.[28] The mean total IEL areas for serial sections in all 3 coronary arteries from IR pigs with severe atherosclerosis was larger than those with moderate atherosclerosis (Table 2.2). This finding is consistent with positive remodeling.[28, 82, 83] Thus, the atherosclerotic plaques in these IR pigs with severe disease exhibit several of the phenotypic characteristics that are found in IR humans.

Study Limitations

First, our study does not include an insulin sensitive control. This means we do not know how much atherosclerosis would develop in insulin sensitive pigs with a comparable degree and duration of hypercholesterolemia. Second, we do not know how much atherosclerosis would develop in insulin resistant pigs fed a low fat diet. However since the absolute level of insulin resistance was comparable in our two groups of animals, this parameter did not appear to account for the differences in disease severity. Nonetheless, it is probable that reducing insulin sensitivity contributed to the development of atherosclerosis that occurred in both groups of

animals. Third, we chose to measure parameters that have been associated with increased atherosclerosis severity in insulin resistant humans: blood pressure, body weight, body fat, hyperlipidemia, inflammatory markers, glycated proteins (i.e., fructosamine), oxLDL, and aldosterone. This study design addressed the extent to which each of these parameters, when measured at 4 time points, were associated with the severity of atherosclerosis that developed in pigs with comparable IR. The grouping of pigs by atherosclerosis severity was only possible after feeding the high fat diet for one year. Likewise, evaluating these parameters for association with atherosclerosis severity could only be done after the groups were identified. This post hoc grouping and analysis could be viewed as possibly introducing bias, although it is comparable to a ranking of the pigs as in a rank correlation statistical test. We have additionally addressed this possibility by analyzing changes over time with appropriate and validated statistical methods.[127] We may have inadvertently omitted other parameters that could be associated with atherosclerosis severity that could also be analyzed in a similar fashion.

Summary

Our goal was to develop a useful animal model of insulin resistance that also develops coronary and aortic atherosclerosis. Several investigators have used pigs to study the impact of diabetes on atherogenesis, most of which have used chemical induction of insulin-deficiency.[23, 48, 49, 128] In contrast, we used pigs that developed increased insulin resistance in association with weight gain, increasing backfat, increased total and LDL and HDL cholesterol levels, and comparable blood

pressure and changes in inflammatory markers. Our model has some features of the metabolic syndrome and a subgroup of animals developed more severe and diffuse atherosclerosis. The metabolic variables that predict this increase in disease severity are increases in fructosamine, oxidized LDL, and aldosterone. If these findings can be confirmed and the degree of glucose abnormality that is required to develop these changes be determined, then these animals should be useful for studying mechanisms of disease and for testing new therapeutic approaches.

Chapter 3

Gene Expression Profiles of Aortic Endothelium in Hyperlipidemic, Hyperinsulinemic Swine

Abstract

We have previously shown that fifty percent of adult insulin resistant pigs fed a high fat diet containing high NaCl developed severe and diffuse distal coronary atherosclerosis and severe and diffuse proximal abdominal aortic atherosclerosis. These pigs also had significantly higher oxLDL and greater increases in fructosamine and aldosterone values consistent with increased oxidative stress than the fifty percent with moderate atherosclerotic disease. Endothelial dysfunction is an early and critical step in atherosclerosis. OxLDL is known to cause changes in endothelial cells that alter endothelial barrier function. In the current study, we use gene expression profiles from normal and atherosclerotic endothelium of both the severe and moderate disease groups to identify potential molecular targets involved in oxidative stress (pathway for increased oxLDL), protein glycation, and/or the renin-angiotensin-aldosterone system. We identified three genes (*MERP-1, RABGAP1L, and COL12A1*) that were uniquely expressed in atherosclerotic endothelium of the severe group and one gene (*SERPINI1*) that was uniquely expressed in normal endothelium of the severe group. Overall comparison of the severe disease group to the moderate disease group identified genes involved in cell

adhesion, migration, and proliferation or transcription and translation that were either significantly up- (*PTPRM, FAM5C, CLOCK, MYCPBP, LPHN2*, *HIPK2*) or down (*TMSB4X, EIF2S3, JARID1C*) -regulated in the severe disease group. This study identifies potentially important genes for further investigation of the endothelial dysfunction seen in these pigs.

Introduction

Normal, healthy endothelium has numerous beneficial effects, including: promotion of vasodilation; antioxidant, anti-inflammatory, anticoagulant, and profibrinolytic effects; and inhibition of leukocyte adhesion and migration, smooth muscle cell proliferation and migration, and platelet aggregation and adhesion.[8] Endothelial dysfunction, while an early and potentially reversible step, can lead to the initiation and progression of atherosclerosis.

The progression of endothelium from normal to dysfunctional to atherosclerotic may parallel the progression of insulin resistance to overt diabetes.[10] Studies have shown that insulin resistance co-associates with other factors that lead to endothelial dysfunction, especially changes in lipoproteins.[11] Insulin works through both the phosphatidylinositol 3-kinase pathway to regulate endothelial nitric oxide (NO) production and as a growth factor through the mitogen activated protein kinase (MAPK) pathway to affect cell growth and movement, increase endothelial cell (EC) adhesion markers and mediate expression of certain prothrombotic factors.[11] Pathologic changes, such as increases in oxLDL and subsequent expression of TNF-α by macrophages, can lead to changes in endothelial gene expression. An initial change is an increase in leukocyte adhesion molecules on the surface of ECs. Other changes include an increase in inducible nitric oxide synthase and a decrease or suppression of endothelial nitric oxide synthase. Changes in gene expression continue as the underlying lesion progresses.

A study of changes in aortic EC gene expression from streptozotocin induced type-1 diabetic rats showed a significant number of up and down-regulated genes. Insulin treatment in these rats normalized about half of the genes, suggesting that levels of both glucose and insulin are important in EC gene expression and subsequent development of diabetic cardiovascular complications.[129] Likewise, studies of cultured human aortic endothelial cells subjected to high glucose had increases in eNOS gene expression.[130]

Novel insight into the molecular mechanisms underlying endothelial dysfunction and hence initiation and progression of atherosclerosis may be possible through gene expression studies. Seo *et al* used human aorta samples with varying degrees of atherosclerosis to establish gene expression profiles. Using the list of genes generated, they were able to predict disease burden and potential susceptibility to atherosclerosis related to anatomic location.[131] However, this study utilized RNA extracted from whole aortic tissue and may not be reflective of specific changes in the endothelium.

A recent study by our group looked at atherosclerosis severity in adult insulin resistant pigs (n=18) fed a high fat diet that also contained high NaCl (56% above recommended levels) for 1 year. Fifty percent of the pigs in this study developed severe and diffuse distal coronary atherosclerosis and severe and diffuse proximal abdominal aortic atherosclerosis. The other fifty percent had moderate atherosclerosis. There were comparable elevations in total and LDL and HDL cholesterol, weight gain, increase in backfat, blood pressure, and inflammatory markers, and increase in insulin resistance without overt diabetes between both

groups. There was no correlation between insulin resistance and the severity of atherosclerosis. Nonetheless, the pigs with severe atherosclerosis had significantly higher oxLDL and greater increases in fructosamine and aldosterone values consistent with increased oxidative stress than the pigs with moderate atherosclerosis.

In this paper, we used endothelium from both normal and atherosclerotic aortic of both groups of pigs (severe and moderate disease) in the previous study. Through microarray technology we identified both up and down-regulation of endothelial cell genes based on the severity of atherosclerosis or state of the endothelium. This approach should provide some insight into the patterns of gene expression, potentially from atherosclerosis initiation through progression to advanced disease. Special attention was paid to identifying genes that may be involved in endothelial dysfunction relating specifically to oxidative stress (pathway for increased oxLDL), protein glycation, and/or the renin-angiotensin-aldosterone system. Our long range goal is to develop novel methods for the noninvasive detection of endothelial dysfunction that occurs during atherogenesis in a relevant animal model.

Methods

Experimental Pigs

All pigs were treated according to the standards set in the Guide for Care and Use of Laboratory Animals (National Institutes of Health publication No. 85-23). All procedures and protocols were in accordance with institutional guidelines and approved by the Institutional Animal Care and Use Committee. All pigs were produced and maintained in the same environmental conditions at the Francis Owen Blood Research Laboratory at the University of North Carolina at Chapel Hill. Male and female pigs were from Spotted Poland/China and Yorkshire crosses. At study termination all pigs were euthanized with an overdose of pentobarbital (6 grains/ 10 lbs. IV).

Study design

Eighteen pigs were entered into the year-long study (11 males, 7 females). Aortic endothelium was only available from 10 pigs (6 males, 4 females); average age at start of study was 4.4 ± 2.1 years. Pigs from the following two genotypes were used: normocholesterolemic (n=7), and heterozygous familial hypercholesterolemic (FH) which are also normocholesterolemic at baseline (n=3). Neither normocholesterolemic nor heterozygous familial hypercholesterolemic pigs exhibit hypercholesterolemia unless they are fed a high fat diet. The animals were fed a high fat diet that consisted of pig chow (5NP8 Wayne™ 15% Pig & Sow Pellets, Granville Milling, Granville NC) supplemented with 1% cholesterol, 20% beef tallow, and 0.75% cholate by weight. The aortas of the pigs were collected at

euthanasia and placed on ice to minimize postmortem changes. Endothelium was collected from both normal and atherosclerotic abdominal aorta. Disease burden was segregated into two phenotypes, severe and moderate. Severe abdominal aortic atherosclerosis was defined as >50% of abdominal aorta with raised atherosclerosis lesions. By collecting both normal and atherosclerotic aortic endothelium from the same pig, a matched set of samples was then available for analysis.

Other variables were measured at baseline, 3, 6, and 12 months and included: weight, backfat, blood pressure, insulin sensitivity, fructosamine, total and LDL and HDL cholesterol, triglycerides, oxidized LDL, inflammatory makers, and aldosterone. For detailed methods used to measure each of these variables, see Chapter 1 – Methods section.

Endothelial Cell Isolation

RNase-free techniques, reagents, materials, and tools were used during all procedures. Porcine aortas were obtained from necropsy, and all endothelial cell isolations were performed immediately after necropsy on fresh tissue to minimize transcriptional changes and RNA degradation. Aortic endothelial RNA isolation was based on a method by Simmons et al[132], as follows. Immediately after necropsy, aortas were rinsed with diethyl pyrocarbonate (DEPC)-treated phosphate buffered saline (PBS). Aortas were then cut longitudinally, spread on a cutting surface with the orientation of the aorta luminal surface side up. A 12-mm #1 glass coverslip was dipped into isopentane on dry ice, blotted to remove excess isopentane and carefully

placed on the luminal surface so as to be in contact only with endothelial cells. The coverslip was pressed firmly with a cold aluminum rod (stored in isopentane on dry ice between uses) for 5-10 seconds (See Figure 3.1), which froze the endothelial layers to the glass coverslips. The circular surface area of the aluminum rod on the "pressed" end ensured wide contact of the endothelium with the coverslip. The coverslips with endothelial cells frozen to them were then gently peeled off and immediately placed/covered in lysis buffer for RNA extraction or in 4% paraformaldehyde for immunostaining. This procedure was repeated several times on each aorta and covered both raised lesions (atherosclerotic) and "normal" (non-atherosclerotic) aortic surfaces.

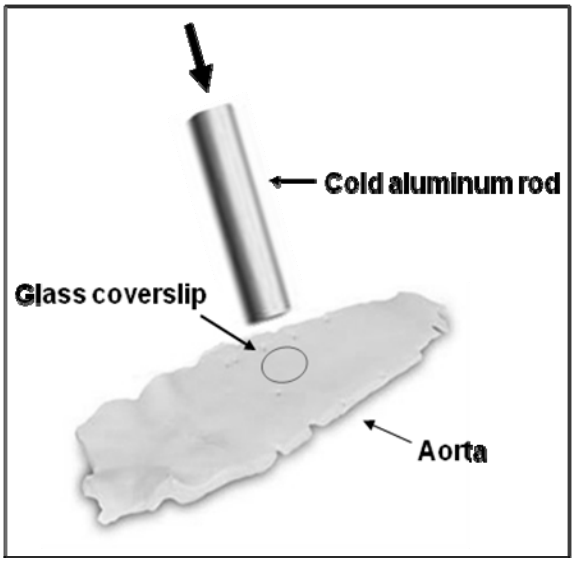

Figure 3.1. Endothelial cell isolation via frozen coverslip technique.

Immunohistochemistry

Coverslips with frozen cells were fixed in 4% paraformaldehyde for 5 min at room temperature. After fixation, the slides were rinsed in PBS for 5 min and then permeabilized with a solution of 0.3% Triton-X and 0.1% Tween-20 in PBS for 15 min at room temperature. Following a 5-min PBS wash, nonspecific primary antibody binding was blocked with 10% normal goat serum (NGS) for 30 min at 37°C. After blocking, the slides were incubated overnight at 4°C with the following antibodies: rabbit anti-human von Willebrand Factor (vWF, 1:250 dilution in 10% NGS; Dako Cytomation, Carpinteria, CA); mouse anti-human α-smooth muscle actin (α-SMA, 1:250 dilution in 5% goat serum; Sigma). A no-primary control for one slide for each antibody was incubated with 5% NGS instead of the primary antibody. Following overnight incubation, the coverslips were washed 3 × 10 min in PBS, and nonspecific secondary antibody binding was blocked by incubating the slides in 10% NGS at 37°C for 30 min. Secondary antibody staining was at room temperature for 1 hour, with Alexa-fluor 594 goat anti-rabbit and Alexa-fluor 488 goat anti-mouse (1:500 dilution in blocking buffer; Invitrogen). The coverslips were washed 3 × 10 min in PBS and placed on a microscope slide with 5 µl of a medium containing DAPI (Invitrogen, Carlsbad, CA). The cells were observed on a Zeiss microscope, and images were acquired using a CCD camera (Jenoptik, Jupiter, FL) and processed using CCD camera software (Jenoptik, Jupiter, FL).

RNA Isolation and Amplification

Total RNA was isolated using the Absolutely RNA Nanoprep Kit (Stratagene, Cedar Creek, TX) according to the manufacturer's instructions. Briefly, coverslips with attached frozen endothelium were quickly placed endothelium side up into guanidine thiocyanate (GITC) lysis buffer (Absolutely RNA Nanoprep Kit, Stratagene). The coverslips were scraped vigorously with sterile disposable cell scrapers, and the cell lysate was collected in microfuge tubes, vortexed and frozen at -80°C for future processing. For processing, cell lysates were thawed and mixed with an equal volume of 70% ethanol, and loaded onto spin columns which contained a silica-based fiber matrix that binds RNA during centrifugation (Absolutely RNA Nanoprep Kit, Stratagene). Any DNA contamination was digested on the column matrix by adding a DNase I treatment at 37°C. DNases and other contaminants were removed by a series of washes in low and high salt buffers. The remaining purified RNA was eluted from the fiber matrix by using RNase-free dH_20. The resulting RNA solution was concentrated by vacuum centrifugation. Total RNA quantity and integrity were evaluated using an Agilent Bioanalyzer 2100 (Agilent Technologies, Santa Clara, CA), a microfluidics-based platform that permits electrophoretic separation of picogram quantities of fluorescently-labeled RNA, allowing measurements of RNA quantity and quality. Total RNA samples and RNA standards (RNA 6000 Ladder, Ambion, Inc., Austin, TX), were prepared and processed according to the manufacturer's protocol. Using Agilent Bio-Sizing software, ribosomal RNA fragments of 28S and 18S and their concentrations were automatically detected on the RNA electropherogram. Total RNA was judged to be intact if the ribosomal fragments were present in a 28S:18S ratio of 2:1 and scored

using an RIN assessment numbering system. 10-100ng of total RNA was extracted for all samples. Affymetrix 2 cycle IVT kit was used to generate cRNA probes according to the manufacturer's instructions.

Microarray Analysis

Amplified RNAs were hybridized to the Porcine GeneChip (Affymetrix, Santa Clara, CA), which interrogates 23,256 transcripts that represent 20,201 genes. The expression intensities for all genes across the samples were normalized using the robust multi-array average (RMA), including probe-level quantile normalization and background correction. Based on quality control metrics, 4 arrays from two pigs were removed from the dataset due to poor Affymetrix chip hybridizations as seen by Affymetrix's QC metrics analysis. All four samples had high scaling factors and low signal intensities outside the acceptable boundaries. These four RNA preparations may have entered the RNA amplification steps with poorly degraded or too low abundant total starting RNA. We will exclude these 4 samples from further analysis.

Data analysis was performed using Partek Genomics Suite Version 6.4 (Partek, St. Louis, MO). A principal component analysis (PCA) was modeled to assess the global analysis of the array data in order to identify major effects influencing expression values in this experiment. PCA mapping of the samples provides a multidimensional gene space that helps visualize gene expression trends. In particular it is also useful analysis in identifying outliers, which could be indicative of poor quality RNA, flawed hybridizations, or experimental batch effects.

Analysis of variance (ANOVA) of the microarray data was performed on the dataset of 16 arrays using Partek software to partition variance due to RNA isolation/preparation of sample, gender, age, and disease burden in order to determine which genes were significantly up or down regulated in the severe/moderate lesions vs. matched non-atherosclerotic tissue, and in the comparison of severe versus moderate lesions. A false discovery rate (FDR) of $q<0.05$ was used as a significance threshold. Partek uses FDR for multiple test correction using the step up[133], step down[134], and q-Value[135] methodology.

Statistical Analysis

Descriptive statistics for weight, backfat, blood pressure, triglycerides, total and LDL cholesterol, oxLDL, fructosamine, inflammatory markers, insulin, glucose, Bergman S_i values, coronary and aortic atherosclerosis measurements are reported for all groups as means ± SD. In the original study, the Wilcoxon signed rank test was used to assess within group change and for pair-wise comparisons of conditions within groups. The Wilcoxon rank sum test was used for comparisons between two groups. A p value of < 0.05 was considered significant.

Results

While eighteen pigs were entered into the year-long study, both normal and atherosclerotic aortic endothelium was only available from ten pigs. Based on quality control metrics, endothelial RNA from two of the remaining pigs was removed from the dataset due to poor Affymetrix chip hybridizations and has been excluded from further analysis.

Severity of Atherosclerosis

The eight remaining pigs were segregated into two groups based on the amount of aortic atherosclerosis. Severe abdominal aortic atherosclerosis was defined as having >50% of abdominal aorta with raised atherosclerosis lesions and moderate abdominal aortic atherosclerosis was defined as having <50% of abdominal aorta with raised atherosclerosis lesions. Atherosclerosis morphometry measurements are shown in Table 3.1 for both aorta and coronary arteries. While the abdominal aortic surface area and medial areas did not vary significantly between groups, the severe group had significantly greater area with raised lesion, percent aortic area with raised lesions, intimal area, and intimal area as percent of medial area than the moderate group. Similar results were seen when comparing coronary arteries. (Results for coronary artery morphometry are shown in Table 3.1 for completeness and comparison.) Differences between the groups for the distal half of the abdominal aorta tended to be absent or less evident than those for the proximal half. Distinctions between proximal and distal are important as abdominal aortic atherosclerosis in swine and humans begins at the aortoiliac junction and progresses in a retrograde fashion.[77-81]

Table 3.1. Atherosclerosis Morphometry in IR Pigs

	Moderate (n=4)	Severe (n=4)
Abdominal aorta:		
Total aortic surface area (cm2)	34.0 ± 6.5	29.8 ± 5.2
Area with raised lesion (cm2)*	11.5 ± 3.4	20.2 ± 5.3
% aortic surface with raised lesions*	33.4 ± 6.6	66.8 ± 7.9
Medial area (mm2)	37.9 ± 11.4	31.4 ± 7.2
Intimal area (mm2)*	2.4 ± 1.6	6.0 ± 2.1
Intimal area as % medial area*	5.9 ± 2.7	19.3 ± 8.0
Proximal Half Abdominal Aorta:		
Total aortic surface area (cm2)	16.8 ± 2.5	15.1 ± 3.4
Area with raised lesion (cm2)*	3.2 ± 0.9	9.5 ± 2.9
% aortic surface with raised lesions*	19.5 ± 7.6	62.0 ± 7.0
Medial area (mm2)	38.7 ± 10.3	29.3 ± 7.3
Intimal area (mm2)*	1.2 ± 0.3	5.5 ± 2.2
Intimal area as % medial area*	3.4 ± 1.6	18.1 ± 6.2
Distal Half Abdominal Aorta:		
Total aortic surface area (cm2)	17.2 ± 4.2	14.7 ± 2.0
Area with raised lesion (cm2)	8.3 ± 3.3	10.7 ± 2.5
% aortic surface with raised lesions*	47.3 ± 12.6	71.7 ± 9.4
Medial area (mm2)	37.3 ± 14.1	33.2 ± 9.8
Intimal area (mm2)	3.7 ± 3.5	6.6 ± 2.0
Intimal area as % medial area	8.7 ± 5.4	20.7 ± 9.9
Coronary arteries:		
Medial area (mm2)	6.7 ± 0.9	5.3 ± 1.2
Intimal area (mm2)*	2.4 ± 0.7	7.1 ± 2.2
% Stenosis*	42.7 ± 13.2	73.9 ± 7.5
Intimal area as % medial area*	46.8 ± 20.3	180.7 ± 64.8

***p≤0.04 between groups

Demographic and Metabolic Characterization

Demographic and metabolic data at the start and end of the study are shown in Table 3.2. There were no significant differences between groups at start or end for age, weight, backfat, fasting insulin, fasting glucose, triglycerides, blood pressure, aldosterone, or inflammatory markers. Slight differences are seen from the original study due to the drop (n=8 vs. n=18) in animal numbers.

Table 3.2. Pig Demographic and Metabolic Characterization at Start and End of 12 Months of Study

	Moderate (n=4)		**Severe** (n=4)	
	Start	End	Start	End
Age (years)	5.3 ± 1.7	6.4 ± 1.7	2.9 ± 0.9	3.9 ± 1.0
Weight (lb)	496 ± 30	639 ± 27	484 ± 47	619 ± 81
Backfat (cm)	6.3 ± 2.3	9.6 ± 0.2	7.9 ± 1.4	9.7 ± 1.1
Insulin Sensitivity:				
Bergman Si (*start)	3.8 ± 0.2	3.5 ± 0.3	4.3 ± 0.1	3.7 ± 0.3
Fasting insulin (µU/ml)	8.0 ± 2.3	14.5 ± 2.3	11.1 ± 5.1	17.9 ± 11.1
Fasting glucose (mg/dl) - sedated	110 ± 11	122 ± 8	101 ± 18	119 ± 21
Fasting glucose (mg/dl) - conscious	71 ± 6	79 ± 10	80 ± 11	75 ±2
Fructosamine (mmol/L) († end)	1.4 ± 0.2	1.4 ± 0.1	1.5 ± 0.2	1.6 ± 0.2
Lipid analysis:				
Total cholesterol (mg/dl) (*start)	64 ± 9	357 ± 73	97 ± 21	389 ± 91
LDL cholesterol (mg/dl) († start)	36 ± 9	148 ± 7	56 ± 14	171 ± 32
HDL cholesterol (*end)	33 ± 7	102 ± 12	38 ± 9	72 ± 12
Triglycerides (mg/dl)	20 ± 9	25 ±17	25 ± 12	29 ± 14
oxLDL (U/L) († start and end)	19.6 ± 2.5	28.7 ± 3.4	23.0 ± 1.6	36.1 ± 5.2
Blood Pressure:				
Systole	157 ± 35	156 ± 21	133 ± 8	140 ± 11
Diastole	98 ± 22	107 ± 17	86 ± 9	98 ± 9
Mean arterial pressure	122 ± 29	126 ± 19	103 ± 10	112 ± 10
Pulse	79 ± 15	92 ± 11	102 ± 17	97 ± 10
Aldosterone (pg/ml)	207 ± 97	208 ± 98	210 ± 115	236 ± 53
Inflammatory markers:				
TNFα (pg/ml)	11.3 ± 22.5	69.3 ± 59.3	3.0 ± 5.9	63.4 ± 52.5
IL-6 (pg/ml)	13.4 ± 15.9	ND	ND	43.2 ± 86.4
PAI-1 (ng/ml)	1.6 ± 2.5	0.7 ± 0.5	3.1 ± 3.4	1.3 ± 1.1
CRP(µg/ml)	7.8 ± 4.6	4.5 ± 3.7	10.1 ± 8.9	18.8 ± 16.1

*****$p \leq 0.05$ between groups, †trend toward significance (p=0.051-0.067)

Purity of Endothelial Samples

First pass and second pass coverslips with frozen aortic endothelium were used to establish endothelial purity. First pass coverslips appeared fairly homogenous for ECs as seen by VWF staining (Figure 3.2). While second pass coverslips still contained some ECs, smooth muscle cells (SMC) predominate as seen by staining for SMC actin (Figure 3.2). Only first pass coverslips were used for RNA isolation.

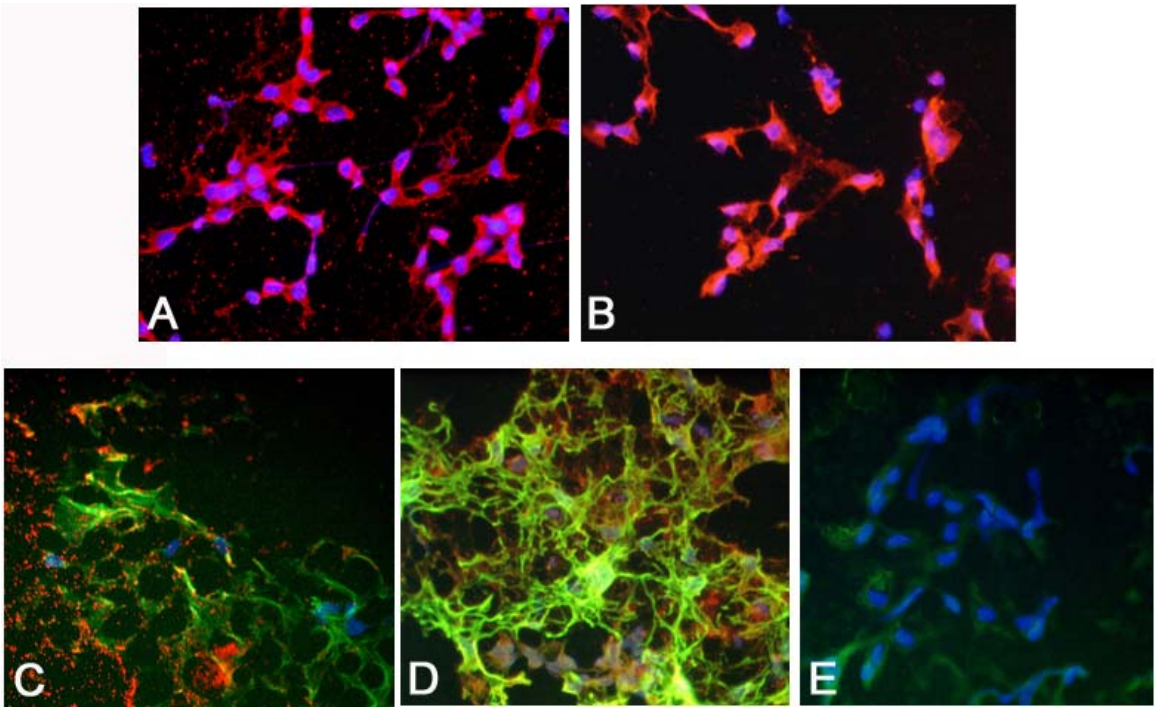

Figure 3.2. VWF and SMC staining of aortic cells obtained by frozen coverslip technique. To ensure a pure population of endothelial cells, coverslips were stained for VWF (red), smooth muscle cell actin (green), and DAPI (blue-nuclei). The first pass is the first time a coverslip is frozen over a particular area and should recover only the endothelial cell monolayer. First pass cell layers are shown from normal aorta (A) and atherosclerotic aorta (B). The second pass is the second time a coverslip is frozen over the same area and should pick up the underlying smooth muscle cells. Second pass cell layers are shown from normal aorta (C) and atherosclerotic aorta (D). Secondary antibody control is also shown (E). In our preparations, the first pass picked up only ECs as evidenced by VWF staining and not SMC staining. Therefore, only first pass coverslips were used for EC RNA.

Gene Expression

Aortic endothelial cells were collected from normal and atherosclerotic areas of abdominal aorta in pigs with severe atherosclerosis and pigs with moderate atherosclerosis. The ratio of normalized expression intensities after hybridization of amplified RNAs to the Affymetrix Porcine Gene Chip were evaluated as below to determine which genes were significantly up or down regulated in the severe/moderate atherosclerotic endothelium vs. matched normal endothelium, and in the comparison of severe versus moderate disease.

Severe vs. moderate disease

Initial analysis looked for the genes which were up- or down-regulated in both normal and atherosclerotic endothelium of severe vs. moderate disease (1-severe disease, normal endothelium vs. moderate disease, normal endothelium and 2- severe disease, atherosclerotic endothelium vs. moderate disease, atherosclerotic endothelium). Gene changes common to both normal and atherosclerotic endothelium are shown in Table 3.3. There were five genes that were up-regulated in both groups (*PTPRM, FAM5C, CLOCK, MYCPBP, LPHN2, HIPK2*). Three down-regulated genes were identified in both groups (*TMSB4X, EIF2S3, JARID1C*). Genes unique to either normal or atherosclerotic endothelium of the severe group are shown in Table 3.4. They include *SERPINI1* for the normal endothelium and *MERP1* and *RABGAP1L* for the atherosclerotic endothelium.

Table 3.3. Comparison of Severe disease to Moderate disease – gene changes common to both normal and atherosclerotic endothelium (fold change is severe disease, normal endothelium-**SN** over moderate disease, normal endothelium-**MN** and severe disease, atherosclerotic endothelium-**SA** over moderate disease, atherosclerotic endothelium-**MA**)

Gene designation	Gene name	Function	SN vs. MN		SA vs. MA	
			Fold change	p	Fold change	p
TMSB4X	thymosin beta 4, X-linked	cytoskeleton cell proliferation, migration, and differentiation	-1310.53	1.76E-09	-1588.23	1.42E-09
EIF2S3	Eukaryotic translation initiation factor 2 subunit 3	translation VEGF signaling	-361.009	8.32E-11	-440.476	6.39E-11
JARID1C	Jumonji/ARID domain-containing protein 1C	transcription oxidoreductase activity	-44.2064	3.64E-06	-33.5628	6.43E-06
HIPK2	Homeodomain-interacting protein kinase 2	Apoptosis TGF-β signaling	16.5955	7.04E-07	18.6776	5.12E-07
LPHN2	Latrophilin 2 precursor	Cell adhesion Signal transduction	147.408	1.20E-08	91.0159	2.67E-08
MYCPBP	c-myc promoter binding protein	Regulation of transcription	459.86	3.79E-12	484.71	3.54E-12
CLOCK	Circadian locomoter output cycles kaput protein	transcription	674.391	2.57E-11	563.496	3.22E-11
FAM5C	Family with sequence similarity 5, member C	Migration, invasion hypertension	840.099	1.74E-10	667.556	2.29E-10
PTPRM	Receptor-type protein-tyrosine phosphatase mu precursor	Cell adhesion Negative regulation of angiogenesis, EC migration, and EC proliferation hypertension	826.804	5.48E-10	828.515	5.47E-10

Table 3.4. Comparison of Severe disease to Moderate disease - genes unique to normal or atherosclerotic endothelium of severe disease group (fold change is severe over moderate)

Gene designation	Gene name	Function	Fold change	p
Normal endothelium			***SN vs. MN***	
SERPINI1	Serine proteinase inhibitor 12	regulation of cell adhesion cell death serine-type endopeptidase inhibitor activity	3.2942	3.58E-06
Atherosclerotic endothelium			***SA vs.MA***	
MERP1	Mammalian ependymin related protein-1 precursor	cell-matrix adhesion	8.76324	1.97E-06
RABGAP1L	RAB GTPase activating protein 1-like	GTPase activator activity	3.24004	6.93E-08

Normal vs. atherosclerotic endothelium

A second analysis evaluated genes that were up or down regulated in the atherosclerotic endothelium of each disease group vs. their respective normal endothelium (1-severe disease, atherosclerotic endothelium vs. severe disease, normal endothelium and 2- moderate disease, atherosclerotic endothelium vs. moderate disease, normal endothelium). Gene changes common to both severe and moderate disease are shown in Table 3.5. These common changes include down-regulation of two genes (*KLHL13, SYNJ1*) and up-regulation of four genes (*FAP, COL4A1, COL4A2, CYP7B1*). Gene changes unique to severe disease, atherosclerotic endothelium are shown in Table 3.6. Two genes (*MERP1*, *RABGAP1L)* are the same as seen by the previous analysis (Table 3.4) and fold changes were comparable to the previous analysis. *COL12A1* was additional up-regulated. For completeness, genes unique to moderate disease, atherosclerotic endothelium are shown in Table 3.7.

Table 3.5. Comparison of atherosclerotic to normal endothelium – gene changes common to both severe and moderate disease groups (fold change is severe disease, atherosclerotic endothelium-**SA** over severe disease, normal endothelium-**SN** and moderate disease, atherosclerotic endothelium-**MA** over moderate disease, normal endothelium-**MN**)

Gene designation	Gene name	Function	SA vs. SN		MA vs. MN	
			Fold change	p	Fold change	p
KLHL13	Kelch-like protein 13	protein binding	-4.37148	2.18E-05	-3.99779	3.44E-05
SYNJ1	Synaptojanin 1	Inositol Phosphate Metabolism	-2.49799	2.03E-06	-2.55892	1.66E-06
KIAA1715	Lunapark	blood coagulation	6.95726	1.88E-05	12.8776	2.39E-06
CYP7B1	Cytochrome P450 7B1	cholesterol metabolic process lipid metabolic process oxidation reduction	31.7243	1.09E-06	69.8156	2.23E-07
COL4A2 (2hits)	Collagen, type IV, alpha 2	extracellular matrix organization negative regulation of angiogenesis	33.4807 31.0193	1.82E-05 2.28E-05	57.6233 39.4786	6.26E-06 1.39E-05
COL4A1	Collagen alpha 1(IV) chain precursor	extracellular matrix structural constituent platelet-derived growth factor binding	54.6855	1.75E-05	73.9564	1.02E-05
FAP	Seprase	metalloendopeptidase activity	86.9546	8.65E-07	83.5107	9.28E-07

Table 3.6. Comparison of atherosclerotic to normal endothelium – genes unique to atherosclerotic endothelium of the severe disease group (fold change is severe disease, atherosclerotic endothelium-**SA** over severe disease, normal endothelium-**SN**)

Gene designation	Gene name	Function	Fold change	p
			SA vs. SN	
RABGAP1L	RAB GTPase activating protein 1-like	GTPase activator activity	2.72829	2.38E-07
MERP1	Mammalian ependymin related protein-1 precursor	cell-matrix adhesion	10.5267	1.06E-06
COL12A1	Collagen alpha 1(XII) chain precursor	extracellular matrix structural constituent cell adhesion	54.8302	2.27E-05

Table 3.7. Comparison of atherosclerotic to normal endothelium – genes unique to atherosclerotic endothelium of the moderate disease group (fold change is moderate disease, atherosclerotic endothelium-**MA** over moderate disease, normal endothelium-**MN**)

Gene designation	Gene name	Function	Fold change	p
			MA vs. MN	
PYGB	Glycogen phosphorylase	carbohydrate metabolism	-2.34974	2.72E-05
GRB10	Growth factor receptor-bound protein 10	cell-cell signaling, insulin-like growth factor receptor signaling pathway, negative regulation of glucose import, negative regulation of insulin receptor signaling pathway, signal transduction	2.17855	1.61E-05
PLXNB2	Plexin B2 precursor	signal transduction cell migration	2.7376	3.53E-05
FGF18	Fibroblast growth factor-18 precursor	fibroblast growth factor receptor binding, growth factor activity	3.89323	4.31E-05
COL3A1 (2 hits)	Collagen alpha 1(III) chain precursor.	extracellular matrix structural constituent, integrin binding, platelet-derived growth factor binding	7.30677 24.9137	1.24E-05 3.54E-06
TPM2 (2hits)	Tropomyosin beta chain	actin binding, protein binding	8.66148 8.7091	2.71E-05 7.06E-06
PIK3R3	Phosphatidylinositol 3-kinase regulatory gamma subunit	insulin receptor signaling pathway	10.2481	5.60E-05
ABI3BP	Target of Nesh-SH3 precursor	extracellular matrix organization, positive regulation of cell-substrate adhesion	10.7799	4.00E-05
SLIT3	Slit homolog 3 protein precursor	calcium ion binding, protein binding, receptor binding, structural molecule activity	12.5587	4.68E-05
ADORA1	Adenosine A1 receptor	activation of MAPKK activity, cell-cell signaling, inflammatory response, positive regulation of blood pressure	13.4092	4.81E-05

Table 3.7. Continued

Gene designation	Gene name	Function	Fold change	p
BCHE	Cholinesterase precursor	carboxylesterase activity, choline binding, cholinesterase activity, enzyme binding, hydrolase activity	24.9536	1.84E-05
ACTA2	alpha 2 actin	cell motility, structure and integrity Integrin Signaling Leukocyte extravasation signaling NRF2-mediated oxidative stress response VEGF Signaling	25.9124	6.56E-06
COL4A1	Collagen alpha 1(IV) chain precursor	binding, extracellular matrix structural constituent, platelet-derived growth factor binding	63.2243	4.63E-05

Discussion

Our goal was to identify molecular targets by comparing differential gene expression from normal and atherosclerotic aortic endothelial cells obtained from insulin resistant pigs with moderate and severe aortic atherosclerotic disease. These pigs were fed a high fat diet for one year and segregated into two groups with varying atherosclerotic severity. The group with severe atherosclerosis had higher oxLDL and greater increases in fructosamine values consistent with increased oxidative stress than the group with moderate atherosclerosis.

For many years, oxLDL has been postulated to alter endothelial barrier function[136] and may do so via changes in cytosolic calcium and subsequent reorganization of the cytoskeleton.[137] Even mildly oxidized LDL was shown to cause rapid actin cytoskeleton organization.[138] The cytoskeleton plays an essential role in endothelial repair as well.[139] Endothelial integrity is maintained through tight complexes with neighboring cells. Cadherins, calcium dependent adhesion molecules, play an important role in cell-cell interactions and are regulated by tyrosine phosphorylation. Cadherins interact with catenins, which in turn link cadherins to the actin cytoskeleton. Cadherin function is also regulated by Rho and Rac. Rho regulates stress fiber formation and is controlled by three regulatory proteins: GDIs, GEFs, and GAPs. GAPs in turn stimulate GTPase activity.

In the present study many of the genes identified as differentially expressed in the severe disease group may be involved in cell adhesion/cytoskeletal signaling pathways. The gene with highest increase was *PTPRM* which encodes receptor-type protein tyrosine phosphatase mu precursor. The presence of *PTPRM* in

vascular endothelium, especially in large arteries, has been established with localization at sites of cell-cell contact .[140] It has been associated with cadherins in various tissues, in regulating cadherin function[141] and is thought to play an important role in controlling the integrity of endothelial cell junctions[140] thus preserving the endothelial barrier.[142] It would be expected that increased *PTPRM* would protect against increases in endothelial permeability and may seem counter intuitive that it is increased in the severe disease group. However, ex vivo studies of porcine endothelial cells exposed to shear stress for extended periods of time show that changes in both localization as well as protein levels of VE-cadherin and catenins are transient and return to a steady state.[143] PTPs may have transient changes due to the tight association of PTPs with these adhesion proteins. It has also been show that the intracellular domains of PTPmu may be required to restore cell adhesion mediated by E-cadherin[144] and that PTPmu may indirectly influence other downstream signaling events, including negative regulation of angiogenesis.[145]

A large decrease was seen in the expression of *TMSB4X* which encodes thymosin-beta 4. Thymosin B4 inhibits the polymerization of actin monomers and thus plays a role in actin polymerization. In addition to its role in actin polymerization, it is also involved in cell proliferation, migration, and differentiation. It has been shown in murine bone marrow ECs (where it has significant inhibitory effects on cell proliferation)[146, 147], and cultured human umbilical ECs (where it increased the production of matrix metalloproteinases and induction of the PAI-1 gene)[148-150], as well as in a variety of tumor cells.[151-154] Perhaps the property most relevant to

the current study is the ability of thymosin B4 to inhibit the inflammatory response[155, 156] and the further suggestion that a decrease in *TMSB4X* gene expression and its subsequent protein may lead to increased inflammatory events in the endothelium.

Other genes differentially expressed in the severe group included *LPHN2* (encodes latrophilin 2 precursor, a G-protein coupled receptor[157] which may facilitate calcium signaling in the cell[158]), *HIPK2* (encodes homeodomain interacting protein kinase, a transcriptional cofactor which regulates apoptosis[159], cell growth and proliferation[160]), and *FAM5C* (encodes family with sequence similarity 5, member C which promotes proliferation, migration and invasion in neuronal and fibroblasts cells[161] as well as aortic smooth muscles cells[162]). Several other genes involved in transcription and translation were also noted: *CLOCK, MYCPBP, JARID1C, EIF2S3* (Table 3.3).

Gene changes common to the atherosclerotic endothelium of the severe disease group were identified using two different analysis groupings. Fold changes were comparable between the two analyses (Tables 3.4 and 3.6). *MERP-1, RABGAP1L,* and *COL12A1* were up-regulated unique to atherosclerotic endothelium of the severe disease group. *COL12A1* encodes the alpha chain of type XII collagen. It is a member of the fibril-associated collagens with interrupted triple helices family of extracellular matrix proteins and is thought to bridge the interactions of collagen I fibrils with the surrounding matrix[163] and may play a part in tissue remodeling[164]. *MERP-1* encodes mammalian ependymin related protein-1 precursor and has been shown to be expressed at high levels in human CD34+

hematopoietic stem cells (where it may play a role in proliferation and differentiation) as well as in brain, heart, skeletal muscle and malignant tissues.[165] It is thought to be a Type II transmembrane glycoprotein with possible calcium binding capabilities suggesting a possible role in calcium dependent cell adhesion.[166] *RABGAP1L* encodes RAB GTPase activating protein1-like. RAB GTPases are part of the Ras superfamily of monomeric G proteins and are involved in membrane traffic pathways[167, 168]. *RABGAP1L* was found to be down regulated in platelets of a patient with inherited platelet dysfunction and was linked to impaired integrin activation[169].

Interestingly, only one gene was found to be differentially expressed in normal endothelium of the severe disease group. *SERPINI1* encodes serine proteinase inhibitor 12. It has been identified in neural cells (where it regulates axonal outgrowth[170]), glioblastoma[171], endocrine cells (where it may function in cell adhesion, communication and/or migration[172, 173]), and hepatocellular carcinoma (where its presence may serve as a diagnostic aid[174]). While *SERPINI1* has not been reported in endothelial cells its identification in normal endothelium from the severe disease group only may put it at the top of the list as a candidate for investigating potential areas of atherosclerosis development.

To our knowledge, this is the first report linking a number of these genes to aortic atherosclerosis. A replicate study with a larger number of animals is underway to substantiate these data. Genes identified through this and further studies can hopefully be used to develop novel methods for the noninvasive detection of endothelial dysfunction that occurs during atherogenesis.

Chapter 4

Albuminuria and Renal Histopathology in Hyperlipidemic, Hyperinsulinemic Swine

Abstract

Human diabetic nephropathy is characterized by progressive renal insufficiency, albuminuria, and characteristic histopathology. Both insulin resistance (IR) without overt diabetes as well as hyperglycemia in diabetes are risk factors for chronic renal disease in humans. *Objective***:** To determine the extent of renal dysfunction and histopathology in hypercholesterolemic IR pigs and if these changes mirror the nephropathy seen in IR humans. *Methods***:** 18 adult IR pigs were fed a high fat diet (DH) and 6 adult familial hypercholesterolemic (FH) insulin sensitive (IS) pigs were fed a low fat diet for 12 months. Urine was analyzed for albumin/creatinine ratio ($U_{A/C}$) and kidneys for histopathology. *Results***:** All pigs had comparable hypercholesterolemia. One IR pig died with renal failure after 3 months on study (serum creatinine 9.4 mg/dl). No other pig had an increase in serum creatinine. 9/18 DH-IR pigs that completed 12 months of study had $U_{A/C}$ >30 and these 9 had higher blood pressure, aldosterone, and renal histopathology: glomerulosclerosis, tubulointerstitial fibrosis, and arteriolar hyalinosis ($p < 0.04$), as well as mesangial matrix expansion, decrease in podocyte density, and

glomerulobasement membrane thickening. 0/6 FH-IS pigs had a $U_{A/C}$> 30 or renal histopathology. *Conclusion:* Renal histopathology in DH-IR pigs appears to mirror the human phenotype of an insulin resistant and/or diabetic nephropathy when moderate blood pressure elevation, increased aldosterone, and $U_{A/C}$ >30 are present. These data also suggest that IR is necessary but insufficient for nephropathogenesis in pigs.

Introduction

Both insulin resistance (IR) without overt diabetes as well as hyperglycemia in diabetes are risk factors for chronic renal disease in humans. IR is generally a precursor of type 2 diabetes mellitus (DM), in which there is improper use of insulin by muscle, fat, and liver cells. Compensatory insulin secretion by the pancreas leads to increased insulin in the blood. When the pancreas can no longer compensate for the needed increase in insulin, glucose increases as well. Patients with high normal glucose and increased insulin are in a "pre-diabetic" state. According to the US Department of Health and Human Services, there is an increased prevalence of pre-diabetes in the US. Many of these patients go on to develop DM. The incidence of insulin resistant, type 2 DM is increasing at epidemic rates globally. In the United States alone, in 2007, there were 1.6 million new cases of diabetes diagnosed in people aged 20 years or older and a total of 7.8 percent of the population with diabetes.[1]

Insulin resistance and hyperinsulinemia have been independently associated with chronic kidney disease in numerous analyses[19, 175, 176], showing significant correlations with albuminuria[176-179] and decreased renal function[180]. Insulin is thought to alter urinary sodium excretion by effects on the tubules, to promote mesangial cell proliferation, and increase the action of angiotensin II.[19] Insulin resistance may be an independent predictor of the development of nephropathy in diabetics. Progression to human diabetic nephropathy leads to a clinical syndrome characterized by progressive renal insufficiency in the setting of diabetes, albuminuria, and characteristic pathological changes[181-183] including mesangial

matrix expansion and sclerosis, arteriolar hyalinosis, glomerulobasement membrane thickening, tubulointerstitial fibrosis, a general absence of immune complex deposits, and podocyte changes (including drop out and foot process effacement).

Creation of an animal model of diabetic nephropathy is a major goal of the Animal Models of Diabetic Complications Consortium (AMDCC, www.amdcc.org) and considerable progress towards this goal has been made in mice.[182] To date, few pig models of insulin resistance and diabetes have focused on nephropathy.[23, 184] Our goal was to characterize the extent to which functional and anatomic renal changes occur in diet-induced hypercholesterolemic, insulin resistant (DH-IR) pigs and, most importantly, how closely these changes resemble those found in humans with IR[175] and/or type 2 diabetes. These data will be essential for the design of future mechanistic studies that will characterize the mechanisms that mediate the pathogenesis of nephropathy in insulin resistant states.

MATERIALS AND METHODS

Experimental Pigs, High Fat Diet, and Sampling Protocol during Year Long Study

All pigs were treated according to the standards set in the Guide for Care and Use of Laboratory Animals (National Institutes of Health publication No. 85-23). All procedures and protocols were in accordance with institutional guidelines and approved by the Institutional Animal Care and Use Committee. All pigs were produced and maintained in the same environmental conditions at the Francis Owen Blood Research Laboratory at the University of North Carolina at Chapel Hill. Male and female pigs were from Spotted Poland/China and Yorkshire crosses. The mean age at study entry was 3.3 ± 2.0 yr. Pigs from the following three genotypes were used: normocholesterolemic (n=11), heterozygous familial hypercholesterolemic (n=8) and familial hypercholesterolemic (n=6).[50-52] Both normocholesterolemic and heterozygous familial hypercholesterolemic (FH) pigs do not express hypercholesterolemia unless they are fed a high fat diet. These animals were fed a high fat diet that consisted of pig chow (5NP8 Wayne™ 15% Pig & Sow Pellets, Granville Milling, Granville NC) supplemented with 1% cholesterol, 20% beef tallow, and 0.75% cholate by weight.[53, 54] The NaCl content of the diets was measured (Eurofins Scientific Inc, Des Moines, IA) and 5NP8 provided 0.35% or 8 grams/day as recommended[55] and the high fat diet provided 0.55% or 12.5 grams/day, a 56% increase. The total calories in this diet were distributed as: 43% fat, 12.5% protein, and 44.5% carbohydrate. Familial hypercholesterolemic pigs exhibit spontaneously

elevated levels of cholesterol and were fed normal pig chow (5NP8 Wayne™ 15% Pig & Sow Pellets, Granville Milling, Granville NC).

The variables that were measured at baseline, 3, 6, and 12 months included: weight, backfat, blood pressure, insulin sensitivity, total and LDL and HDL cholesterol, triglycerides, serum creatinine, inflammatory makers, oxidized LDL, fructosamine, and aldosterone. For detailed methods used to measure each of these variables, see Chapter 1 – Methods section.

At study termination all pigs were euthanized with an overdose of pentobarbital (6 grains/ 10 lbs. IV) and urine and kidney samples for morphometry were collected.

Kidney Morphometry

Formalin fixed, paraffin embedded kidney sections were stained with PAS and evaluated for glomerulosclerosis, glomerular mesangial matrix expansion, arteriolar hyalinosis, and tubulointerstitial fibrosis. On average, 50 glomeruli per pig were evaluated, only glomeruli with hylum or near equatorial plane were included in the analysis. Glomerulosclerosis is described as a percent (sclerotic glomeruli per total glomeruli). Morphometric analysis used Image J to measure diameter, circumference, area, and nuclei count of non-sclerotic glomeruli. Mesangial matrix area was assessed by using Image J to measure PAS stained area of mesangium. Mesangial matrix area is expressed as average area per glomerular section. Nuclei were counted in each glomerular section and expressed as number of nuclei per glomerular section. Kidneys were also processed for electron microscopy by

standard methods. Calibrated, digital micrographs were taken of nine random areas of glomerulobasement membrane (GBM) from each pig. Image J was used to measure GBM thickness.

Podocytes were visualized in frozen kidney sections placed onto Probe-On Plus charged microscopic slides, dried, and fixed in acetone and paraformaldehyde. Endogenous peroxidases were quenched by exposure of the tissue sections to a hydrogen peroxide/methanol solution before antigen retrieval was performed. Non-specific binding was blocked by exposure of the sections to avidin D and biotin solutions and 2% horse serum (Vector Laboratories). The kidney sections were incubated with anti-WT-1(Wilm's tumor antigen 1, 1:200 dilution, C-19, Santa Cruz Biotechnology, CA) overnight at 4°C. (WT-1 is a marker for mature, differentiated podocytes.[185]) This was followed by incubation with a universal secondary antibody and Vectastain R.T.U. Elite ABC reagent supplied in the Vectastain Universal Elite ABC kit (Vector Laboratories). The stain was visualized using NovaRed (Vector Laboratories) and counterstained with PAS for enhanced contrast. Omitting the primary antibody created negative controls. WT-1 positive nuclei were counted in each glomerular section and expressed as a percent of the total number of nuclei.

Urine Albumin and Creatinine

Urinary albumin was measured by ELISA (Bethyl Labs, Montgomery, TX, sensitivity 7.8 ng/ml, Pig Albumin) and urine creatinine was measured by automated methods (Antech). The reference interval for normal human urine albumin/creatinine

ratio ($U_{A/C}$) is 0-30 µg albumin/mg creatinine, microalbuminuria is 30-300 and clinical albuminuria is >300. Since reference ranges have not been established for insulin resistant pigs, we have tentatively used human ranges as guidelines for evaluating urinary albuminuria.

Statistical Analysis

Descriptive statistics for weight, backfat, blood pressure, triglycerides, total and LDL and HDL cholesterol, oxLDL, fructosamine, inflammatory markers, insulin, glucose, Bergman S_i values, and kidney morphometry measurements are reported for all groups as means ± SD. The Wilcoxon rank sum test was used to assess within group change and for pair wise comparisons of conditions between groups. A p value of < 0.05 was considered significant.

Results

Twenty five pigs were entered into the year-long study. Nineteen normocholesterolemic hyperinsulinemic pigs were fed a high fat diet to induce hypercholesterolemia (DH) and developed worsening insulin resistance (IR) when eating this diet. Six familial hypercholesterolemic (FH) insulin sensitive (IS) pigs were used as controls. All pigs had comparable hypercholesterolemia. The detailed results of the renal evaluation are presented first followed by the metabolic parameters that were monitored during the yearlong study to determine which were associated with the development of nephropathy.

One DH-IR pig died with renal failure after 3 months on diet (serum creatinine 9.4 mg/dl) and was excluded from further study. Urine was not available from this pig, however several of the histopathological findings consistent with insulin resistant/diabetic nephropathy were present, most notably, mesangial sclerosis, GBM thickening, tubulointerstitial fibrosis, podocyte foot process effacement, and protein resorption droplets in renal tubules.

Albuminuria

None of the six control FH-IS pigs had an elevated $U_{A/C}$. Urine was not available from one of the DH-IR pigs and this pig was excluded from further analysis. Of the remaining 17 DH-IR pigs, eight (47%) had a $U_{A/C}$ <30 and nine (53%) had $U_{A/C}$ >30 (Figure 4.1).

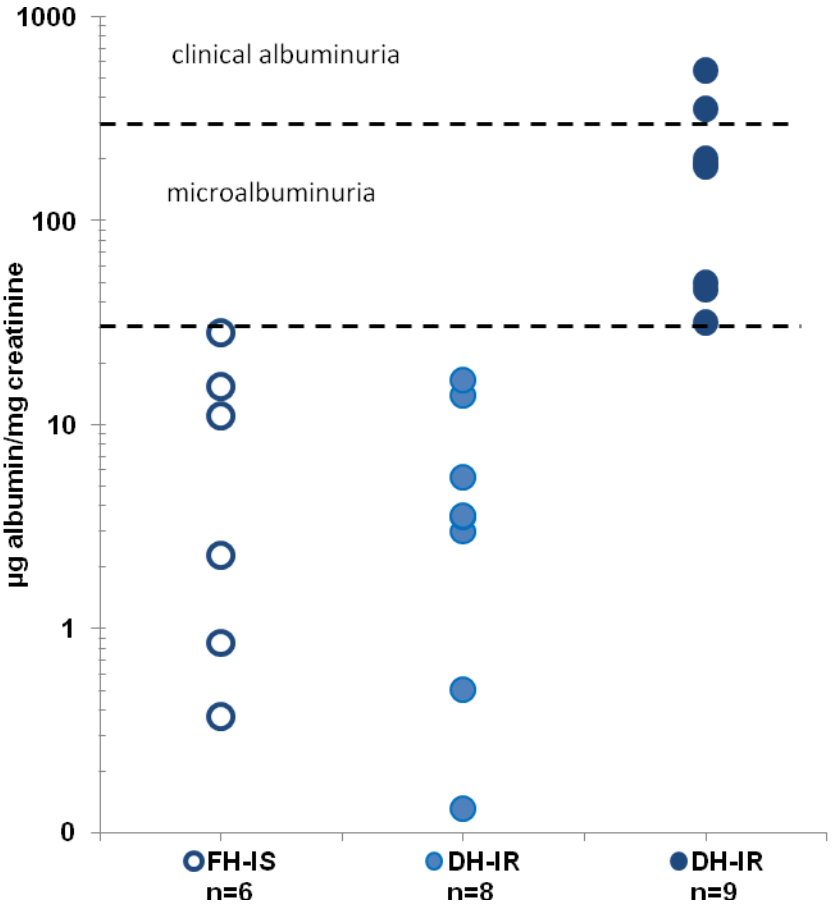

Figure 4.1. Albuminuria in IS and IR pigs. None of the six control FH-IS pigs exhibited albuminuria. Eight (47%) of the DH-IR pigs had a $U_{A/C}$ <30 and nine (53%) had $U_{A/C}$ >30. The reference interval for normal human urine albumin/creatinine ratio ($U_{A/C}$) is 0-30 µg albumin/mg creatinine, microalbuminuria is 30-300 and clinical albuminuria is >300. Since reference ranges have not been established for insulin resistant pigs, we have tentatively used human ranges as guidelines for evaluating urinary albuminuria.

Renal Histopathology

The FH-IS pigs exhibited no detectible renal histopathology (Table 4.1). Four of the eight DH-IR pigs with $U_{A/C}$ <30 had glomerulosclerosis, six had mesangial matrix expansion, and five had podocyte changes (Table 4.1). The glomerulosclerosis was perihylar and focal segmental. Tubulointerstitial fibrosis, arteriolar hyalinosis and GBM thickening were not detected in any of the DH-IR pigs with $U_{A/C}$ <30. Seven of the nine DH-IR pigs with $U_{A/C}$ >30 had glomerulosclerosis, six had mesangial matrix expansion, six had tubulointerstitial fibrosis, four had arteriolar hyalinosis, two showed glomerulobasement membrane thickening, and seven had podocyte changes (Table 4.1, Figure 4.2). The glomerulosclerosis was predominantly perihylar and focal segmental, with three of the pigs also exhibiting global sclerosis. None of the pigs exhibited immune complex deposition (Table 4.1).

Table 4.1. Pig Demographic and Metabolic Characterization at End of 12 Months of Study

	FH-IS	DH-IR	
Age (years)	2.9 ± 0.4	3.8 ± 1.0	5.3 ± 2.0
Weight (lb)	484 ± 46	604 ± 86	661 ± 60
Weight (% increase from baseline)	9.7 ± 5.1	23.7 ± 8.0	26.2 ± 6.2
Bergman Si	4.6 ± 0.4	3.4 ± 0.3	3.5 ± 0.4
Fasting insulin (μU/ml)	7.6 ± 2.9	15.3 ± 4.0	19.7 ± 9.2
Fasting glucose (mg/dl) - sedated	76 ± 6	125 ± 28	116 ± 22
Fasting glucose (mg/dl) - conscious	71 ± 2	72 ± 4	76 ± 7
Fructosamine (mmol/L)	1.9 ± 0.2	1.5 ± 0.2	1.5 ± 0.2
Blood pressure (mmHG)	137/85	130/84	154/108*
Mean arterial pressure	105 ± 20	100 ± 16	125 ± 17*
Aldosterone (pg/ml)	47 ± 16	175 ± 75	194 ± 94
Total cholesterol (mg/dl)	383 ± 43	333 ± 74	385 ± 63
Serum creatinine (mg/dl)	2.3 ± 0.4	1.9 ± 0.3	1.5 ± 0.3
Urine albumin/creatinine ratio:			
$U_{A/C}$ >30	0/6	0/8	9/9*
Average $U_{A/C}$	9.7 ± 10.9	5.8 ± 6.1	181 ± 174*
Renal Histopathology:			
Glomerulosclerosis	0/6	4/8	7/9
% glomeruli with sclerosis	0	4 ± 7	26 ± 16*
Mesangial matrix (MM) expansion	0/6	6/8	6/9
MM area ($x10^3$ μm^2)	2.3 ± 0.6	3.8 ± 1.5	5.0 ± 1.9
Tubulointerstitial fibrosis	0/6	0/8	6/9*
Arteriolar hyalinosis	0/6	0/8	4/9*
GBM thickening	0/6	0/8	2/9
Thickness (nm)	161 ± 14	229 ± 41	210 ± 32
Podocyte density (% of total cells in glomeruli)	14.5 ± 3.8	7.9 ± 2.1	7.3 ± 1.8
Immune complex deposition	0/6	0/8	0/9
Glomerular tuft area ($x10^4$ μm^2)	2.2 ± 0.2	3.0 ± 0.3	3.6 ± 0.5*
Nuclei per glomerular section	179 ± 18	225 ± 18	248 ± 26*

*$p \leq 0.046$ for DH-IR pigs with $U_{A/C}$ >30 vs. DH-IR pigs with $U_{A/C}$>30

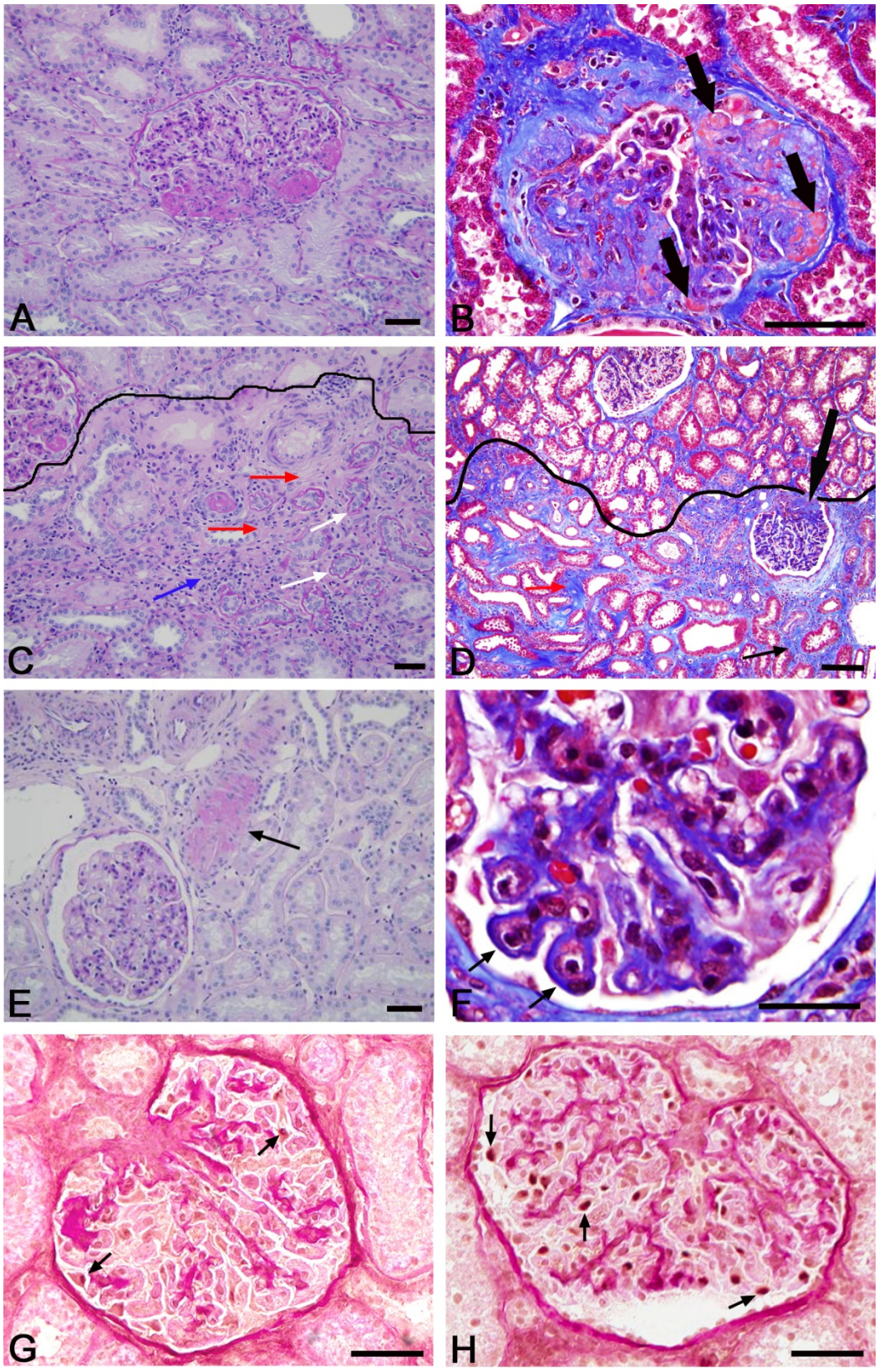
A
B
C
D
E
F
G
H

Figure 4.2. Renal Histopathology in Hyperlipidemic, Hyperinsulinemic Pigs with $U_{A/C}$ >30. Characteristic changes of renal pathology seen in humans with insulin resistance were also noted in the DH-IR pigs. They include both segmental (A) and global (B) sclerosis, arrows in B show residual fuchsinophilic (red) hyalinosis. Tubulointerstitial fibrosis (C and D) is seen by the pink area below the black line in C (red arrows, PAS staining) or the blue staining below the black line in D (small black arrow, Masson's trichrome stain), indicating collagen deposition. A sclerotic glomerulus is also noted by large black arrow (D); tubular atrophy (white arrows) and chronic inflammation (blue arrows) are also present in C. Arteriolar hyalinosis (E) was also present as indicated by the black arrow. Glomerulobasement membrane thickening (F) is noted by the black arrows. Decrease in podocyte density is seen in G (podocyte detection by immunohistochemical staining with antibody to WT-1, C-19, Santa Cruz Biotechnology, Nova Red detection, arrows). Podocyte staining from FH-IS control pig for comparative purposes is seen in H.
Magnification bars A, B, C, E, G, & H = 50 μm; D = 100 μm; F = 25 μm.

Glomerular analysis – While the control FH pigs had no glomerulosclerosis, the DH-IR pigs with $U_{A/C}$ <30 averaged 3.9 ± 6.8 percent glomeruli with sclerosis. Both were significantly lower than DH-IR pigs with $U_{A/C}$ >30 which averaged 25.9 ± 16.1 percent glomeruli with sclerosis (Table 4.1, $p \leq 0.016$). Glomeruli from DH-IR pigs with $U_{A/C}$ >30 also had significantly larger tuft surface area than glomeruli from either DH-IR pigs with $U_{A/C}$ <30 or control FH-IS pigs (Table 4.1, $p \leq 0.008$). Both DH-IR groups showed an increase in mesangial matrix area. The DH-IR pigs with $U_{A/C}$ >30 had a mesangial matrix area (MMA) of 5.0 ± 1.9 x $10^3 \mu m^2$, and the DH-IR pigs with $U_{A/C}$ <30 had an MMA of 3.8 ± 1.5 x $10^3 \mu m^2$. These were significantly larger than in the control FH-IS pigs (2.3 ± 0.6 x $10^3 \mu m^2$, $p \leq 0.043$, Table 4.1).

Glomerular cellularity was increased in both the DH-IR groups. The DH-IR pigs with $U_{A/C}$ >30 had an average of 248 ± 26 nuclei per glomerular section which was significantly higher than either the DH-IR pigs with $U_{A/C}$ <30 (225 ± 18) or the control FH-IS pigs (179 ± 19, Table 4.1, $p \leq 0.046$).

There was a significant decrease in podocyte density between the DH-IR pigs and the control FH-IS control pigs (Figure 4.2, G & H). In the FH-IS pigs 14.5 ± 3.8% of the total cells were podocytes, compared to 7.9 ± 2.1% for the DH-IR pigs with $U_{A/C}$ <30 and 7.3 ± 1.8% for the DH-IR pigs with $U_{A/C}$ >30 (Table 4.1, $p \leq 0.005$).

While GBM thickening was noted by light microscopy on two of the DH-IR pigs with $U_{A/C}$ >30, GBM thickness measurements taken from digital electron micrographs of nine random areas of GBM for each pig showed no significant difference in thickness between the two DH-IR groups. Both groups of DH-IR pigs had significantly thicker GBM measurements than the FH-IS pigs (Table 4.1,

$p \leq 0.03$).

Creatinine

Serum creatinine was not elevated in the study animals at any time point (Table 4.1).

Fasting Insulin, Glucose, and Insulin Sensitivity by Bergman FSIVGTT and Fructosamine

Fasting glucose values in conscious pigs at months 1, 2, 4, 5, 7, 8, 9, 10, and 11 are shown in Table 4.2, and their counterparts for sedated pigs during the Bergman FSIVGTT at baseline, 3, 6, and 12 months are in Table 4.3. The glucose values are higher when the pigs were sedated, possibly due to the stress of the procedure or the sedatives used.[84, 85]

Fasting insulin values measured during the Bergman FSIVGTT were not significantly different between the three groups at baseline. The DH-IR pigs with $U_{A/C}$ >30 had insulin levels significantly higher than the FH-IS pigs at 3, 6, and 12 months ($p \leq 0.005$). The DH-IR pigs with $U_{A/C}$ <30 had insulin values significantly higher that the FH-IS pigs at 12 months ($p \leq 0.001$). The only difference in insulin values between the two DH-IR groups was at 3 months and was significantly higher in the DH-IR pigs with $U_{A/C}$ >30 ($p \leq 0.006$). The DH-IR pigs with $U_{A/C}$ >30 also had fasting insulin values significantly higher at 12 months compared to baseline ($p \leq 0.004$), whereas the DH-IR pigs with $U_{A/C}$ <30 and the FH-IS pigs showed little or no evidence of change in insulin values over the 12 months on diet (Table 4.3).

Fasting glucose values during the Bergman FSIVGTT showed little or no

evidence of change over the 12 months on diet for any of the three groups. There was no significant difference in glucose between the two DH-IR groups at any time point but both were significantly higher than the FH-IS pigs at all time points ($p \leq 0.05$, Table 4.3).

The mean S_i values decreased significantly in the DH-IR pigs with $U_{A/C}$ >30 at 3, 6 and 12 months and in the DH-IR pigs with $U_{A/C}$ <30 at 12 months consistent with increased insulin resistance ($p \leq 0.003$ compared to baseline). There was no change in Si values for the control FH-IS pigs during the 12 months of study. Si values for both DH-IR groups were significantly lower than FH-IS pigs at all time points ($p \leq 0.014$, Table 4.3).

Fasting fructosamine values are shown in Table 4.3. Values for FH and DH-IR pigs with $U_{A/C}$ <30 remained relatively unchanged over the 12 months of study. DH-IR pigs with $U_{A/C}$ >30 had significant increases over baseline at 3 and 6 months ($p \leq 0.02$). Values for FH pigs were significantly higher than both groups of DH pigs at all time points ($p \leq 0.02$).

Table 4.2. Fasting Glucose in Conscious IS and IR Pigs on the Year Long Study

Fasting Glucose (mg/dl)		**FH-IS** $U_{a/c}$<30 (n = 6)	**DH-IR** $U_{a/c}$<30 (n = 8)	**DH-IR** $U_{a/c}$>30 (n = 9*)
Month:	1	76 ± 7	74 ± 8	73 ± 6
	2	66 ± 10	74 ± 6	74 ± 5
	4	71 ± 3	74 ± 7	76 ± 7
	5	71 ± 8	75 ± 13	72 ± 7
	7	72 ± 5	77 ± 8	72 ± 5
	8	71 ± 3	75 ± 9	73 ± 9
	9	71 ± 4	80 ± 15	72 ± 5
	10	71 ± 3	73 ± 12	75 ± 3
	11	71 ± 2	72 ± 4	76 ± 7

*One pig was euthanized due to inappetance at 6 months, thus n = 8 for months 7 to 11.

Table 4.3. Fasting Insulin and Glucose, Bergman S_i, and Fructosamine Values

	FH-IS $U_{a/c}$<30 (n = 6)	**DH-IR** $U_{a/c}$<30 (n = 8)	**DH-IR** $U_{a/c}$>30 (n = 9*)
Fasting Insulin (µU/ml)			
Baseline	9.3 ± 2.4	11.0 ± 4.2	15.5 ± 12.7
3 month	7.8 ± 1.4	11.6 ± 4.0	18.9 ± 4.4
6 month	7.5 ± 1.2	14.4 ± 9.3	19.6 ± 14.5
12 month	7.6 ± 2.9	15.3 ± 4.0	19.7 ± 9.2†
Fasting Glucose (mg/dl)			
Baseline	88.0 ± 13.0	108.4 ± 19.6	114.6 ± 27.7
3 month	75.4 ± 4.5	107.2 ± 22.4	106.5 ± 21.1
6 month	77.6 ± 11.9	100.6 ± 19.7	117.0 ± 39.2
12 month	75.6 ± 6.3	125.2 ± 27.7	116.2 ± 21.5
Bergman S_i			
Baseline	4.8 ± 0.6	4.0 ± 0.2	3.9 ± 0.5
3 month	4.6 ± 0.5	3.9 ± 0.4	3.6 ± 0.4†
6 month	4.5 ± 0.6	3.8 ± 0.4	3.5 ± 0.5†
12 month	4.6 ± 0.4	3.4 ± 0.3†	3.5 ± 0.4†
Fasting Fructosamine (mmol/L)			
Baseline	2.0 ± 0.3	1.5 ± 0.2	1.4 ± 0.1
3 month	2.0 ± 0.1	1.7 ± 0.2	1.7 ± 0.2†
6 month	2.1 ± 0.2	1.6 ± 0.2	1.6 ± 0.2†
12 month	1.9 ± 0.2	1.5 ± 0.2	1.5 ± 0.2

*One pig was euthanized due to inappetance at 6 months, thus n = 8 for month 12.
†$p<0.05$, Wilcoxon signed rank statistic for change from baseline within group.

Weight and Backfat

The baseline, 3, 6, and 12 month weight and backfat values are shown in Table 4.4. Weight increased significantly over time compared to baseline in both the DH-IR pigs with $U_{A/C}$ >30 and the FH-IS pigs at 3, 6 and 12 months and in the DH-IR pigs with $U_{A/C}$ <30 at 6 and 12 months ($p<0.04$). The weights for DH-IR pigs with $U_{A/C}$ >30 were significantly increased compared to DH-IR pigs with $U_{A/C}$ <30 at 3 months ($p=0.010$) and were also significantly increased at all time points compared to FH-IS pigs ($p\leq0.016$). The weights for DH-IR pigs with $U_{A/C}$ <30 were significantly increased over the FH-IS pigs at 12 months only ($p=0.004$).

Backfat increased significantly in DH-IR pigs with $U_{A/C}$ >30 at all time points ($p \leq 0.016$). There was no significant change in backfat for DH-IR pigs with $U_{A/C}$ <30 at any time point. Backfat values were significantly different between the two DH-IR groups at 12 months ($p=0.003$). Backfat values were not available for the FH-IS pigs.

Table 4.4. Weight and Backfat in IS and IR Pigs in Year Long Study

	FH-IS $U_{a/c}$<30 (n = 6)	**DH-IR** $U_{a/c}$<30 (n = 8)	**DH-IR** $U_{a/c}$>30 (n = 9*)
Weight (lb)			
Baseline	421 ± 51	457 ± 41	512 ± 59
3 month	457 ± 50†	479 ± 72	578 ± 47†
6 month	449 ± 38†	525 ± 86†	606 ± 35†
12 month	484 ± 46†	604 ± 86†	661 ± 60†
Backfat (cm)			
Baseline	NA	6.2 ± 1.8	7.4 ± 2.0
3 month	NA	7.4 ± 1.0	8.1 ±1.5†
6 month	NA	7.8 ± 0.8	8.8 ± 1.4†
12 month	NA	8.5 ± 1.1	9.9 ± 0.6†

NA = not available.
Data are listed for pigs for which there was a complete 12 month data set except for *one pig that was euthanized at 6 months due to inappetance, thus n = 8 for month 12.
†p<0.05, Wilcoxon signed rank statistic for change from baseline within group.

Blood Pressure

Blood pressure data are listed in Table 4.5. Data are listed for pigs for which there was a complete 12 month data set except for one pig that was euthanized at 6 months due to inappetance. Blood pressure values were only available for one FH-IS pig at baseline and two FH-IS pigs at all other time points.

Blood pressure in DH-IR pigs with $U_{A/C}$ >30 did not change significantly over the 12 months of study and was in a range that would be considered mildly hypertensive in humans. Blood pressure in DH-IR pigs with $U_{A/C}$ >30 was significantly higher than DH-IR pigs with $U_{A/C}$ <30 at baseline, 3, and 12 months ($p \leq 0.045$) and significantly higher than FH-IS pigs at 3 months ($p=0.036$).

Table 4.5. Arterial Blood Pressure (mm Hg) in IR Pigs on the Year Long Study

	FH-IS $U_{a/c}$<30 (n = 1,2)	**DH-IR** $U_{a/c}$<30 (n = 5)	**DH-IR** $U_{a/c}$>30 (n = 9*)
Systolic			
Baseline	127	123 ± 7	144 ± 24
3 month	126 ± 4	130 ± 8	147 ± 17
6 month	121 ± 8	154 ± 24	146 ± 27
12 month	137 ± 31	130 ± 16	154 ± 17
Diastolic			
Baseline	86	73 ± 4	95 ± 13
3 month	83 ± 1	80 ± 9	99 ± 16
6 month	80 ± 6	101 ± 15	104 ± 31
12 month	85 ± 25	84 ± 16	108 ± 14
MAP			
Baseline	106	93 ± 7	114 ± 19
3 month	101 ± 2	102 ± 6	121 ± 17
6 month	94 ± 1	123 ± 22	120 ± 31
12 month	105 ± 20	100 ± 16	125 ± 17
Pulse			
Baseline	61	91 ± 11	99 ± 23
3 month	94 ± 11	89 ± 11	105 ± 19
6 month	86 ± 10	86 ± 17	109 ± 23
12 month	81 ± 13	99 ± 18	96 ± 13

Data are listed for pigs for which there was a complete 12 month data set except for *one pig that was euthanized at 6 months due to inappetance, thus n = 8 for month 12.
$^{\dagger}p<0.05$, Wilcoxon signed rank statistic for change from baseline within group.

Aldosterone

Aldosterone values are listed in Table 4.6. DH-IR pigs with $U_{A/C}$ >30 had aldosterone values significantly higher than the FH-IS pigs at all time points ($p \leq 0.018$). DH-IR pigs with $U_{A/C}$ <30 had aldosterone values significantly higher than the FH-IS pigs at 3, 6, and 12 months ($p \leq 0.013$). While the mean aldosterone levels were higher in the DH-IR pigs with $U_{A/C}$ >30, they were not statistically different from the DH-IR pigs with $U_{A/C}$ <30.

Table 4.6. Fasting Aldosterone Values in IS and IR Pigs

	FH-IS $U_{a/c}$<30 (n = 6)	**DH-IR** $U_{a/c}$<30 (n = 8)	**DH-IR** $U_{a/c}$>30 (n = 9*)
Aldosterone (pg/ml)			
Baseline	58 ± 24	127 ± 111	202 ± 108
3 month	40 ± 12	125 ± 80	185 ± 100
6 month	42 ± 32	126 ± 70	203 ± 85
12 month	47 ± 16	175 ± 75	194 ± 94

*****One pig in this group was euthanized due to inappetance at 6 months, thus n = 8 for month 12.

Total, LDL, and HDL Cholesterol, oxLDL and Triglyceride Levels

Lipoprotein values are listed in Table 4.7. FH-IS pigs had no significant changes in total, LDL, and HDL cholesterol, oxLDL, or triglycerides at any time point. Both groups of DH-IR pigs had significant increases above baseline in total, LDL, and HDL cholesterol, and oxLDL at all time points ($p \leq 0.004$). The only significant difference seen between the DH-IR groups was in HDL cholesterol at baseline, DH-IR pigs with $U_{A/C}$ >30 had a significantly higher value than DH-IR pigs with $U_{A/C}$ <30 ($p=0.016$).

FH-IS pigs had significantly higher total cholesterol at baseline than either group of DH-IR pigs ($p \leq 0.001$). This due a LDL receptor mutation (i.e., not diet induced). Total cholesterol levels were comparable between the three groups throughout the remainder of the study. FH-IS pigs had significantly higher triglycerides at baseline than both DH-IR groups and significantly higher triglycerides at 3 months than the DH-IR pigs with $U_{A/C}$ <30 ($p \leq 0.008$). LDL cholesterol values were significantly higher at all time points for FH-IS pigs than either DH-IR group ($p \leq 0.013$). FH-IS pigs had HDL cholesterol values significantly lower than DH-IR pigs with $U_{A/C}$ >30 at all time points and significantly lower than DH-IR pigs with $U_{A/C}$ <30 at 3, 6 and 12 months ($p \leq 0.001$). FH-IS pigs also had oxLDL levels significantly higher than DH-IR pigs with $U_{A/C}$ <30 at baseline, 3 and 12 months and significantly higher than DH-IR pigs with $U_{A/C}$ >30 at baseline and 6 months ($p \leq 0.005$).

Table 4.7. Fasting Total, LDL, and HDL Cholesterol, oxLDL, and Triglyceride Levels

	FH-IS $U_{a/c}$<30 (n = 6)	**DH-IR** $U_{a/c}$<30 (n = 8)	**DH-IR** $U_{a/c}$>30 (n = 9*)
Total cholesterol (mg/dl)			
Baseline	391 ± 104	69 ± 16	86 ± 18
3 month	394 ± 54	434 ± 204†	435 ± 95†
6 month	410 ± 73	402 ± 185†	317 ± 118†
12 month	383 ± 43	333 ± 74†	385 ± 63†
LDL cholesterol (mg/dl)			
Baseline	291 ± 76	36 ± 14	49 ± 11
3 month	305 ± 43	198 ± 80†	201 ± 40†
6 month	302 ± 48	174 ± 58†	151 ± 59†
12 month	291 ± 27	134 ± 15†	172 ± 22†
HDL cholesterol (mg/dl)			
Baseline	20 ± 4	26 ± 7	36 ± 6
3 month	22 ± 4	95 ± 38†	91 ± 24†
6 month	22 ± 4	85 ± 26†	82 ± 26†
12 month	22 ± 3	77 ± 19†	84 ± 18†
oxLDL (U/L)			
Baseline	42 ± 3	20 ± 2	22 ± 2
3 month	40 ± 5	30 ± 6†	34 ± 6†
6 month	40 ± 4	33 ± 8†	30 ± 6†
12 month	40 ± 4	30 ± 6†	36 ± 5†
Triglycerides (mg/dl)			
Baseline	56 ± 9	22 ± 6	24 ± 9
3 month	35 ± 5	22 ± 8	31 ± 16
6 month	46 ± 32	24 ± 14	26 ± 20
12 month	32 ± 20	24 ± 13	25 ± 12

*One pig in this group was euthanized due to inappetance at 6 months, thus n = 8 for month 12.
†$p<0.05$, Wilcoxon signed rank statistic for change from baseline within group.

Inflammatory Markers

Values for inflammatory markers are shown in Table 4.8. DH-IR pigs with $U_{A/C}$ <30 had significant increases in TNFα and PAI-1 at 3 months compared to baseline ($p \leq 0.05$). DH-IR pigs with $U_{A/C}$ >30 had a significant increase in PAI-1 at 3 months compared to baseline ($p \leq 0.02$). FH-IS showed no significant differences in inflammatory markers over the study period.

There were no significant differences in any marker, at any time point between the two DH-IR groups. TNFα values for DH-IR pigs with $U_{A/C}$ <30 were significantly increased at all time points compared to FH-IS pigs ($p \leq 0.033$) and CRP values for DH-IR pigs with $U_{A/C}$ <30 were significantly lower than FH-IS pigs at baseline ($p=0.008$). Significant differences between DH-IR pigs with $U_{A/C}$ >30 and FH-IS pigs included increased TNFα at 12 months and increased PAI-1 at 3 months ($p<0.05$).

Table 4.8. Inflammatory Markers

	FH-IS $U_{a/c}$<30 (n = 6)	**DH-IR** $U_{a/c}$<30 (n = 8)	**DH-IR** $U_{a/c}$>30 (n = 9*)
TNF-alpha (pg/ml)			
Baseline	4.8 ±6.9	42.3 ± 40.0	17.5 ± 18.7
3 month	9.4 ± 13.1	111.1 ± 91.6†	53.3 ± 72.0
6 month	5.5 ± 8.5	61.9 ± 39.2	31.3 ± 35.2
12 month	2.0 ± 0.0	101.8 ± 124.1	51.1 ± 58.2
IL-6 (pg/ml)			
Baseline	12.0 ± 8.8	11.1 ± 11.9	7.9 ± 8.7
3 month	8.9 ± 5.4	38.6 ± 43.7	10.6 ± 12.0
6 month	9.7 ± 10.6	25.6 ± 58.4	5.0 ± 0.0
12 month	5.0 ± 0.0	24.3 ± 27.6	26.0 ± 59.3
PAI-1 (ng/ml)			
Baseline	1.7 ± 3.9	1.5 ± 1.2	4.4 ± 5.2
3 month	3.1 ± 5.0	6.2 ± 4.8	10.6 ± 6.9†
6 month	2.3 ± 1.7	3.1 ± 2.3	4.9 ± 4.9
12 month	2.2 ± 2.1	3.0 ± 5.3	1.4 ± 1.3
CRP (µg/ml)			
Baseline	37.7 ± 42.0	6.7 ± 11.5	8.8 ± 6.2
3 month	10.6 ± 5.3	8.9 ± 5.2	16.3 ± 20.5
6 month	40.0 ± 38.3	11.4 ± 9.6	8.8 ± 7.6
12 month	26.1 ± 25.9	9.2 ± 9.7	13.4 ± 12.4

*One pig was euthanized due to inappetance at 6 months, thus n = 8 for month 12.
†$p<0.05$, Wilcoxon signed rank statistic for change from baseline within group.

Discussion

This study demonstrates renal histopathology consistent with human insulin resistant/pre-diabetic nephropathy in a subset of insulin resistant, hypercholesterolemic pigs fed a high fat diet with increased sodium content. The two groups of DH-IR pigs were similar in degree of hyperinsulinemia, decrease in insulin sensitivity, weight gain, backfat, lipid profiles, and inflammatory markers. However, one group exhibits albuminuria, moderate elevation in blood pressure, and persistent elevations in aldosterone levels. We must mention that none of these pigs became hyperglycemic (glucose $\geq$ 126 mg/dl). While insulin resistance without overt hyperglycemia has been shown to be a risk factor for chronic renal disease, this study suggests that IR is necessary but insufficient for nephropathogenesis in our pigs. The scope of this paper is not meant to be mechanistic in nature, but to characterize the extent to which functional and anatomic changes occur in our insulin resistant (IR) pigs and, most importantly, how closely these changes resemble those found in humans with insulin resistance.

Albuminuria

Glomeruli act as a size and charge barrier to keep albumin and other proteins present in the blood from entering the urine. When glomeruli are damaged, albumin is able to pass through and is then excreted in the urine. The DH-IR pigs were segregated based on the presence or absence of albuminuria. The presence of even small amounts of albumin in the urine, “microalbuminuria” ($U_{A/C}$ of 3-300), is often undetectable by urine dipstick, can occur long before the onset of overt

nephropathy, and is an important finding as it indicates that there is already significant deterioration or impairment in renal function. Albuminuria may be a transient finding; therefore the sustained presence of albuminuria (repeat sampling) is a more reliable indicator of glomerular damage. In the current study, urine was only evaluated for albuminuria at the end of the 12 months of study. In conjunction with the other findings of glomerular and tubular injury, we conclude that this is likely not a transient finding but a true indicator of renal disease in these animals. Additionally insulin resistance and hyperinsulinemia have been significantly associated with the presence of albuminuria in numerous studies.[19, 175, 176]

Mesangial Expansion, Podocyte changes, and Glomerular hypertrophy

Mesangial expansion can be caused by an increase in mesangial matrix and/or an increase in mesangial cells[186]. Studies have shown rat mesangial cells grown in vitro in the presence of supplemental insulin had alterations in their phenotype and the expression of collagens leading to increased cell proliferation and accumulation of extracellular matrix.[187, 188] When compared to the insulin sensitive pigs, both groups of DH-IR pigs had increases in mesangial matrix as well as increased cellularity (Table 4.1).

Mesangial matrix expansion may also result in part from reduced degradation because of a decrease in matrix metalloproteinases (MMP). Plasminogen activator inhibitor 1 (PAI-1) has been shown in animal models to inhibit MMPs.[189] While sustained increases of PAI-1 were not seen over the course of the study, both groups of DH-IR did have significant increases in PAI-1 at 3 months.

Both groups of DH-IR pigs had a decreased number of podocytes compared to the FH-IS control pigs. Immortalized human podocytes have been shown to be insulin responsive[190] and podocyte number and density in patients with obesity related glomerulopathy have been shown to correlate with insulin levels.[191] Likewise, hyperinsulinemia and insulin resistance have been associated with podocyte injury in Zucker rats.[192] Only recently has podocyte injury been recognized as an early event in IR/diabetic nephropathy.[193] Our DH-IR pig model is consistent with this early finding.

Both mesangial matrix expansion and podocyte injury are thought to lead to glomerular hypertrophy.[194] We have shown an increase in glomerular size (Table 4.1) in our DH-IR pigs over FH-IS controls. Estimated glomerular volumes for the DH-IR pigs were increased 1.6 and 1.8 times ($U_{A/C}$ <30 and $U_{A/C}$ >30, respectively) those of the FH-IS control pigs. This is also consistent with data from rhesus monkeys showing an association between glomerular hypertrophy and hyperinsulinemia which appeared before the onset of diabetes.[195]

Arteriolar hyalinosis, GBM thickening, and tubulointerstitial fibrosis

Only DH-IR pigs with $U_{A/C}$ >30 exhibited the most abnormal finding of renal nephropathy including arteriolar hyalinosis, GBM thickening, and tubulointerstitial fibrosis. While GBM thickening was noticed by light microscopy in two of these pigs, electron microscopy offers relatively few glomeruli for measurements. Therefore no significant changes were observed between the means for the two groups of DH-IR pigs, although both were significantly thicker than the control pigs. A combination of

GBM thickening, podocyte pathology, and hemodynamic changes was associated with proteinuria and the most abnormal findings of nephropathy, including tubulointerstitial fibrosis and tubular atrophy.[196]

Aldosterone and blood pressure

The associations between insulin resistance, systemic hypertension, the renin-angiotensin-aldosterone system (RAAS), and renal disease are well established.[197-199] Both obesity and insulin resistance lead to activation of RAAS which in turn contributes to renal injury. The hormone aldosterone regulates electrolyte reabsorption and secretion in the kidneys leading to regulation of blood volume and pressure. Continuous infusing of aldosterone in rats fed a high salt diet led to podocyte injury and resultant proteinuria.[200] It is also suggested that both proteinuria and podocyte injury are related to aldosterone signaling in a rat model of metabolic syndrome.[201] Both groups of DH-IR pigs had increased aldosterone levels over controls and those with $U_{A/C}$ >30 had the highest values. The potential effects of elevated aldosterone are also seen in the decreased numbers of podocytes present in the DH-IR pigs. The contribution of insulin resistance to increased blood pressure via the actions of aldosterone is also observed in the DH-IR pigs. Study pigs with increased aldosterone levels had higher blood pressure than those with lower aldosterone levels. Findings in our IR pigs are consistent with those in non-diabetic insulin resistant humans who exhibit higher blood pressure in subjects with microalbuminuria.[176]

Obesity

Obesity may incite insulin resistance as well as add to its severity. Additional similarities between human studies and our findings include increased obesity in non-diabetic subjects with microalbuminuria.[176] When glomerular gene expression profiles from obesity related glomerulopathy (ORG) patients were compared to normal controls, ORG glomeruli were found to have significant changes in genes related to lipid metabolism, inflammatory cytokines and insulin resistance.[202] It is suggested that in addition to alterations in lipid metabolism, the upregulation of insulin resistance genes indicates a role for local insulin resistance in ORG lesion development. Another study showed a correlation between insulin resistance and decreased podocyte number and density in patients with ORG.[191] Weight increased significantly in both groups of DH-IR pigs over the yearlong study and backfat was significantly increased at 12 months in the DH-IR pigs with $U_{A/C}$ >30 compared to DH-IR pigs with $U_{A/C}$ <30. Other obesity related renal findings in our pigs include glomerular hypertrophy (glomerulomegaly), focal segmental glomerulosclerosis, decreased podocyte number and density, and GBM thickening.

Study Limitations

The use of a high fat, high salt diet leads to significant increases in weight gain, back fat and insulin resistance. The use of FH-IS pigs was to provide a control with comparable hypercholesterolemia while avoiding the change in metabolic parameters associated with a high fat diet.

The nephropathy seen in the DH-IR pigs resembles perihilar focal segmental

glomerulosclerosis (FSGS). FSGS presents with perihilar sclerosis in greater than 50% of glomeruli with segmental lesions, glomerulomegaly is usually present and it may be associated with obesity. In a study of patients with FSGS variants, those with perihylar FSGS had the highest frequency of hypertension.[203] The nephropathology seen in the DH-IR pigs with $U_{A/C}$ >30 does resemble perihylar FSGS, however, when the other metabolic factors are taken into consideration, an insulin resistant/hyperinsulinemic nephropathy seems more likely.

Summary

Increased insulin levels and insulin resistance have been independently associated with chronic kidney disease[19, 175, 176, 204] and are present early in the course of renal disease.[180, 205-207] Our goal was to characterize the extent to which functional and anatomic changes occur in our insulin resistant (IR) pigs and, most importantly, how closely these changes resemble those found in humans with IR. We have detected $U_{A/C}$ >30 in 9 of 17 (52%) IR pigs and 8 of these 9 (88.8%) had renal lesions consistent with insulin resistance. Hyperglycemia is a major determinant of risk for diabetic nephropathy in humans.[208, 209] Although our IR pigs did not develop overt diabetes, all had increases in insulin resistance and DH-IR pigs with $U_{A/C}$ >30 had increases in fructosamine at some point during the study consistent with an increase in glucose to some degree. Notably, insulin resistance in humans without diabetes is associated with an increased risk of developing chronic kidney disease and one of the key manifestations is microalbuminuria.[88-93] These data suggest that our IR pigs with $U_{A/C}$ >30,

moderate blood pressure elevations (at least 140/90), and increased aldosterone levels provide a model of the nephropathy found in IR humans without overt diabetes and that IR is necessary for initial glomerular changes (mesangial matrix expansion and podocyte injury) but insufficient for the nephropathy seen in our pigs with albuminuria. This work provides a model of early (pre-diabetic) renal damage that exhibits the associations between insulin resistance, hypertension, and obesity that are already established from observational studies in humans. The model should prove useful in elucidating mechanisms as well as testing treatment strategies for IR/hyperinsulinemic associated chronic kidney disease.

Chapter 5

Discussion and Future Directions

Summary

Development and characterization of this porcine model of insulin resistance and hyperlipidemia has identified an animal model that 1-develops severe and diffuse coronary and aortic atherosclerosis with morphology that recapitulates the disease phenotype that develops in IR humans, and 2-develops renal histopathology when albuminuria is present that is consistent with human insulin resistant/pre-diabetic nephropathy. Additionally, we have identified a promising set of aortic endothelial cell genes that can be used for further investigation of the endothelial dysfunction seen in these pigs and to develop novel methods for the noninvasive detection of endothelial dysfunction that occurs during atherogenesis in a relevant animal model. To our knowledge, this is the first description of an animal model of insulin resistance and hyperlipidemia that exhibits all of these components.

Cardiovascular Disease

Feeding insulin resistant pigs a high fat, high salt diet induced two atherosclerosis phenotypes: a severe and diffuse coronary and aortic atherosclerosis and a moderate coronary and aortic atherosclerosis. Surprisingly, the presence of insulin resistance alone did not correlate with the severity of

atherosclerotic disease. The most significant finding was that pigs in the severe atherosclerosis group had significantly higher oxLDL along with greater increases in fructosamine and aldosterone levels when compared to the moderate atherosclerosis group. Hence, the severity of atherosclerosis development may be enhanced through changes in oxidative stress that accompany feeding a high fat, high salt diet. Furthermore, the atherosclerotic lesions present in these pigs were morphologically identical to those found in human coronary atherosclerosis[28, 30] and included fibrous caps, intimal thickening, calcium deposits, medial thinning, hemorrhage, and necrosis.

Endothelial Cell Gene Expression

Differential gene expression studies from both normal and atherosclerotic endothelium of the severe and moderate disease groups identified genes involved in cell adhesion, migration, and proliferation or transcription and translation that were either significantly up- (*PTPRM, FAM5C, CLOCK, MYCPBP, LPHN2, HIPK2*) or down (*TMSB4X, EIF2S3, JARID1C*) -regulated in the severe disease group. Three genes (*MERP-1, RABGAP1L, COL12A1*) were uniquely expressed in atherosclerotic endothelium of the severe disease group and one gene (*SERPINI1*) was uniquely expressed in normal endothelium of the severe disease group. These have been shown in other studies and cell systems to be involved in cell adhesion[163, 166, 169, 172, 173], proliferation[165], and differentiation[165] as well as tissue remodeling[164]. Their identification provides a basis for further investigational studies on the role of oxLDL in endothelial dysfunction and atherosclerosis.

Renal Dysfunction

Feeding insulin resistant pigs a high fat, high salt diet also resulted in two different renal phenotypes. Approximately half of the animals exhibited albuminuria ($U_{A/C}$ >30), while the other half showed minimal or no albuminuria ($U_{A/C}$ <30). Both groups exhibited mesangial matrix expansion, decrease in podocyte density, and glomerulobasement membrane thickening, however, only the group with $U_{A/C}$ >30 had moderate elevation in blood pressure, and persistent elevations in aldosterone levels as well as glomerulosclerosis, tubulointerstitial fibrosis, and arteriolar hyalinosis – findings consistent with those seen in humans with insulin resistant/diabetic nephropathy.[181-183] Both groups also had a similar degree of hyperinsulinemia, decrease in insulin sensitivity, weight gain, backfat, lipid profiles, and inflammatory markers. The group with $U_{A/C}$ >30 provides a model of early (pre-diabetic) renal damage that exhibits the associations between insulin resistance, hypertension, and obesity that are already established. This model should prove useful in elucidating mechanisms as well as treatment strategies for IR/hyperinsulinemic associated chronic kidney disease.

Additional Studies

Endothelial dysfunction can lead to a host of hemostatic, thrombotic, inflammatory and other factors that may or may not have potential in predicting the onset and severity of atherosclerosis.[210, 211] Many of these factors have also been associated with diabetes mellitus and insulin resistance and may be predictive

of cardiovascular events in these patients.[212-214] It has been suggested that in IR-DM patients, activation of coagulation is driven by increases in glucose whereas impairments in fibrinolysis are driven by insulin levels.[215] Initial characterization of this model sought to evaluate selected plasma markers of coagulation, fibrinolysis, and endothelial cell dysfunction and their correlation with glycemic control, inflammatory markers, and atherosclerosis in hypercholesterolemic, hyperinsulinemic pigs. aPTT, PT, VWF and fibrinogen levels were assessed. No differences were seen between atherosclerosis groups for any of these parameters. However, aPTT for all pigs did significantly shorten (compared to baseline) at all time points measured over the course of the year-long study (Figure 5.1) suggesting some degree of change in coagulation most likely due to the hyperlipidemic state created by the high fat diet. This is supported by the finding that the greatest decreases occurred in the first 3 months and leveled off thereafter. There were no differences in PT, VWF, or fibrinogen over the course of the year. Due to a lack of any variation in these parameters between the two atherosclerotic groups, we did not further pursue coagulation or fibrinolytic changes.

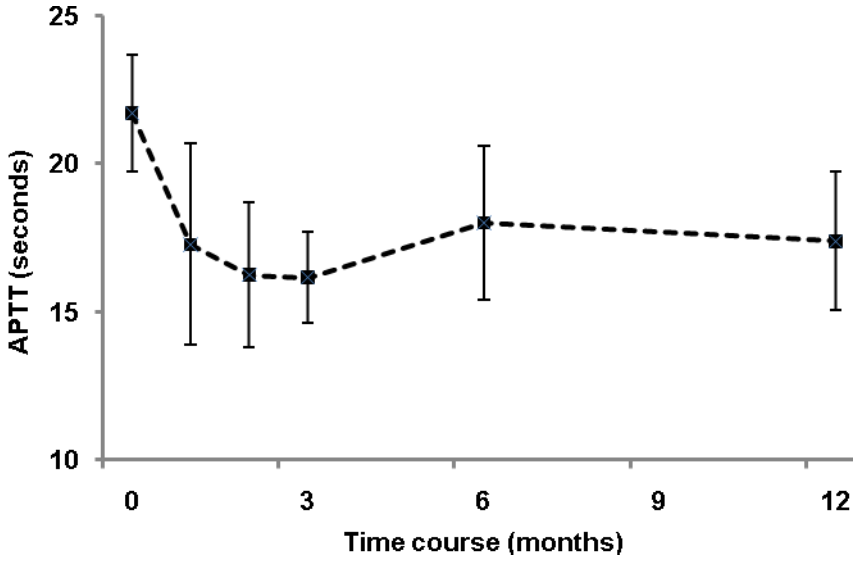

Figure 5.1 – aPTT measurements in DH-IR pigs. aPTT was measured by clot assay on the ST4 (Diagnostica Stago, Parsippany, NJ) using plasma from all 18 study pigs at baseline, 1, 2, 3, 6, and 12 months. Results are mean ± SD for all pigs at each time point. Baseline values fall within normal ranges of those reported for pigs.[216]

Future directions

A second study is currently underway to confirm and strengthen the data presented here. An additional 20 pigs have been entered into a comparable year-long high fat, high salt diet study. Furthermore, 5 pigs have been added that will not receive high fat, high salt diet (only standard pig chow) and therefore serve as normocholesterolemic controls. By using a combined total of 38 animals with insulin resistance and hyperlipidemia we should be able to 1-follow elevations in oxLDL, fructosamine, and aldosterone to more accurately predict the extent to which they correlate with atherosclerosis severity, 2- increase the number of aortic EC RNA samples collected in order to substantiate genes identified in Chapter 3 and 3-to better monitor renal status in order to determine specificity and sensitivity with which renal histopathological findings may be predicted by elevated urinary albumin. In order to better assess any renal insufficiencies over the course of the year, urine is being collected monthly. This will hopefully allow us to better evaluate the time of onset, frequency and degree of albuminuria.

Pigs from both studies are from a mixed genetic background, including Spotted Poland/China and Yorkshire crosses as well as pigs that are heterozygous for familial hypercholesterolemic (one normal allele and one FH allele). As mentioned in previous chapters, cholesterol levels at baseline and while ingesting a high fat, high salt diet are comparable for both groups of pigs and heterozygous familial hypercholesterolemic (HFH) pigs do not exhibit hypercholesterolemia unless they are fed a high fat diet. Nonetheless we controlled for this genotype in our

analyses of severity of atherosclerosis and metabolic variables. At this point we do not feel that the presence of one FH allele is influencing the data presented. The present study of 18 pigs contains 10 normal and 8 HFH pigs and the additional study of 20 pigs contains 6 normal and 14 HFH pigs. This gives us a combined total of 16 normal and 22 HFH. Based on statistical power analyses from results of the first 18 pigs, the addition of 20 more pigs should render a sufficient number of animals to determine if the FH allele is exerting an influence on atherosclerosis severity or metabolic variables. The inclusion of 5 normocholesterolemic (2 normal and 3 HFH) controls will allow us to look at the effects of hyperinsulinemia/insulin resistance independent of increases in cholesterol and changes in lipoprotein profiles.

Additionally, this pig model has already been used in pilot studies for the *in vivo* detection of nonstenotic plaques and the material assessment of these plaques via a novel imaging method known as acoustic radiation force impulse (ARFI) ultrasound.[217] These studies have shown ARFI detection of nonstenotic plaques not revealed by conventional B-mode ultrasound as well as correlations between elastin and collagen contents and peak displacement and recovery time parameters.[217] During the second study (mentioned above) all 25 pigs (20 diet fed and 5 control) will be monitored via ARFI for changes in femoral artery atherosclerosis over the course of the year. Images taken at 12 months will be compared with ex vivo measurements of atherosclerosis and histological assessments of vessel material content. Results of ARFI assessments will allow us to monitor the progression of atherosclerosis over the year as well as to determine if

a more aggressive atherosclerosis phenotype is associated with increases in oxLDL and fructosamine.

This work supports the long range goal of this laboratory: to provide the scientific community with a well-characterized, reproducible animal model of insulin resistance that develops human-like coronary and aortic atherosclerosis and kidney disease. This model will not only be of considerable value for mechanistic studies that investigate the underlying pathophysiology but also for intervention studies to test new therapeutic approaches.

Chapter 6

Related Publications and Presentations During the Course of this Work

Peer Reviewed Publications:

Bellinger DA, **Merricks EP**, Nichols TC. *Diabetes,* in *The Minipig in Biomedical Research*, Peter McAnulty, Editor. 2010, CRC Press (Taylor & Francis Group), publication in progress.

Maile LA, Busby WH, Nichols TC, Bellinger DA, **Merricks EP**, Rowland M, Veluvolu U, Clemmons DR. A Monoclonal Antibody Against aVb3 Integrin Inhibits Development of Atherosclerotic Lesions in Diabetic Pigs. *Sci. Transl. Med*. 2, 18ra11 (2010).

Behler RH, Nichols TC, Zhu H, **Merricks EP**, Gallippi CM. ARFI Imaging for Noninvasive Material Characterization of Atherosclerosis Part II: Toward In Vivo Characterization. *Ultrasound Med Biol*. 2009 Feb;35(2):278-95. Epub 2008 Nov 21.

Nichols TC, Busby WH Jr, **Merricks E**, Sipos J, Rowland M, Sitko K, Clemmons DR. Protease Resistant IGFBP-4 Inhibits IGF-I Actions and Neointimal Expansion in a Porcine Model of Neointimal Hyperplasia. *Endocrinology*. 2007 Jul 19

Dumont D, Behler R, Nichols TC, **Merricks EP**, and Gallipp C. (2006) Toward ARFI Classification of Atherosclerosis for Non-Invasive CVD Assessment. *Ultrasound in Medicine and Biology.* , 32:1703–1711, 2006.

Bellinger DA, **Merricks EP**, Nichols TC. Swine models of type 2 diabetes mellitus: Insulin resistance, glucose tolerance, and cardiovascular complications. ILAR Journal. 2006;47:243-258.

Brodala N, **Merricks EP**, Bellinger DA, Damrongsri D, Offenbacher S, Beck J, Madianos P, Sotres D, Chang YL, Koch G, Nichols TC. Porphyromonas gingivalis bacteremia induces coronary and aortic atherosclerosis in normocholesterolemic and hypercholesterolemic pigs. *Arterioscler Thromb Vasc Biol*. 2005 Jul;25(7):1446-51. Epub 2005 Apr 21.

Baer JT, duLaney TV, Wyrick PB, McCain AD, Fischer TA, **Merricks EP**, Baldwin AS, Nichols TC: NF-κB activation in endothelium by *Chlamydia pneumoniae* without active infection. *J Infect Dis*., 203:1094-1097, 2003.

Pye J, Ardeshirpour F, McCain A, Bellinger DA, **Merricks E**, Adams J, Elliott PJ, Pien C, Fischer TH, Baldwin AS, Nichols TC: Proteasome inhibition ablates activation of NF-κB in myocardial reperfusion and reduces reperfusion injury. *Am. J. Physiol Heart Circ Physiol* 284: H919-H926, 2003.

Abstracts and Conference Proceedings:

Merricks E, Bellinger D, Clemmons D, Jennette C, Raymer R, and Nichols T. Albuminuria and Renal Histopathology in Hyperlipidemic, Insulin Resistant Swine. *FASEB J.* 2009 23:930.6

Presnell SC, Bruce A, Wallace SM, Choudhury S, Kelley RW, Tatsumi P, Werdin E, Rivera E, **Merricks E,** Nichols TC, Jennette JC, Jayo MJ, and Bertram TA. Isolation and Characterization of Bioresponsive Renal Cells from Human and Large Mammal with Chronic Renal Failure. *FASEB J.* 2009 23:LB143

Merricks EP, Bellinger DA, Nyangweso P, Deans C, Koch G, Busby WH, Clemmons DR, Raymer RA, Nichols TC. Severe and diffuse coronary and aortic atherosclerosis in hyperlipidemic insulin resistant pigs. Proceedings of the Swine in Biomedical Research Conference, San Diego, CA, 2008, pg 59.

Merricks E, Bellinger D, Clemmons D, Jennette C, Raymer R, Nichols T. Albuminuria and renal renal histopathology in hyperlipidemic, hyperinsulinemic swine. Proceedings of the Swine in Biomedical Research Conference, San Diego, CA, 2008, pg 57.

Behler RH, Nichols TC, **Merricks EP**, and Gallippi CM. ARFI Ultrasound for Discrimination of Calcification in Arterial Plaques: Additional Progress Toward Improved Atherosclerosis Imaging in Women. Journal of Womens Health. 17(8):1243, 2008

Behler RH, Nichols TC, **Merricks EP**, and Gallippi CM. The Impact of Calcium on ARFI Imaging of Atherosclerotic Plaques. The Seventh International Conference on the Ultrasonic Measurement and Imaging of Tissue Elasticity. Lake Travis, Austin, Texas, USA. 6 pages, October 2008.

Behler RH, Nichols TC, **Merricks EP**, and Gallippi CM. Comparison of Multiple Beam Sequences in Arterial ARFI Imaging. 2008 IEEE International Ultrasonics Symposium Proceedings, Beijing, China. 6 pages, October 2008.

Behler RH, **Merricks EP**, Nichols TC, and Gallippi CM. In Vivo ARFI Atherosclerosis Imaging with Validation in a Relevant Pig Model of CVD. 19th International Congress on Acoustics 38(3-4) ult-01-007 (6 pages), Madrid, Spain, September 2007.

Behler RH, Nichols TC, **Merricks EP**, and Gallippi CM. ARFI Ultrasound for Enhanced Delineation of Atherosclerosis in Women. *Journal of Women's Health* 16(8)1112, 2007

Behler RH, Dumont DM, Nichols TC, **Merricks EP**, and Gallippi CM. ARFI ultrasound for characterizing atherosclerosis. IEEE Ultrasonics Symposium, 2006. pages 722–727, 2006.

Behler RH, Nichols TC, **Merricks EP**, et al. A Rigid Wall Approach to Physiological Motion Rejection in Arterial ARFI Imaging: Simulation and In Vivo Demonstration. IEEE Ultrasonics Symposium, 2006. 722–727, 2006

Merricks EP, Mccain AS, Baer JT, Du Laney TV, Wyrick PB, Fischer TH, Baldwin AS, Nichols TC. NF-κB Activation in Endothelium by Chlamydia pneumoniae without Active Infection. CCID Research Day 2003

Literature Cited

1. http://diabetes.niddk.nih.gov/dm/pubs/statistics. [cited.

2. www.diabetesatlas.org. [cited.

3. Ervin, R.B., *Prevalence of metabolic syndrome among adults 20 years of age and over, by sex, age, race and ethnicity, and body mass index: United States, 2003-2006.* Natl Health Stat Report, 2009(13): p. 1-7.

4. Kahn, S.E., R.L. Hull, and K.M. Utzschneider, *Mechanisms linking obesity to insulin resistance and type 2 diabetes.* Nature, 2006. **444**(7121): p. 840-6.

5. Qatanani, M. and M.A. Lazar, *Mechanisms of obesity-associated insulin resistance: many choices on the menu.* Genes Dev, 2007. **21**(12): p. 1443-55.

6. Kahn, B.B. and J.S. Flier, *Obesity and insulin resistance.* J Clin Invest, 2000. **106**(4): p. 473-81.

7. Ogden, C.L., et al., *Obesity among adults in the United States--no statistically significant chance since 2003-2004.* NCHS Data Brief, 2007(1): p. 1-8.

8. Bonetti, P.O., L.O. Lerman, and A. Lerman, *Endothelial dysfunction: a marker of atherosclerotic risk.* Arterioscler Thromb Vasc Biol, 2003. **23**(2): p. 168-75.

9. Vedanthan, R. and V. Fuster, *Disease Prevention: The moving target of global cardiovascular health.* Nat Rev Cardiol, 2009. **6**(5): p. 327-8.

10. Hsueh, W.A., C.J. Lyon, and M.J. Quinones, *Insulin resistance and the endothelium.* Am J Med, 2004. **117**(2): p. 109-17.

11. Hsueh, W.A. and M.J. Quinones, *Role of endothelial dysfunction in insulin resistance.* Am J Cardiol, 2003. **92**(4A): p. 10J-17J.

12. Pyorala, K., *Relationship of glucose tolerance and plasma insulin to the incidence of coronary heart disease: results from two population studies in Finland.* Diabetes Care, 1979. **2**(2): p. 131-41.

13. Welborn, T.A. and K. Wearne, *Coronary heart disease incidence and cardiovascular mortality in Busselton with reference to glucose and insulin concentrations.* Diabetes Care, 1979. **2**(2): p. 154-60.

14. Ducimetiere, P., et al., *Relationship of plasma insulin levels to the incidence of myocardial infarction and coronary heart disease mortality in a middle-aged population.* Diabetologia, 1980. **19**(3): p. 205-10.

15. Fontbonne, A., et al., *Hyperinsulinaemia as a predictor of coronary heart disease mortality in a healthy population: the Paris Prospective Study, 15-year follow-up.* Diabetologia, 1991. **34**(5): p. 356-61.

16. McNeill, A.M., et al., *Prevalence of coronary heart disease and carotid arterial thickening in patients with the metabolic syndrome (The ARIC Study).* Am J Cardiol, 2004. **94**(10): p. 1249-54.

17. McNeill, A.M., et al., *The metabolic syndrome and 11-year risk of incident cardiovascular disease in the atherosclerosis risk in communities study.* Diabetes Care, 2005. **28**(2): p. 385-90.

18. Ballantyne, C.M., et al., *Metabolic syndrome risk for cardiovascular disease and diabetes in the ARIC study.* Int J Obes (Lond), 2008. **32 Suppl 2**: p. S21-4.

19. Sarafidis, P.A. and L.M. Ruilope, *Insulin resistance, hyperinsulinemia, and renal injury: mechanisms and implications.* Am J Nephrol, 2006. **26**(3): p. 232-44.

20. Martins, C., et al., *Insulin resistance is associated with circulating fibrinogen levels in nondiabetic patients receiving peritoneal dialysis.* J Ren Nutr, 2007. **17**(2): p. 132-7.

21. Yamagata, K., et al., *Risk factors for chronic kidney disease in a community-based population: a 10-year follow-up study.* Kidney Int, 2007. **71**(2): p. 159-66.

22. Chandie Shaw, P.K., et al., *Central obesity is an independent risk factor for albuminuria in nondiabetic South Asian subjects.* Diabetes Care, 2007. **30**(7): p. 1840-4.

23. Bellinger, D.A., E.P. Merricks, and T.C. Nichols, *Swine models of type 2 diabetes mellitus: insulin resistance, glucose tolerance, and cardiovascular complications.* Ilar J, 2006. **47**(3): p. 243-58.

24. Zimmet, P., K.G. Alberti, and J. Shaw, *Global and societal implications of the diabetes epidemic.* Nature, 2001. **414**(6865): p. 782-7.

25. Kohen-Avramoglu, R., A. Theriault, and K. Adeli, *Emergence of the metabolic syndrome in childhood: an epidemiological overview and mechanistic link to dyslipidemia.* Clin Biochem, 2003. **36**(6): p. 413-20.

26. Pinhas-Hamiel, O. and P. Zeitler, *Acute and chronic complications of type 2 diabetes mellitus in children and adolescents.* Lancet, 2007. **369**(9575): p. 1823-31.

27. Meigs, J.B., et al., *Coronary artery calcification in type 2 diabetes and insulin resistance: the framingham offspring study.* Diabetes Care, 2002. **25**(8): p. 1313-9.

28. Burke, A.P., et al., *Morphologic findings of coronary atherosclerotic plaques in diabetics: a postmortem study.* Arterioscler Thromb Vasc Biol, 2004. **24**(7): p. 1266-71.

29. Graner, M., et al., *Insulin resistance as predictor of the angiographic severity and extent of coronary artery disease.* Ann Med, 2007. **39**(2): p. 137-44.

30. Virmani, R., et al., *Lessons from sudden coronary death: a comprehensive morphological classification scheme for atherosclerotic lesions.* Arterioscler Thromb Vasc Biol, 2000. **20**(5): p. 1262-75.

31. Weckbach, S., et al., *Systemic cardiovascular complications in patients with long-standing diabetes mellitus: comprehensive assessment with whole-body magnetic resonance imaging/magnetic resonance angiography.* Invest Radiol, 2009. **44**(4): p. 242-50.

32. Angeja, B.G., et al., *Impact of diabetes mellitus on epicardial and microvascular flow after fibrinolytic therapy.* Am Heart J, 2002. **144**(4): p. 649-56.

33. Flaherty, J.D. and C.J. Davidson, *Diabetes and coronary revascularization.* Jama, 2005. **293**(12): p. 1501-8.

34. Finn, A.V., et al., *Drug-eluting stents for diabetes mellitus: a rush to judgment?* J Am Coll Cardiol, 2005. **45**(4): p. 479-83.

35. Yamagishi, S., et al., *Molecular mechanism for accelerated atherosclerosis in diabetes and its potential therapeutic intervention.* Int J Clin Pharmacol Res, 2004. **24**(4): p. 129-34.

36. Moreno, P.R. and V. Fuster, *New aspects in the pathogenesis of diabetic atherothrombosis.* J Am Coll Cardiol, 2004. **44**(12): p. 2293-300.

37. Hsueh, W., et al., *Recipes for creating animal models of diabetic cardiovascular disease.* Circ Res, 2007. **100**(10): p. 1415-27.

38. Keren, P., et al., *Effect of hyperglycemia and hyperlipidemia on atherosclerosis in LDL receptor-deficient mice: establishment of a combined model and association with heat shock protein 65 immunity.* Diabetes, 2000. **49**(6): p. 1064-9.

39. Forbes, J.M., et al., *Advanced glycation end product interventions reduce diabetes-accelerated atherosclerosis.* Diabetes, 2004. **53**(7): p. 1813-23.

40. Goldberg, I.J. and H.M. Dansky, *Diabetic vascular disease: an experimental objective.* Arterioscler Thromb Vasc Biol, 2006. **26**(8): p. 1693-701.

41. Kanter, J.E., et al., *Do glucose and lipids exert independent effects on atherosclerotic lesion initiation or progression to advanced plaques?* Circ Res, 2007. **100**(6): p. 769-81.

42. Kunjathoor, V.V., D.L. Wilson, and R.C. LeBoeuf, *Increased atherosclerosis in streptozotocin-induced diabetic mice.* J Clin Invest, 1996. **97**(7): p. 1767-73.

43. Wu, L., et al., *Addition of dietary fat to cholesterol in the diets of LDL receptor knockout mice: effects on plasma insulin, lipoproteins, and atherosclerosis.* J Lipid Res, 2006. **47**(10): p. 2215-22.

44. Goldberg, I.J., *Why does diabetes increase atherosclerosis? I don't know!* J Clin Invest, 2004. **114**(5): p. 613-5.

45. Roy, H., et al., *VEGF-A, VEGF-D, VEGF receptor-1, VEGF receptor-2, NF-kappaB, and RAGE in atherosclerotic lesions of diabetic Watanabe heritable hyperlipidemic rabbits.* Faseb J, 2006. **20**(12): p. 2159-61.

46. Tanaka, A., et al., *Insulin and nateglinide reduce monocyte adhesion to endothelial cells in Goto-Kakizaki rats exhibiting repetitive blood glucose fluctuation.* Biochem Biophys Res Commun, 2006. **350**(1): p. 195-201.

47. Xi, S., et al., *A minipig model of high-fat/high-sucrose diet-induced diabetes and atherosclerosis.* Int J Exp Pathol, 2004. **85**(4): p. 223-31.

48. Dixon, J.L., et al., *Dyslipidemia and vascular dysfunction in diabetic pigs fed an atherogenic diet.* Arterioscler Thromb Vasc Biol, 1999. **19**(12): p. 2981-92.

49. Gerrity, R.G., et al., *Diabetes-induced accelerated atherosclerosis in swine.* Diabetes, 2001. **50**(7): p. 1654-65.

50. Hasler-Rapacz, J.O., et al., *Familial and diet-induced hypercholesterolemia in swine. Lipid, ApoB, and ApoA-I concentrations and distributions in plasma and lipoprotein subfractions.* Arterioscler Thromb, 1994. **14**(6): p. 923-30.

51. Hasler-Rapacz, J., et al., *Identification of a mutation in the low density lipoprotein receptor gene associated with recessive familial hypercholesterolemia in swine.* Am J Med Genet, 1998. **76**(5): p. 379-86.

52. Grunwald, K.A., et al., *Identification of a novel Arg-->Cys mutation in the LDL receptor that contributes to spontaneous hypercholesterolemia in pigs.* J Lipid Res, 1999. **40**(3): p. 475-85.

53. Nichols, T.C., et al., *Reduction in atherosclerotic lesion size in pigs by alphaVbeta3 inhibitors is associated with inhibition of insulin-like growth factor-I-mediated signaling.* Circ Res, 1999. **85**(11): p. 1040-5.

54. Brodala, N., et al., *Porphyromonas gingivalis bacteremia induces coronary and aortic atherosclerosis in normocholesterolemic and hypercholesterolemic pigs.* Arterioscler Thromb Vasc Biol, 2005. **25**(7): p. 1446-51.

55. *Nutrient Requirements of Swine*. Tenth Revised Edition ed. Subcommitte on Swine Nutrition. 1998: The National Academies Press.

56. Bergman, R.N., D.T. Finegood, and M. Ader, *Assessment of insulin sensitivity in vivo.* Endocr Rev, 1985. **6**(1): p. 45-86.

57. Bergman, R.N., et al., *Equivalence of the insulin sensitivity index in man derived by the minimal model method and the euglycemic glucose clamp.* J Clin Invest, 1987. **79**(3): p. 790-800.

58. Moses, A.C., et al., *Recombinant human insulin-like growth factor I increases insulin sensitivity and improves glycemic control in type II diabetes.* Diabetes, 1996. **45**(1): p. 91-100.

59. O'Connell, T. and D.R. Clemmons, *IGF-I/IGF-binding protein-3 combination improves insulin resistance by GH-dependent and independent mechanisms.* J Clin Endocrinol Metab, 2002. **87**(9): p. 4356-60.

60. Black, M.H., et al., *Evidence of interaction between PPARG2 and HNF4A contributing to variation in insulin sensitivity in Mexican Americans.* Diabetes, 2008. **57**(4): p. 1048-56.

61. Sam, S., et al., *Evidence for pancreatic beta-cell dysfunction in brothers of women with polycystic ovary syndrome.* Metabolism, 2008. **57**(1): p. 84-9.

62. Hausman, G.J., D.R. Campion, and G.B. Thomas, *Adipose tissue cellularity and histochemistry in fetal swine as affected by genetic selection for high or low backfat.* J Lipid Res, 1983. **24**(3): p. 223-8.

63. Buhlinger, C.A., et al., *Body composition, in vitro lipid metabolism and skeletal muscle characteristics in fast-growing, lean and in slow-growing, obese pigs at equal age and weight.* Growth, 1978. **42**(2): p. 225-36.

64. Etherton, T.D., *Subcutaneous adipose tissue cellularity of swine with different propensities for adipose tissue growth.* Growth, 1980. **44**(3): p. 182-91.

65. Etherton, T.D. and P.M. Kris-Etherton, *Characterization of plasma lipoproteins in swine with different propensities for obesity.* Lipids, 1980. **15**(10): p. 823-9.

66. McNamara, J.P. and R.J. Martin, *Muscle and adipose tissue lipoprotein lipase in fetal and neonatal swine as affected by genetic selection for high or low backfat.* J Anim Sci, 1982. **55**(5): p. 1057-61.

67. Dyson, M.C., et al., *Components of metabolic syndrome and coronary artery disease in female Ossabaw swine fed excess atherogenic diet.* Comp Med, 2006. **56**(1): p. 35-45.

68. Krege, J.H., et al., *A noninvasive computerized tail-cuff system for measuring blood pressure in mice.* Hypertension, 1995. **25**(5): p. 1111-5.

69. Mesangeau, D., D. Laude, and J.L. Elghozi, *Early detection of cardiovascular autonomic neuropathy in diabetic pigs using blood pressure and heart rate variability.* Cardiovasc Res, 2000. **45**(4): p. 889-99.

70. Springett, R., Y. Sakata, and D.T. Delpy, *Precise measurement of cerebral blood flow in newborn piglets from the bolus passage of indocyanine green.* Phys Med Biol, 2001. **46**(8): p. 2209-25.

71. Kalela, A., et al., *Association of serum sialic acid and MMP-9 with lipids and inflammatory markers.* Eur J Clin Invest, 2000. **30**(2): p. 99-104.

72. Lau, C.L., et al., *The role of antibodies and von Willebrand factor in discordant pulmonary xenotransplantation.* Am J Transplant, 2003. **3**(9): p. 1065-75.

73. Daghini, E., et al., *Acute inhibition of the endogenous xanthine oxidase improves renal hemodynamics in hypercholesterolemic pigs.* Am J Physiol Regul Integr Comp Physiol, 2006. **290**(3): p. R609-15.

74. Chade, A.R., et al., *Effects of proteasome inhibition on the kidney in experimental hypercholesterolemia.* J Am Soc Nephrol, 2005. **16**(4): p. 1005-12.

75. Chade, A.R., et al., *Pathways of renal fibrosis and modulation of matrix turnover in experimental hypercholesterolemia.* Hypertension, 2005. **46**(4): p. 772-9.

76. Nichols, T.C., et al., *Porcine von Willebrand disease and atherosclerosis. Influence of polymorphism in apolipoprotein B100 genotype.* Am J Pathol, 1992. **140**(2): p. 403-15.

77. Gerrity, R.G., J.A. Goss, and L. Soby, *Control of monocyte recruitment by chemotactic factor(s) in lesion-prone areas of swine aorta.* Arteriosclerosis, 1985. **5**(1): p. 55-66.

78. Thomas, W., Lee KT, Kim DN, *Pathogenesis of Atherosclerosis in the Abdominal aorta and coronary arteries of swine in the first 90 days of hyperlipidemic diet*, Tumbleson ME, Editor. 1985, Plenum Press. p. 1511-1525.

79. Thomas, W.A., K.T. Lee, and D.N. Kim, *Cell population kinetics in atherogenesis. Cell births and losses in intimal cell mass-derived lesions in the abdominal aorta of swine.* Ann N Y Acad Sci, 1985. **454**: p. 305-15.

80. Mohiaddin, R.H., et al., *Glagov remodeling of the atherosclerotic aorta demonstrated by cardiovascular magnetic resonance: the CORDA asymptomatic subject plaque assessment research (CASPAR) project.* J Cardiovasc Magn Reson, 2004. **6**(2): p. 517-25.

81. Benvenuti, L.A., et al., *Different patterns of atherosclerotic remodeling in the thoracic and abdominal aorta.* Clinics (Sao Paulo), 2005. **60**(5): p. 355-60.

82. Glagov, S., et al., *Compensatory enlargement of human atherosclerotic coronary arteries.* N Engl J Med, 1987. **316**(22): p. 1371-5.

83. Holvoet, P., et al., *LDL hypercholesterolemia is associated with accumulation of oxidized LDL, atherosclerotic plaque growth, and compensatory vessel enlargement in coronary arteries of miniature pigs.* Arterioscler Thromb Vasc Biol, 1998. **18**(3): p. 415-22.

84. Otis, C.R., B.R. Wamhoff, and M. Sturek, *Hyperglycemia-induced insulin resistance in diabetic dyslipidemic Yucatan swine.* Comp Med, 2003. **53**(1): p. 53-64.

85. Laber-Laird, K., et al., *Effects of isoflurane anesthesia on glucose tolerance and insulin secretion in Yucatan minipigs.* Lab Anim Sci, 1992. **42**(6): p. 579-81.

86. Howard, B.V., *Insulin resistance and lipid metabolism.* Am J Cardiol, 1999. **84**(1A): p. 28J-32J.

87. Taskinen, M.R., *Insulin resistance and lipoprotein metabolism.* Curr Opin Lipidol, 1995. **6**(3): p. 153-60.

88. Spijkerman, A.M., et al., *Microvascular complications at time of diagnosis of type 2 diabetes are similar among diabetic patients detected by targeted screening and patients newly diagnosed in general practice: the hoorn screening study.* Diabetes Care, 2003. **26**(9): p. 2604-8.

89. Kurella, M., J.C. Lo, and G.M. Chertow, *Metabolic syndrome and the risk for chronic kidney disease among nondiabetic adults.* J Am Soc Nephrol, 2005. **16**(7): p. 2134-40.

90. Sosenko, J.M., et al., *Albuminuria in recent-onset type 2 diabetes: the Strong Heart Study.* Diabetes Care, 2002. **25**(6): p. 1078-84.

91. Kohler, K.A., et al., *Risk factors for microalbuminuria in black americans with newly diagnosed type 2 diabetes.* Am J Kidney Dis, 2000. **36**(5): p. 903-13.

92. Lucove, J., et al., *Metabolic syndrome and the development of CKD in American Indians: the Strong Heart Study.* Am J Kidney Dis, 2008. **51**(1): p. 21-8.

93. Bonnet, F., et al., *Waist circumference and the metabolic syndrome predict the development of elevated albuminuria in non-diabetic subjects: the DESIR Study.* J Hypertens, 2006. **24**(6): p. 1157-63.

94. Wahid, S.T., et al., *Serum fructosamine as a marker of 5-year risk of developing diabetes mellitus in patients exhibiting stress hyperglycaemia.* Diabet Med, 2002. **19**(7): p. 543-8.

95. Higgins, P.J., R.L. Garlick, and H.F. Bunn, *Glycosylated hemoglobin in human and animal red cells. Role of glucose permeability.* Diabetes, 1982. **31**(9): p. 743-8.

96. Herdzik, E., K. Safranow, and K. Ciechanowski, *Diagnostic value of fasting capillary glucose, fructosamine and glycosylated haemoglobin in detecting diabetes and other*

glucose tolerance abnormalities compared to oral glucose tolerance test. Acta Diabetol, 2002. **39**(1): p. 15-22.

97. Thornalley, P.J., *Glycation, receptor-mediated cell activation and vascular complications of diabetes.* Diab Vasc Dis Res, 2004. **1**(1): p. 21-2.

98. Zhang, Y.F., et al., *Hyperglycaemia after glucose loading is a major predictor of preclinical atherosclerosis in nondiabetic subjects.* Clin Endocrinol (Oxf), 2006. **64**(2): p. 153-7.

99. Gokulakrishnan, K., et al., *Oxidized low-density lipoprotein and intimal medial thickness in subjects with glucose intolerance: the Chennai Urban Rural Epidemiology Study-25.* Metabolism, 2007. **56**(2): p. 245-50.

100. Yegin, A., T. Ozben, and H. Yegin, *Glycation of lipoproteins and accelerated atherosclerosis in non-insulin-dependent diabetes mellitus.* Int J Clin Lab Res, 1995. **25**(3): p. 157-61.

101. Nilsson, J., et al., *Oxidized LDL antibodies in treatment and risk assessment of atherosclerosis and associated cardiovascular disease.* Curr Pharm Des, 2007. **13**(10): p. 1021-30.

102. Meisinger, C., et al., *Plasma oxidized low-density lipoprotein, a strong predictor for acute coronary heart disease events in apparently healthy, middle-aged men from the general population.* Circulation, 2005. **112**(5): p. 651-7.

103. Zhang, L., et al., *Diabetes-induced oxidative stress and low-grade inflammation in porcine coronary arteries.* Circulation, 2003. **108**(4): p. 472-8.

104. Ishigaki, Y., et al., *Impact of plasma oxidized low-density lipoprotein removal on atherosclerosis.* Circulation, 2008. **118**(1): p. 75-83.

105. Schwenke, D.C., et al., *Differences in LDL oxidizability by glycemic status: the insulin resistance atherosclerosis study.* Diabetes Care, 2003. **26**(5): p. 1449-55.

106. Hussein, O.A., et al., *LDL oxidation is associated with increased blood hemoglobin A1c levels in diabetic patients.* Clin Chim Acta, 2007. **377**(1-2): p. 114-8.

107. Veiraiah, A., *Hyperglycemia, lipoprotein glycation, and vascular disease.* Angiology, 2005. **56**(4): p. 431-8.

108. Verhamme, P., et al., *Dietary cholesterol withdrawal reduces vascular inflammation and induces coronary plaque stabilization in miniature pigs.* Cardiovasc Res, 2002. **56**(1): p. 135-44.

109. Knopp, R.H. and P. Paramsothy, *Oxidized LDL and abdominal obesity: a key to understanding the metabolic syndrome.* Am J Clin Nutr, 2006. **83**(1): p. 1-2.

110. Shin, M.J., et al., *Weight loss effect on inflammation and LDL oxidation in metabolically healthy but obese (MHO) individuals: low inflammation and LDL oxidation in MHO women.* Int J Obes (Lond), 2006. **30**(10): p. 1529-34.

111. Ho, R.C., et al., *Whole-body insulin sensitivity, low-density lipoprotein (LDL) particle size, and oxidized LDL in overweight, nondiabetic men.* Metabolism, 2002. **51**(11): p. 1478-83.

112. de Castro, S.H., H.C. Castro-Faria-Neto, and M.B. Gomes, *Association of postprandial hyperglycemia with in vitro LDL oxidation in non-smoking patients with type 1 diabetes--a cross-sectional study.* Rev Diabet Stud, 2005. **2**(3): p. 157-64.

113. Schindhelm, R.K., et al., *Fasting and postprandial glycoxidative and lipoxidative stress are increased in women with type 2 diabetes.* Diabetes Care, 2007. **30**(7): p. 1789-94.

114. Serin, O., et al., *Serum oxidized low density lipoprotein, paraoxonase 1 and lipid peroxidation levels during oral glucose tolerance test.* Horm Metab Res, 2007. **39**(3): p. 207-11.

115. Okopien, B., et al., *The risk of atherosclerosis in patients with impaired glucose tolerance.* Res Commun Mol Pathol Pharmacol, 2003. **113-114**: p. 87-95.

116. Edwards, I.J., et al., *Glycation of plasma low density lipoproteins increases interaction with arterial proteoglycans.* Diabetes Res Clin Pract, 1999. **46**(1): p. 9-18.

117. Edwards, I.J., et al., *Improved glucose control decreases the interaction of plasma low-density lipoproteins with arterial proteoglycans.* Metabolism, 2002. **51**(10): p. 1223-9.

118. Inoue, I., et al., *Acarbose ameliorates atherogenecity of low-density lipoprotein in patients with impaired glucose tolerance.* Metabolism, 2006. **55**(7): p. 946-52.

119. Paniagua, J.A., et al., *Oxidized-LDL levels are changed during short-term serum glucose variations and lowered with statin treatment in early Type 2 diabetes: a study of endothelial function and microalbuminuria.* Diabet Med, 2005. **22**(12): p. 1647-56.

120. Akanji, A.O., N. Abdella, and O.A. Mojiminiyi, *Determinants of glycated LDL levels in nondiabetic and diabetic hyperlipidaemic patients in Kuwait.* Clin Chim Acta, 2002. **317**(1-2): p. 171-6.

121. Karolkiewicz, J., et al., *Insulin resistance, oxidative stress markers and the blood antioxidant system in overweight elderly men.* Aging Male, 2006. **9**(3): p. 159-63.

122. Sies, H., W. Stahl, and A. Sevanian, *Nutritional, dietary and postprandial oxidative stress.* J Nutr, 2005. **135**(5): p. 969-72.

123. Tushuizen, M.E., et al., *Two consecutive high-fat meals affect endothelial-dependent vasodilation, oxidative stress and cellular microparticles in healthy men.* J Thromb Haemost, 2006. **4**(5): p. 1003-10.

124. Cooper, S.A., et al., *Renin-angiotensin-aldosterone system and oxidative stress in cardiovascular insulin resistance.* Am J Physiol Heart Circ Physiol, 2007. **293**(4): p. H2009-23.

125. Joy, T.R. and R.A. Hegele, *The failure of torcetrapib: what have we learned?* Br J Pharmacol, 2008. **154**(7): p. 1379-81.

126. Forrest, M.J., et al., *Torcetrapib-induced blood pressure elevation is independent of CETP inhibition and is accompanied by increased circulating levels of aldosterone.* Br J Pharmacol, 2008. **154**(7): p. 1465-73.

127. LaVange, L.M. and G.G. Koch, *Rank score tests.* Circulation, 2006. **114**(23): p. 2528-33.

128. Renard, C. and E. Van Obberghen, *Role of diabetes in atherosclerotic pathogenesis. What have we learned from animal models?* Diabetes Metab, 2006. **32**(1): p. 15-29.

129. Kobayashi, T., et al., *Changes in aortic endothelial gene expressions and relaxation responses following chronic short-term insulin treatment in diabetic rats.* Atherosclerosis, 2006. **185**(1): p. 47-57.

130. Cosentino, F., et al., *High glucose increases nitric oxide synthase expression and superoxide anion generation in human aortic endothelial cells.* Circulation, 1997. **96**(1): p. 25-8.

131. Seo, D., et al., *Gene expression phenotypes of atherosclerosis.* Arterioscler Thromb Vasc Biol, 2004. **24**(10): p. 1922-7.

132. Simmons, C.A., J. Zilberberg, and P.F. Davies, *A rapid, reliable method to isolate high quality endothelial RNA from small spatially-defined locations.* Ann Biomed Eng, 2004. **32**(10): p. 1453-9.

133. Benjamini, Y. and Y. Hochberg, *Controlling the false discovery rate: a practical and powerful approach to multiple testing.* JRSS, 1995. **B, 57**: p. 289-300.

134. Benjamini, Y. and W. Liu, *A step-down multiple hypotheses testing procedure that controls the false discovery rate under independence.* J. Statist. Plann. Inference, 1999. **82**: p. 163-170.

135. Storey, J., *The positive false discovery rate: A Bayesian interpretation and the q-value.* Annals of Statistics, 2003. **31**: p. 2013-2035.

136. Rangaswamy, S., et al., *Exogenous oxidized low-density lipoprotein injures and alters the barrier function of endothelium in rats in vivo.* Circ Res, 1997. **80**(1): p. 37-44.

137. Zhao, B., et al., *Oxidized low-density lipoprotein increases endothelial intracellular calcium and alters cytoskeletal f-actin distribution.* Eur J Clin Invest, 1997. **27**(1): p. 48-54.

138. Essler, M., et al., *Mildly oxidized low density lipoprotein induces contraction of human endothelial cells through activation of Rho/Rho kinase and inhibition of myosin light chain phosphatase.* J Biol Chem, 1999. **274**(43): p. 30361-4.

139. Lee, J.S. and A.I. Gotlieb, *Understanding the role of the cytoskeleton in the complex regulation of the endothelial repair.* Histol Histopathol, 2003. **18**(3): p. 879-87.

140. Bianchi, C., et al., *Receptor-type protein-tyrosine phosphatase mu is expressed in specific vascular endothelial beds in vivo.* Exp Cell Res, 1999. **248**(1): p. 329-38.

141. Brady-Kalnay, S.M., et al., *Dynamic interaction of PTPmu with multiple cadherins in vivo.* J Cell Biol, 1998. **141**(1): p. 287-96.

142. Young, B.A., et al., *Protein tyrosine phosphatase activity regulates endothelial cell-cell interactions, the paracellular pathway, and capillary tube stability.* Am J Physiol Lung Cell Mol Physiol, 2003. **285**(1): p. L63-75.

143. Noria, S., et al., *Transient and steady-state effects of shear stress on endothelial cell adherens junctions.* Circ Res, 1999. **85**(6): p. 504-14.

144. Hellberg, C.B., et al., *Expression of the receptor protein-tyrosine phosphatase, PTPmu, restores E-cadherin-dependent adhesion in human prostate carcinoma cells.* J Biol Chem, 2002. **277**(13): p. 11165-73.

145. Singleton, P.A., J.G. Garcia, and J. Moss, *Synergistic effects of methylnaltrexone with 5-fluorouracil and bevacizumab on inhibition of vascular endothelial growth factor-induced angiogenesis.* Mol Cancer Ther, 2008. **7**(6): p. 1669-79.

146. Huang, W.Q. and Q.R. Wang, *Bone marrow endothelial cells secrete thymosin beta4 and AcSDKP.* Exp Hematol, 2001. **29**(1): p. 12-8.

147. Huang, W.Q. and Q.R. Wang, *Expression of Thymosin beta4 in Murine Bone Marrow Endothelial Cells, HL-60 Cells and Human Peripheral Blood Mononuclear Cells.* Zhongguo Shi Yan Xue Ye Xue Za Zhi, 2001. **9**(1): p. 10-13.

148. Oh, I.S., et al., *Hepatocyte growth factor upregulates thymosin beta4 in human umbilical vein endothelial cells.* Biochem Biophys Res Commun, 2002. **296**(2): p. 401-5.

149. Bednarek, R., et al., *Ku80 as a novel receptor for thymosin beta4 that mediates its intracellular activity different from G-actin sequestering.* J Biol Chem, 2008. **283**(3): p. 1534-44.

150. Al-Nedawi, K.N., et al., *Thymosin beta 4 induces the synthesis of plasminogen activator inhibitor 1 in cultured endothelial cells and increases its extracellular expression.* Blood, 2004. **103**(4): p. 1319-24.

151. Larsson, L.I. and S. Holck, *Localization of thymosin beta-4 in tumors.* Ann N Y Acad Sci, 2007. **1112**: p. 317-25.

152. Larsson, L.I. and S. Holck, *Occurrence of thymosin beta4 in human breast cancer cells and in other cell types of the tumor microenvironment.* Hum Pathol, 2007. **38**(1): p. 114-9.

153. Olbryt, M., et al., *Gene expression profile of B 16(F10) murine melanoma cells exposed to hypoxic conditions in vitro.* Gene Expr, 2006. **13**(3): p. 191-203.

154. Gyorffy, B., et al., *A snapshot of microarray-generated gene expression signatures associated with ovarian carcinoma.* Int J Gynecol Cancer, 2008. **18**(6): p. 1215-33.

155. Sosne, G., et al., *Thymosin beta 4 promotes corneal wound healing and decreases inflammation in vivo following alkali injury.* Exp Eye Res, 2002. **74**(2): p. 293-9.

156. Young, J.D., et al., *Thymosin beta 4 sulfoxide is an anti-inflammatory agent generated by monocytes in the presence of glucocorticoids.* Nat Med, 1999. **5**(12): p. 1424-7.

157. Matsushita, H., V.G. Lelianova, and Y.A. Ushkaryov, *The latrophilin family: multiply spliced G protein-coupled receptors with differential tissue distribution.* FEBS Lett, 1999. **443**(3): p. 348-52.

158. Doyle, S.E., et al., *Latrophilin-2 is a novel component of the epithelial-mesenchymal transition within the atrioventricular canal of the embryonic chicken heart.* Dev Dyn, 2006. **235**(12): p. 3213-21.

159. Mattiussi, S., et al., *Homeodomain interacting protein kinase 2 activation compromises endothelial cell response to laminar flow: protective role of p21(waf1,cip1,sdi1).* PLoS One, 2009. **4**(8): p. e6603.

160. Wei, G., et al., *HIPK2 represses beta-catenin-mediated transcription, epidermal stem cell expansion, and skin tumorigenesis.* Proc Natl Acad Sci U S A, 2007. **104**(32): p. 13040-5.

161. Shorts-Cary, L., et al., *Bone morphogenetic protein and retinoic acid-inducible neural specific protein-3 is expressed in gonadotrope cell pituitary adenomas and induces proliferation, migration, and invasion.* Endocrinology, 2007. **148**(3): p. 967-75.

162. Connelly, J.J., et al., *Genetic and functional association of FAM5C with myocardial infarction.* BMC Med Genet, 2008. **9**: p. 33.

163. Oh, S.P., et al., *The mouse alpha 1(XII) and human alpha 1(XII)-like collagen genes are localized on mouse chromosome 9 and human chromosome 6.* Genomics, 1992. **14**(2): p. 225-31.

164. Storlazzi, C.T., et al., *Rearrangement of the COL12A1 and COL4A5 genes in subungual exostosis: molecular cytogenetic delineation of the tumor-specific translocation t(X;6)(q13-14;q22).* Int J Cancer, 2006. **118**(8): p. 1972-6.

165. Apostolopoulos, J., et al., *Identification and characterization of a novel family of mammalian ependymin-related proteins (MERPs) in hematopoietic, nonhematopoietic, and malignant tissues.* DNA Cell Biol, 2001. **20**(10): p. 625-35.

166. Gregorio-King, C.C., et al., *MERP1: a mammalian ependymin-related protein gene differentially expressed in hematopoietic cells.* Gene, 2002. **286**(2): p. 249-57.

167. Stenmark, H. and V.M. Olkkonen, *The Rab GTPase family.* Genome Biol, 2001. **2**(5): p. REVIEWS3007.

168. Schimmoller, F., I. Simon, and S.R. Pfeffer, *Rab GTPases, directors of vesicle docking.* J Biol Chem, 1998. **273**(35): p. 22161-4.

169. Sun, L., et al., *Decreased platelet expression of myosin regulatory light chain polypeptide (MYL9) and other genes with platelet dysfunction and CBFA2/RUNX1 mutation: insights from platelet expression profiling.* J Thromb Haemost, 2007. **5**(1): p. 146-54.

170. Parmar, P.K., et al., *Neuroserpin regulates neurite outgrowth in nerve growth factor-treated PC12 cells.* J Neurochem, 2002. **82**(6): p. 1406-15.

171. Rajaraman, P., et al., *Common variation in genes related to innate immunity and risk of adult glioma.* Cancer Epidemiol Biomarkers Prev, 2009. **18**(5): p. 1651-8.

172. Hill, R.M., et al., *Expression and functional characterization of the serine protease inhibitor neuroserpin in endocrine cells.* Ann N Y Acad Sci, 2002. **971**: p. 406-15.

173. Fell, B., et al., *Characterisation of two serine protease inhibitors expressed in the pituitary gland.* Arch Physiol Biochem, 2002. **110**(1-2): p. 26-33.

174. Jia, H.L., et al., *Gene expression profiling reveals potential biomarkers of human hepatocellular carcinoma.* Clin Cancer Res, 2007. **13**(4): p. 1133-9.

175. Ikee, R., et al., *Glucose metabolism, insulin resistance, and renal pathology in non-diabetic chronic kidney disease.* Nephron Clin Pract, 2008. **108**(2): p. c163-8.

176. Mykkanen, L., et al., *Microalbuminuria is associated with insulin resistance in nondiabetic subjects: the insulin resistance atherosclerosis study.* Diabetes, 1998. **47**(5): p. 793-800.

177. Esteghamati, A., et al., *Insulin resistance is an independent correlate of increased urine albumin excretion: a cross-sectional study in Iranian Type 2 diabetic patients.* Diabet Med, 2009. **26**(2): p. 177-181.

178. Okpechi, I.G., et al., *Microalbuminuria and the metabolic syndrome in non-diabetic black Africans.* Diab Vasc Dis Res, 2007. **4**(4): p. 365-7.

179. Hao, Z., et al., *The association between microalbuminuria and metabolic syndrome in the general population in Japan: the Takahata study.* Intern Med, 2007. **46**(7): p. 341-6.

180. Kobayashi, S., et al., *Insulin resistance in patients with chronic kidney disease.* Am J Kidney Dis, 2005. **45**(2): p. 275-80.

181. Fioretto, P., M.L. Caramori, and M. Mauer, *The kidney in diabetes: dynamic pathways of injury and repair. The Camillo Golgi Lecture 2007.* Diabetologia, 2008. **51**(8): p. 1347-55.

182. Breyer, M.D., et al., *Mouse models of diabetic nephropathy.* J Am Soc Nephrol, 2005. **16**(1): p. 27-45.

183. Gross, J.L., et al., *Diabetic nephropathy: diagnosis, prevention, and treatment.* Diabetes Care, 2005. **28**(1): p. 164-76.

184. Liu, Y., et al., *Severe insulin resistance and moderate glomerulosclerosis in a minipig model induced by high-fat/ high-sucrose/ high-cholesterol diet.* Exp Anim, 2007. **56**(1): p. 11-20.

185. Sanden, S.K., et al., *Evaluation of a thick and thin section method for estimation of podocyte number, glomerular volume, and glomerular volume per podocyte in rat kidney with Wilms' tumor-1 protein used as a podocyte nuclear marker.* J Am Soc Nephrol, 2003. **14**(10): p. 2484-93.

186. Herrera, G.A., *Plasticity of mesangial cells: a basis for understanding pathological alterations.* Ultrastruct Pathol, 2006. **30**(6): p. 471-9.

187. Abrass, C.K., *Diabetic nephropathy. Mechanisms of mesangial matrix expansion.* West J Med, 1995. **162**(4): p. 318-21.

188. Abrass, C.K., D. Spicer, and G.J. Raugi, *Induction of nodular sclerosis by insulin in rat mesangial cells in vitro: studies of collagen.* Kidney Int, 1995. **47**(1): p. 25-37.

189. Sowers, J.R., *Metabolic risk factors and renal disease.* Kidney Int, 2007. **71**(8): p. 719-20.

190. Coward, R.J., et al., *The human glomerular podocyte is a novel target for insulin action.* Diabetes, 2005. **54**(11): p. 3095-102.

191. Chen, H.M., et al., *Podocyte lesions in patients with obesity-related glomerulopathy.* Am J Kidney Dis, 2006. **48**(5): p. 772-9.

192. Whaley-Connell, A., et al., *Insulin resistance, oxidative stress, and podocyte injury: role of rosuvastatin modulation of filtration barrier injury.* Am J Nephrol, 2008. **28**(1): p. 67-75.

193. Wolf, G., S. Chen, and F.N. Ziyadeh, *From the periphery of the glomerular capillary wall toward the center of disease: podocyte injury comes of age in diabetic nephropathy.* Diabetes, 2005. **54**(6): p. 1626-34.

194. Li, J.J., et al., *Podocyte biology in diabetic nephropathy.* Kidney Int Suppl, 2007(106): p. S36-42.

195. Cusumano, A.M., et al., *Glomerular hypertrophy is associated with hyperinsulinemia and precedes overt diabetes in aging rhesus monkeys.* Am J Kidney Dis, 2002. **40**(5): p. 1075-85.

196. Wolf, G. and F.N. Ziyadeh, *Cellular and molecular mechanisms of proteinuria in diabetic nephropathy.* Nephron Physiol, 2007. **106**(2): p. p26-31.

197. El-Atat, F.A., et al., *The relationship between hyperinsulinemia, hypertension and progressive renal disease.* J Am Soc Nephrol, 2004. **15**(11): p. 2816-27.

198. Morse, S.A., et al., *Hypertension and the metabolic syndrome.* Am J Med Sci, 2005. **330**(6): p. 303-10.

199. Alpert, M.A., et al., *The role of the renin-angiotensin system in the pathophysiology, prevention, and treatment of renal impairment in patients with the cardiometabolic syndrome or its components.* J Cardiometab Syndr, 2009. **4**(1): p. 57-62.

200. Shibata, S., et al., *Podocyte as the target for aldosterone: roles of oxidative stress and Sgk1.* Hypertension, 2007. **49**(2): p. 355-64.

201. Nagase, M., et al., *Enhanced aldosterone signaling in the early nephropathy of rats with metabolic syndrome: possible contribution of fat-derived factors.* J Am Soc Nephrol, 2006. **17**(12): p. 3438-46.

202. Wu, Y., et al., *Obesity-related glomerulopathy: insights from gene expression profiles of the glomeruli derived from renal biopsy samples.* Endocrinology, 2006. **147**(1): p. 44-50.

203. Thomas, D.B., et al., *Clinical and pathologic characteristics of focal segmental glomerulosclerosis pathologic variants.* Kidney Int, 2006. **69**(5): p. 920-6.

204. Chen, J., et al., *Insulin resistance and risk of chronic kidney disease in nondiabetic US adults.* J Am Soc Nephrol, 2003. **14**(2): p. 469-77.

205. Fliser, D., et al., *Insulin resistance and hyperinsulinemia are already present in patients with incipient renal disease.* Kidney Int, 1998. **53**(5): p. 1343-7.

206. Dzurik, R., V. Spustova, and K. Janekova, *The prevalence of insulin resistance in kidney disease patients before the development of renal failure.* Nephron, 1995. **69**(3): p. 281-5.

207. Becker, B., et al., *Renal insulin resistance syndrome, adiponectin and cardiovascular events in patients with kidney disease: the mild and moderate kidney disease study.* J Am Soc Nephrol, 2005. **16**(4): p. 1091-8.

208. Krolewski, A.S., et al., *Glycosylated hemoglobin and the risk of microalbuminuria in patients with insulin-dependent diabetes mellitus.* N Engl J Med, 1995. **332**(19): p. 1251-5.

209. *The effect of intensive treatment of diabetes on the development and progression of long-term complications in insulin-dependent diabetes mellitus. The Diabetes Control and Complications Trial Research Group.* N Engl J Med, 1993. **329**(14): p. 977-86.

210. Spronk, H.M., D. van der Voort, and H. Ten Cate, *Blood coagulation and the risk of atherothrombosis: a complex relationship.* Thromb J, 2004. **2**(1): p. 12.

211. Kannel, W.B., *Overview of hemostatic factors involved in atherosclerotic cardiovascular disease.* Lipids, 2005. **40**(12): p. 1215-20.

212. Grant, P.J., *Diabetes mellitus as a prothrombotic condition.* J Intern Med, 2007. **262**(2): p. 157-72.

213. Dunn, E.J. and P.J. Grant, *Type 2 diabetes: an atherothrombotic syndrome.* Curr Mol Med, 2005. **5**(3): p. 323-32.

214. Carr, M.E., *Diabetes mellitus: a hypercoagulable state.* J Diabetes Complications, 2001. **15**(1): p. 44-54.

215. Stegenga, M.E., et al., *Hyperglycemia stimulates coagulation, whereas hyperinsulinemia impairs fibrinolysis in healthy humans.* Diabetes, 2006. **55**(6): p. 1807-12.

216. Velik-Salchner, C., et al., *Normal values for thrombelastography (ROTEM) and selected coagulation parameters in porcine blood.* Thromb Res, 2006. **117**(5): p. 597-602.

217. Behler, R.H., et al., *ARFI imaging for noninvasive material characterization of atherosclerosis. Part II: toward in vivo characterization.* Ultrasound Med Biol, 2009. **35**(2): p. 278-95.